Experimental Optimisation of a Simple Basin Solar Still: Improved Heat Loss Management and Evaporation Rate

Heidi Lynn Marais

Experimental Optimisation of a Simple Basin Solar Still: Improved Heat Loss Management and Evaporation Rate

Author: Heidi Lynn Marais

Supervisor: Mr PW Sonnendecker

Co-Supervisor: Prof FJWJ Labuschagné

Dissertation submitted in partial fulfilment of the requirements for the degree

Master of Engineering
(Chemical Engineering)

in the

Department of Chemical Engineering
Faculty of Engineering, Built Environment and Information Technology
University of Pretoria

November 2018

Experimental Optimisation of a Simple Basin Solar Still: Improved Heat Loss Management and Evaporation Rate

Synopsis

Numerous modifications were made to simple basin solar stills with the aim to improve the performance of the stills and develop an understanding of the operation of the system. The changes were focused on reducing energy losses from the system, and increasing the rate of both evaporation and condensation. The stills had a cover area of $0.5\,\mathrm{m}^2$ and were coated with Duram© Durapond as the absorber surface and waterproofing. A cost target of 0.08 ZAR per litre was set in order for the system to be competitive with existing small-scale desalination systems.

To reduce energy losses the effect of insulation thickness was tested. Using Armaflex® foamed nitrile rubber insulation, increasing the thickness such that the thermal resistance values were increased by $0.25\,\mathrm{K}\cdot\mathrm{W}^{-1}$, $0.33\,\mathrm{K}\cdot\mathrm{W}^{-1}$, and $0.58\,\mathrm{K}\cdot\mathrm{W}^{-1}$ resulted in increases in yield of 9 %, 30 %, and 27 % on average when compared to the reference still.

It was observed that the back wall of the still reached exceptionally high temperatures, between 70 °C and 80 °C; to decrease losses through the back wall and better utilise that energy, aluminium panels were added to the inside of the still. This resulted in a higher rate of increase of water temperature and maximum water temperature in the still. The aluminium panels successfully redirected energy from the back wall of the basin still, reducing the temperature of the surface by around 10 °C. This did not result in the desired increase in yield as it was observed that condensation occurred on the panels themselves, overnight, thus resulting in a loss of condensate that would otherwise have been collected.

The evaporation rate was modified primarily by increasing the absorbance of solar irradiation, this was done by testing a polyvinyl chloride (PVC) coated textile as the absorber surface, adding a carbon black nanofluid, adding activated charcoal, and adding a carbon felt. The PVC absorber improved the yield by 98 % on average when compared to the

reference still. The nanofluid proved impractical as the fluid degraded and the particles settled out with multiple heating-cooling cycles, additionally the increase in yield when compared to the reference still increased from 46 % to 72 % as the particles settled suggesting that the nanofluid performed worse when the particles were in suspension. The activated charcoal resulted in an increase in yield of 98 % on average, and the carbon felt gave a 110 % increase. The carbon felt caused lower bulk water temperatures due to the tendency of the felt to float just beneath the surface of the water and allowing for evaporation to occur from a thin film of water which heated up significantly quicker due to its small thermal mass. All modifications significantly reduced the time between start-up and the onset of condensate collection which was shown to increase the yield.

Observation of the still during operation suggested condensation to be a limiting step in the process due to the speed at which droplets would re-form after running down the cover plate. Attempts at increasing the condensation rate included increasing the internal area by milling grooves into a portion of the plate, when compared to the reference still an improvement between 7 % and 27 % was observed in the yield. Other modifications included the addition of a heat sink to the top of the cover plate on the outside of the still where the temperature was highest; visually it could be seen that condensate formed more quickly around the heat sink but no significant effect on the yield or overall cover temperature was observed. Manually tapping on the cover improved the yield by forcing drop movement down the cover, this suggests drop movement to be a limiting step in the production of condensate.

A final still was designed and constructed using the information gained from the experiments performed. The still achieved water temperatures up to 11 °C hotter than the reference still and resulted in a 180 % increase in yield when compared to the reference still.

Analysis of the energy balance for the solar still indicates that the majority of the losses are linked to the cover plate - reflective, radiative, and convective losses, as well as radiative losses from the base of the still. It is of course necessary for some heat to be removed from the cover in order for condensation to occur, but the high temperature of the cover results in unnecessary losses which greatly reduce the efficiency of the system. It is recommended that steps be taken to reduce the cover temperature and provide an additional surface on which condensation can occur.

Acknowledgements

The financial assistance of the National Research Foundation (NRF) towards this research is hereby acknowledged. Opinions expressed and conclusions arrived at, are those of the author and are not necessarily to be attributed to the NRF.

The author would also like to express her gratitude and appreciation to:

The South African Water Research Commission for funding the experimental work.

My supervisor, Paul Sonnendecker, for his help and guidance throughout the project as well as his patience and support through all the problems encountered.

My co-supervisor, Prof. Johan Labuschagné, for his open door policy and willingness to listen to his students.

Jean-Paul André Ivan, for his support and encouragement every step of the way.

My family, for putting up with all the long working hours and always believing in me.

My fellow postgraduate students and office mates, for always being willing to bounce ideas off of each other over a cup of coffee.

Contents

List of Figures

List of Tables

Nomenclature

Greek Symbols

β	Coefficient of Thermal Expansion	K^{-1}
ϵ	Emmisivity	–
η	Efficiency	–
η_i	Instantaneous Efficiency	–
λ_{vap}	Latent Heat of Vaporisation	$\mathrm{J} \cdot \mathrm{kg}^{-1}$
μ	Viscosity	$\mathrm{kg} \cdot \mathrm{m}^{-1} \cdot \mathrm{s}^{-1}$
ρ	Density	$\mathrm{kg} \cdot \mathrm{m}^{-3}$
σ	Stefan-Boltzmann Constant	$\mathrm{W} \cdot \mathrm{m}^{-2} \cdot \mathrm{K}^{-4}$

Roman Symbols

A	Area	m^2
C_p	Specific Heat Capacity at Constant Pressure	$\mathrm{J} \cdot \mathrm{kg}^{-1} \cdot \mathrm{K}^{-1}$
C_v	Specific Heat Capacity at Constant Volume	$\mathrm{J} \cdot \mathrm{kg}^{-1} \cdot \mathrm{K}^{-1}$
E_{total}	Total Energy Available for Use	J
E_{un}	Energy Unaccounted for in the Energy Balance	J
g	Standard Acceleration due to Gravity	$\mathrm{m} \cdot \mathrm{s}^{-2}$
Gr	Grashof Number	–
$\mathcal{H}_{abs}$	Absolute Humidity	$\mathrm{kg} \cdot \mathrm{kg}^{-1}$
H	Enthalpy	$\mathrm{J} \cdot \mathrm{kg}^{-1}$
h	Heat Transfer Coefficient	$\mathrm{W} \cdot \mathrm{m}^{-2} \cdot \mathrm{K}^{-1}$
k	Thermal Conductivity	$\mathrm{W} \cdot \mathrm{m}^{-1} \cdot \mathrm{K}^{-1}$
L_c	Characteristic Length	m
M	Molecular Mass of Fluid	$\mathrm{kg} \cdot \mathrm{kmol}^{-1}$
m	Mass	kg

$\dot{m}$	Mass Flow Rate	$\mathrm{kg} \cdot \mathrm{s}^{-1}$
Nu	Nusselt Number	–
P	Partial pressure of water	Pa
Pr	Prandtl Number	–
$\dot{Q}$	Rate of Heat Transfer	W
Re	Reynold's Number	–
T	Temperature	°C
t	Time	s
U	Internal Energy	$\mathrm{J} \cdot \mathrm{kg}^{-1}$
v	Velocity	$\mathrm{m} \cdot \mathrm{s}^{-1}$
W	Work Rate	W
x	Thickness	m

Subscripts

ci	Cover Inside Surface
$cond$	Conductive
$conv$	Convective
cv	Control Volume
e	Evaporative
fs	Flow Streams
I	Solar Irradiation
o	Evaporation Surface
rad	Radiative
ref	Reflective
s	Surface from which Radiation Occurs
sky	Sky Conditions
w	Water Surface
∞	Bulk Conditions

1 Introduction

Fresh water is a limited resource. South Africa has low levels of rainfall compared to global averages and is facing a potential water crisis (Hedden & Cilliers, 2014). Corrigan (2009) states that one of the main socio-economic problems that Africa is currently facing is water shortage, this impacts the economic growth of the continent, the well being of the population, and reflects poorly on the scientific community.

Desalination is a method of producing distilled water through the removal of salt from seawater or brackish water. Desalination is a highly energy intensive process and consequently has high operating costs associated with it. Due to the high and rising cost of energy in South Africa as well as the fact that many rural communities do not have access to the electric grid it is desirable to use renewable energy sources, such as solar energy, to drive the desalination process and produce distilled water. For this type of situation a simple basin-type solar still is attractive due to its low operating and maintenance costs as well as its ease of construction (Bouchekima, 2003), however, solar stills have low daily yields in the range of $3\,\mathrm{L}\cdot\mathrm{m}^{-2}$ (Li, Goswami & Stefanakos, 2013; Chandrashekara & A Yadav, 2017; S Yadav & Sudhakar, 2015; Bouchekima, 2003; He & Yan, 2009).

Significant research has been done on improving the performance of simple basin solar stills. Some of the areas of focus are improving the absorbance of solar irradiation (Matrawy, Alosaimy & Mahrous, 2015; Rabhi *et al*, 2017; Velmurugan *et al*, 2008; Murugavel, Chockalingam & Srithar, 2008), optimising the still geometry (Feilizadeh, Soltanieh, *et al*, 2017; El-Swify & Metias, 2002; Rajaseenivasan *et al*, 2017; Jamil & Akhtar, 2017; GN Tiwari, Thomas & Khan, 1994; Khalifa & Hamood, 2009c), redirecting energy onto the water (Omara, Kabeel & Abdullah, 2017; Monowe *et al*, 2011; Estahbanati *et al*, 2016), and adding heat storage materials (Murugavel *et al*, 2008; Deshmukh & Thombre, 2017), among many others. Despite this, achieving substantial yields in a basin solar still at a competitive price is not an easy task.

Basin solar stills commonly utilise less than 35 % of the incident irradiation to produce water (Kalogirou, 2014 p. 442). Constraints imposed by heat and mass transfer limitations and losses inherent to the system make achieving a high yield in a simple basin solar still very difficult. Typically designs which have high efficiencies make use of expensive materials or costly additions to the stills (Al-Hussaini & IK Smith, 1995; Eldalil, 2010); in an off grid passive system low efficiencies are near impossible to avoid.

The objective of this project was to maximise the yield, and efficiency, of a simple basin solar still using passive modifications. This was to be done with a cost target of 0.08 ZAR per litre in order for the system to be competitive with existing small scale desalination

systems (Li *et al*, 2013). The system was required to be completely off grid, to be robust, and easy to operate and maintain. The objective included gaining a fundamental understanding of the system in order to isolate where improvements can be made in future designs and variations of the still. The information gained should be applicable to more complex systems, possibly those including active modifications, for future investigations.

The objective was considered by reducing energy losses from the system, and increasing the rate of both evaporation and condensation. Energy losses were investigated through the addition of insulation to the outside of the still, and aluminium panels to the inside. The evaporation rate was modified by the addition of a carbon black nanofluid, activated charcoal, carbon felt, and PVC tarpaulin. And finally the condensation rate was changed by increasing the area for condensation, removing additional energy from the condensation surface, and forcing movement of water droplets from the condensation surface. The investigation was limited to a single geometric design of the basin still in order to allow for better comparison of results, all modifications involved simple additions that could be made to the stills post construction. Due to the requirement of passive modifications, any circulation of air, or water, within the still was not considered.

2 Literature Review

Desalination is the process of removing salt from seawater or brackish water to obtain water with an acceptable concentration of dissolved solids (Joseph, Saravanan & Renganarayanan, 2005). To date desalination has been one of the most expensive ways of producing potable water due to large energy requirements as well as the capital cost associated with it. However, its presence in the production of potable water is rapidly becoming more prominent despite these drawbacks. (Li *et al*, 2013; He & Yan, 2009)

2.1 Solar Desalination

As the use of alternative energy sources is increasing solar energy is rapidly becoming more viable as an energy source for desalination processes (He & Yan, 2009). This is particularly relevant in developing countries where population growth requires large amounts of water but there are insufficient funds for traditional desalination to be feasible. These countries generally have high levels of solar irradiation which makes solar desalination even more promising. (Li *et al*, 2013) South Africa is marked as a country which has high potential for implementation of solar desalination according to Pugsley *et al* (2016).

Solar desalination makes use of solar energy to heat and evaporate salt water in order to obtain distilled water (He & Yan, 2009). There are two types of solar desalination, indirect and direct processes. Indirect methods involve two subsystems: a solar collector to absorb and collect the solar energy, and a separate desalination unit where the distilled water is produced. Alternatively in direct systems both collection of solar energy and production of distilled water occur together in the same unit. Direct solar desalination processes are typically better suited for small scale applications. (Chandrashekara & A Yadav, 2017)

Solar desalination systems generally have low costs of operation and maintenance but do require large installation areas as well as large capital investments (He & Yan, 2009; Delyannis, 1987). In most solar desalination systems the production rate of distilled water is directly proportional to the area of solar collection; this means that the cost of water remains constant regardless of the capacity of the plant and typical cost improvements due to economy of scale do not apply. This results in solar desalination systems often being more suited to small scale applications. (Kalogirou, 2005) Advantages of small scale desalination include the lower capital costs, the ability to operate near the water source thus reducing cost of transportation of the salt or brackish water, and the adaptivity to different water sources (Song *et al*, 2017). For these reasons small scale desalination

is particularly attractive when considering the applications to rural communities and small towns (Bouchekima, 2003). However, despite the lower energy requirements these systems generally produce distilled water at a higher cost per volume than large scale desalination plants (Ayoub & Alward, 1996; Karagiannis & Soldatos, 2008).

In direct solar desalination the most commonly used method is a basin solar still (Chandrashekara & A Yadav, 2017; Bouchekima, 2003), the typical set-up is shown in Figure 1. Basin solar stills typically operate in such a manner that heat collection and distillation occur in the same system; the water evaporates and condenses on the transparent cover through which solar radiation enters the system (Li *et al*, 2013).

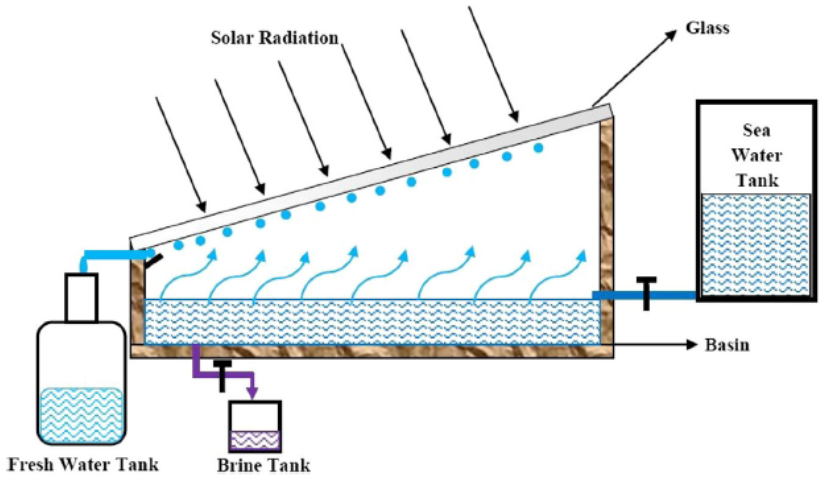

Figure 1: Simple basin-type solar still (Sharon & Reddy, 2015).

The main problems with traditional basin-type solar stills are brought about by evaporation and condensation occurring in the same unit. These problems include difficulties in rejecting the latent heat of condensation, as well as complications in obtaining a high enough temperature for evaporation while lowering the condensation temperature simultaneously (He & Yan, 2009). These drawbacks ultimately result in low yields of between $3\,\mathrm{L}\cdot\mathrm{m}^{-2}\cdot\mathrm{day}^{-1}$ and $4\,\mathrm{L}\cdot\mathrm{m}^{-2}\cdot\mathrm{day}^{-1}$ (Li *et al*, 2013; Chandrashekara & A Yadav, 2017; Bouchekima, 2003). Due to these low yields solar still desalination is not considered viable to address water shortages on a regional scale as of yet (S Yadav & Sudhakar, 2015). However, solar still desalination is the cheapest desalination method available and is feasible when water is desired in very small quantities (Kalogirou, 2005).

Additional disadvantages of solar stills are that they require a large amount of area to produce sizeable amounts of distilled water, require a large initial investment, and require daily maintenance to clean the cover and flush the basin. The maintenance requirements are simple but necessary in order to ensure that the still continues to operate at its

optimum; a build up of dust on the cover hinders incoming radiation and an excess of salt in the still makes evaporation more difficult. (Malik *et al*, 1982 pp. 40–41)

Many investigations have been carried out in attempts to achieve higher yields by addressing these two main problems in a number of different ways. Additionally, many different still designs have been developed from the traditional basin still.

2.2 Principles of Operation

The operation of a simple basin solar still is as follows: a transparent cover allows for solar radiation to enter the still where it is absorbed by an absorber plate beneath the water. The absorber plate causes the water to heat up and evaporate where it can then condense on the cover. (Malik *et al*, 1982 pp. 3-5) This is a simplistic view of the actual energy transfers occurring in the still.

2.2.1 General Heat Transfer Processes

In the solar still system there is both external heat transfer and internal heat transfer occurring. The external heat transfer is losses from the still to the surroundings and includes convection, conduction, and radiation. Internal heat transfer deals primarily with the energy transfers from the water to the cover, as well as from the absorber to the water, and also includes convection, conduction, and radiation.

Conduction is described by Equation 1 (Fourier, 1822), where k is the thermal conductivity of a material and has only a weak dependence on temperature.

$$\dot{Q}_{cond} = -kA\frac{dT}{dx} \tag{1}$$

The driving force for conduction is the temperature difference in the direction of interest.

Convection also uses a temperature difference as the driving force for heat transfer, the equation is shown below (Çengel & Ghajar, 2015 p. 26):

$$\dot{Q}_{conv} = h_{conv}A\Delta T \tag{2}$$

However, h_{conv} is a complicated function of the geometry of the surface, the flow and physical properties of the fluid, as well as the temperatures of operation. For natural

convection the relationship (Malik *et al*, 1982 p. 9; Çengel & Ghajar, 2015 p. 539)

$$Nu = C(GrPr)^n \tag{3}$$

can be used to describe the heat transfer coefficient. Where C and n are constants describing geometry and the physical behaviour of the system. Empirical relationships are commonly used for these constants. In the case of forced convection Equation 4 can be used to describe heat transfer (Çengel & Ghajar, 2015 p. 440);

$$Nu = CRe^m Pr^n \tag{4}$$

where the dimensionless parameters are calculated as:

$$Nu = \frac{h_{conv} L_c}{k} \tag{5}$$

$$Gr = \frac{g\beta {L_c}^3 \rho^2 \Delta T}{\mu^2} \tag{6}$$

$$Pr = \frac{\mu C_p}{k} \tag{7}$$

$$Re = \frac{\rho v L_c}{\mu} \tag{8}$$

The convective heat transfer coefficient is strongly dependent on the wind speed in the case of forced convection.

Radiative heat transfer from the cover of the still is modelled using the Stefan-Boltzmann law shown in Equation 9 (Çengel & Ghajar, 2015 p. 29),

$$\dot{Q}_{rad} = \sigma\epsilon \left((T_s + 273)^4 - (T_{sky} + 273)^4 \right) \tag{9}$$

The subscript s refers to the temperature of the surface from which radiation is occurring.

2.2.2 Internal Heat Transfer

The most important heat transfer processes occurring inside the still are conduction from the absorber surface to the water, evaporation from the water surface, convection from the water surface to the cover surface, and condensation of water onto the cover surface.

In a solar still convection occurs, most commonly, in the form of natural convection. Equation 3 is used to describe this process. However, as simultaneous mass and heat

transfer is taking place inside the still a modified Grashof number should be used. A common form of this modified Grashof number is shown in Equation 10 (Malik *et al*, 1982 p. 10).

$$Gr' = \frac{g{L_c}^3\rho^2}{\mu^2}\left(\frac{M_\infty\left(T_o + 273\right)}{M_o\left(T_\infty + 273\right)} - 1\right) \tag{10}$$

The subscripts o and ∞ refer to the conditions at the evaporation surface and at a point far away from the surface.

Manipulation of the equations and relevant empirical correlations yields Equation 12 (Malik *et al*, 1982 pp. 10–11) to describe the heat transfer by convection inside a basin solar still:

$$\dot{Q}_{conv} = h_{conv}A\left(T_w - T_{ci}\right) \tag{11}$$

$$\dot{Q}_{conv} = 0.884\left[T_w - T_{ci} + \frac{\left(P_w - P_{ci}\right)\left(T_w + 273\right)}{\left(269.9 \times 10^3 - P_w\right)}\right]^{\left(\frac{1}{3}\right)} A\left(T_w - T_{ci}\right) \tag{12}$$

where the subscripts w and ci refer to the conditions at the water surface and at the inside cover surface respectively.

While many models exist to model the evaporative heat transfer occurring in a basin solar still (C Elango, Gunasekaran & Sampathkumar, 2015), the most commonly used model for evaporation in a basin solar still is that of Dunkle (1961),

$$\dot{Q}_e = 16.273 \times 10^{-3} h_{conv} A(P_w - P_{ci}) \tag{13}$$

where the vapour pressures are calculated with the following relationship:

$$P_i = exp\left[25.317 - \left(\frac{5144}{T_i + 273}\right)\right] \tag{14}$$

The rate of evaporation in $\mathrm{kg \cdot s^{-1}}$ can further be calculated using the latent heat of vaporisation and the evaporative heat transfer rate.

$$\dot{m}_e = \frac{\dot{Q}_e}{\lambda_{vap}} \tag{15}$$

This relationship is largely empirical but is widely used in the field and has been tested extensively. It is clear from these relationships that the driving force for evaporation is the temperature difference between the water and the condensation surface.

The two main mechanisms for condensation are film condensation and dropwise condensation. In a simple basin solar still dropwise condensation is the observed mode of condensation. In dropwise condensation the vapour condenses as droplets of varying sizes which slide down the surface when they reach a specific size exposing the surface to allow for more drops to form. As there is no film of water hindering heat transfer between the vapour and the solid surface the rate of heat transfer is orders of magnitude larger than that associated with film condensation. (Çengel & Ghajar, 2015 p. 612; Coulson *et al*, 1999 pp. 476–478) In order for these drops to move along the condensation surface they must become large enough to overcome adhesive forces due to surface tension.

The presence of non-condensable gases in the system can cause a drastic reduction in the rate of condensation. The non-condensable gases collect near the surface and form a barrier which the vapour must first diffuse through subsequently hindering condensation. However, a higher velocity of the gas mixture aids in removing the non-condensable gases from the area adjacent to the surface which reduces this effect. (Çengel & Ghajar, 2015 p. 620) This is a problem in the simple basin solar still as the only movement of the air within the still is due to buoyancy forces and natural convection. Increased temperature differences between the absorber and the cover would aid in increased movement of air within the still.

2.2.3 The Energy Balance

In order to understand the system and determine where inefficiencies and losses are most prevalent it is important to do an energy balance of the system.

The general form of the energy balance is given in Equation 16 (JM Smith, Van Ness & Abbott, 2005 p. 48),

$$\frac{d(mU)_{cv}}{dt} = \dot{Q} + W - \Delta\left[\dot{m}\left(H + \frac{1}{2}v^2 + zg\right)\right]_{fs} \tag{16}$$

where subscripts cv and fs refer to the control volume and flowing streams respectively.

For the basin solar still there is only an outlet stream, no inlet, and kinetic and potential energy of this stream is negligible. Additionally there is no work input or output in the system, this reduces the equation to

$$\frac{d(mU)_{cv}}{dt} = \dot{Q}_{net} - \dot{m}_{out}H \tag{17}$$

The terms of Equation 17 can be further expanded to a place where the fundamental laws of heat transfer can be applied. Working from left to right, the first term represents the internal energy change of the system. The internal energy change of the system will be the sum of the internal energy changes of the various components included in the control volume. The control volume is not a general control volume and will be discussed in depth in Section 3.3.3.

Expanding the heat transfer term,

$$\dot{Q}_{net} = \dot{Q}_{in} - \dot{Q}_{out} \tag{18}$$

where the subscripts *in* and *out* could be replaced by *incident irradiation* and *losses*. In a passive solar still the only significant heat input to the system is in the form of solar irradiation, thus allowing for the $\dot{Q}_{in}$ term to be replaced with $\dot{Q}_I$ where $\dot{Q}_I$ is the incident solar irradiation.

Losses from the system are numerous, and dependent on the control volume selected. They can include convective losses from the cover plate, radiative losses from the cover, reflective losses from the cover, and conductive losses through the insulation. These can in turn be expressed using the heat transfer relations described previously. The losses are considered in depth in Section 3.3.3.

2.2.4 Thermal Efficiency

The thermal efficiency of a solar still is traditionally calculated as the ratio of water produced to the input of solar energy. In a passive solar still the instantaneous thermal efficiency can be calculated as the ratio of the rate of heat transfer related to evaporation to the rate of incident solar radiation, this is seen in Equation 19 (GN Tiwari, A Tiwari & Shyam, 2016 pp. 523–524),

$$\eta_i = \frac{\dot{Q}_e}{\dot{Q}_I} \tag{19}$$

and can be rewritten as

$$\eta_i = \frac{h_e A(T_w - T_{cover})}{\dot{Q}_I} \tag{20}$$

showing that as the temperature difference between the water and the cover increases the theoretical thermal efficiency of the still increases. Similarly an overall thermal efficiency

can be determined by Equation 21:

$$\eta = \frac{\lambda_{vap} \int_{t_0}^{t_n} \dot{m}_e dt}{\int_{t_0}^{t_n} \dot{Q}_I dt} \tag{21}$$

2.3 Modifications of Simple Basin Solar Stills

A main factor to consider throughout all of the modifications is the temperature difference between the water and the still cover (Sharshir, Yang, *et al*, 2016; Sharshir, Peng, *et al*, 2017). Increasing this temperature difference can increase the movement of humid air in the still and improve both the condensation rate and the evaporation rate. There are many ways to increase this temperature difference, such as active cooling of the cover with air or water, which results in an increase in production of distilled water (Omara, Abdullah, *et al*, 2017).

The performance of a solar still is a function of many different parameters which can be classified as design, operational, and meteorological parameters. As the meteorological parameters are not controllable variables within the system they will not be discussed in great detail. However, it is known that as the wind velocity increases the yield of the still increases, and as ambient temperature increases the yield also increases. (Malik *et al*, 1982 pp. 54) The design parameters include the size of the basin, the material of the absorber plate, the inclination angle of the cover, the material and thickness of the cover, and the type and thickness of insulation. While operational parameters include the depth of water in the still, and the temperature of water fed to the still. (Taghvaei *et al*, 2014; Jamil & Akhtar, 2017) Optimisation of the design and operational parameters are key to maximising the yield of the solar still.

The following subsections discuss many of the modifications that can be made regarding both design and operational parameters in order to improve the yield of a simple basin solar still.

2.3.1 Basin Height

Optimisation of the geometry of the basin still is of the utmost importance to this work as different geometries are not to be investigated in this project. It is for that reason that literature pertinent to the height of the basin still is relevant in order to design and construct a good base still to which further modifications can be made. The following

two sections, Section 2.3.2 and Section 2.3.3, are also relevant to the geometry of the basin still and are important for the same reason.

The height of the basin is an important parameter in the design of the solar still. The main effects of changing the basin height are that the volume available for evaporation increases, the distance water vapour must travel to condense increases, and additional shadows are added to the still. Additionally, if the ratio of the height of the back wall to the front wall is not kept constant changing the height can cause an increase in cover area.

Feilizadeh, Soltanieh, *et al* (2017) investigated the effect of basin height on the yield of the solar still while keeping the inclination angle of the cover constant. They found that increasing the height decreases the yield. The same result was found by Rajaseenivasan *et al* (2017) where they observed that decreasing the height from 0.45 m to 0.15 m resulted in a 84 % increase in yield. Jamil & Akhtar (2017) investigated heights varying from 0.366 m to 0.266 m and found that as the height decreased the yield increased from $1.341\,\mathrm{L}\cdot\mathrm{m}^{-2}\cdot\mathrm{day}^{-1}$ to $4.186\,\mathrm{L}\cdot\mathrm{m}^{-2}\cdot\mathrm{day}^{-1}$, a 212 % increase in yield. Feilizadeh, Estahbanati, *et al* (2016) achieved similar results for heights between 0.09 m and 0.23 m, observing approximately a 27 % increase in yield as the height of the basin decreased in summer conditions and 35 % in winter.

The explanation for this increase in yield for decrease in height is that the distance for the vapour to travel before it condenses decreases while the driving force remains more or less constant, a lower basin height also promotes convective heat transfer within the still due to the reduced distance between evaporation surface and condensation surface. Decreasing the volume of air in the still causes there to be more heat available per unit volume of vapour in the still and for there to be less volume that must be saturated before condensation can occur. Finally the additional shadows, which higher walls produce, hinder incoming radiation and decrease the temperature, and consequently yield, of the still.

2.3.2 Basin Aspect Ratio

Modifying the geometry of the still is a simple and cheap change that can be made in order to increase the yield. The change is implemented in the design and manufacturing of the still and changes nothing of the day to day operation of the solar still. The geometry of a simple basin solar still is shown in Figure 2.

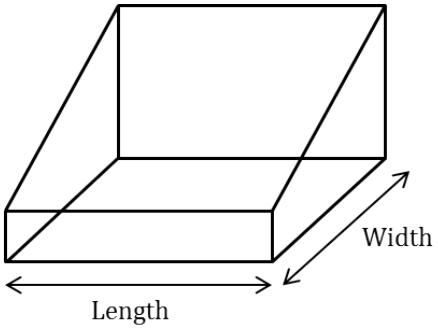

Figure 2: Geometry of simple basin type solar still.

Feilizadeh, Soltanieh, *et al* (2017) investigated the effect of basin geometries on the yield of a solar still. For a constant width of 1 m they found that increasing the ratio of length to width as lengths varied from 0.5 m to 1 m increased the yield by 26 % while increasing the lengths from 3.5 m to 4 m only increased the yield by 2 %, yields were reported in $\mathrm{L} \cdot \mathrm{m}^{-2} \cdot \mathrm{day}^{-1}$ so the results compensated for the increase in area. The large increase at small length to width ratios is due to the shadows cast by the walls as well as the walls receiving a large portion of the incoming radiation instead of the basin. They concluded that for length to width ratios greater than two the change in yield is insignificant and the lowest possible length should be used to minimise maintenance costs. The length to width ratio of two is also recommended by El-Swify & Metias (2002). It is necessary to note that this does depend on the orientation of the still; the length of the still should be parallel to the equator, with the low side nearest to the equator.

When changing the width of the still while maintaining a constant inclination angle the height of the still changes accordingly, meaning that the effects discussed in Section 2.3.1 are relevant. Feilizadeh, Soltanieh, *et al* (2017) found that as the width is increased the yield of the still increases up to a point after which the yield decreases. They found that the optimum ratio of width to length is around a value of 0.4 (or a length to width ratio of 2.5). This optimum point is likely due to the trade off between additional incoming solar radiation and the effects of increased basin height.

The modifications in this section and in Section 2.3.1 are easy to make and do not influence the operational costs of the still significantly. For this reason they are attractive options to optimise the performance of a simple basin solar still.

2.3.3 Angle of Inclination of Cover

The tilt angle of the cover is harder to discuss than some other factors as the optimum depends on both the latitude and season of where the tests are being done.

Changing the angle of inclination causes a number of changes within the still such as the speed at which condensed water collects, the volume available for water to evaporate into, the cover area available for heat transfer, and the amount of radiation that is reflected by the cover. (Khalifa & Hamood, 2009c; Lal *et al*, 2017)

The speed of water collection is important because if the water travels too slowly along the cover it is more likely to fall from the condensation surface back into the still. Additionally, slow movement of the water on the cover can result in a lack of cover space for new water to condense on. GN Tiwari, Thomas, *et al* (1994) state that a minimum inclination angle of 10° is required to prevent condensate falling back into the basin.

Considering the volume available for evaporation, a larger volume requires a larger amount of time in order to become saturated with vapour at which point condensation begins. This is mentioned briefly in Section 2.3.10 as the depth of water in the still will contribute to the available volume, and was discussed in full in Section 2.3.1 where the height of the still basin was considered. The net effect is that an increase in cover angle results in an increase in height which decreases the yield as was previously discussed.

The effect of the cover area influences both the losses and the amount of incoming radiation. For a constant basin area as the angle of inclination increases the area of the cover increases. Larger cover areas increase the losses which occur as the cover is the only uninsulated surface in the still, but it also increases the area through which solar radiation can enter the still. These are two competing effects and an optimum angle should therefore exist.

Khalifa & Hamood (2009c) attempted to obtain a general relationship between the productivity of the still and the tilt angle of the cover, they found that as the angle of inclination increased the yield increased, passed through an optimum, and decreased. The investigation done by Nafey *et al* (2000) showed that in winter months increasing the inclination angle increased the yield while in summer months the opposite held true. For this reason it is suggested that the optimum angle of inclination is the latitude of where the still is located; this is confirmed by GN Tiwari, Thomas, *et al* (1994) and Singh & GN Tiwari (2004). Note that the above results were all for stills in the northern hemisphere.

The cover angle is a simple way to optimise the still and should always be taken into account in the design of the solar still.

2.3.4 Absorber Surface

In a conventional basin solar still the bottom of the basin, or the absorber surface, is responsible for capturing energy from the incident solar radiation in the form of heat and transferring this energy to the water in the basin. Evidently the properties of this surface will affect the still performance.

One of the main things to consider is the surface area of the absorber, increasing the surface area improves the transfer of heat between the absorber surface and the water within the still due to increased area for heat conduction. An increase in area can be achieved through many different means such as corrugating the absorber plate, adding fins, pins, or wicks to the plate, or by the addition of a porous medium such as a sponge.

Matrawy *et al* (2015) compared a still with a corrugated wick absorber to a conventional still, both with external reflectors, and observed that the modified still reached higher temperatures and consequently had a higher yield: the modified still achieved $5.9\,\mathrm{L}\cdot\mathrm{m}^{-2}\cdot\mathrm{day}^{-1}$ while the conventional still achieved $4.4\,\mathrm{L}\cdot\mathrm{m}^{-2}\cdot\mathrm{day}^{-1}$, indicating a 35 % increase in yield due to the corrugated wick absorber. This result is similar to that obtained by Velmurugan *et al* (2008) who observed a 30 % increase in yield when comparing a conventional still to a still with wicks on the absorber plate.

Velmurugan *et al* (2008) also compared a conventional still and a finned still and achieved a 49 % increase in yield in the modified still with yields of $1.88\,\mathrm{L}\cdot\mathrm{m}^{-2}\cdot\mathrm{day}^{-1}$ and $2.81\,\mathrm{L}\cdot\mathrm{m}^{-2}\cdot\mathrm{day}^{-1}$ for the conventional and modified still respectively. Similarly Rabhi *et al* (2017) compared a conventional unmodified solar still to a solar still with a pin fins absorber. They found that both the cover temperature, and the absorber temperature were higher in the still with the pin fins absorber plate and that the modified still produced $2.83\,\mathrm{L}\cdot\mathrm{m}^{-2}\cdot\mathrm{day}^{-1}$ of distilled water compared to the $2.47\,\mathrm{L}\cdot\mathrm{m}^{-2}\cdot\mathrm{day}^{-1}$ produced by the conventional still, only a 15 % increase in yield. The difference in these numbers illustrates the large effect that a finned absorber can have on the performance of the still and how the effect is dependent on the specific dimensions of the fins (neither of which were well documented in the respective papers for the sake of comparison).

As mentioned, the addition of a porous medium serves to increase the exposure area of the water to the absorber surface. An example of this is shown by Abu-Hijleh & Rababa'h (2003) where sponge cubes are added to the still. The sponge is most useful when it protrudes from the water surface allowing capillary action to draw water into the sponge. The water in the sponge, above the water surface, can be heated more quickly due to volume of water exposed to the solar irradiation being smaller. Additionally, the small pores in the sponge can cause a reduction in the surface tension of the water

allowing for easier evaporation. (Murugavel *et al*, 2008; Abu-Hijleh & Rababa'h, 2003) This is observed again in the study done by Velmurugan *et al* (2008) where they achieved yields of $1.88\,\mathrm{L}\cdot\mathrm{m}^{-2}\cdot\mathrm{day}^{-1}$ in a conventional still and $2.26\,\mathrm{L}\cdot\mathrm{m}^{-2}\cdot\mathrm{day}^{-1}$ in a still with sponges; a 20 % increase in yield between the two stills. Madani & Zaki (1995) used a 2.5 cm layer of soot, which is essentially a porous mass, to increase the absorbance and when compared to a simple black painted absorber they found that the soot increased the yield by approximately 35 %.

While the absorbing surface is typically the bottom of the still it is of great benefit if the heat can be absorbed near the surface of the water instead of at the absorber plate at the bottom. This can be achieved using a suspended absorber which separates the water into two sections causing a smaller volume to receive heat and for the heat to be added nearer to the surface. The use of a suspended absorber is advantageous as it removes the need for the entire volume of water in the still to be heated before evaporation can begin. Small volumes of water above the absorber are heated much quicker allowing for evaporation to occur at an increased rate due to the effective decreased thermal mass of the water capturing heat. A disadvantage of the warm up period experienced when heat is absorbed from the bottom is that heat is lost in this period largely by conduction through the basin to the environment, maintaining the base of the still at a cooler temperature reduces losses to the surroundings. (Szulmayer, 1973)

El-Sebaii *et al* (2000) compared the use of four different materials on the effect of the suspended absorber plate. They observed that the metallic absorber materials: aluminium, copper, and stainless steel all caused between a 15 % and 20 % increase in yield compared to a conventional still while a mica absorber plate caused a 42 % increase in yield. Not only the material type but also the amount of water above it influences the effect it has on the yield. A perforated black aluminium sheet increases the yield by 15 % and 40 % for water layers of 3 cm and 6 cm respectively (Murugavel *et al*, 2008).

Szulmayer (1973) investigated the use of different floating absorber surfaces, suspended between 2 mm and 6 mm below the surface of the water. They made use of a woven shading cloth over a polyethylene lining, carbon black powder, a black plastic grid with 6 mm holes over a polyethylene lining, and a simple polyethylene sheet. They found the combination of shading cloth and liner to have been the most effective in increasing the evaporation rate within the still. Similarly, Srivastava & Agrawal (2013) placed floats covered with black burlap on the surface of the water, this allowed for capillary action to draw the water from the basin into the cloth to be evaporated, and observed a significant improvement in the still performance.

In general the absorber material is required to have a high radiation absorbance, to be

corrosion resistant, and to have a low cost (Madani & Zaki, 1995). The absorber is one of the most important parts of the still and it is clear that extensive research has been done on modifications to enhance the absorber performance. The modifications that have been investigated in this section all involve improving the absorbance of solar irradiation or improving the rate of heat transfer from the absorber to the water. As Equation 13 and Equation 15 state that the evaporation rate is proportional to the temperature difference between the water and the cover, it is clear that increasing the water temperature through modifications to the absorber could result in an increase in evaporation rate.

2.3.5 Agitation of Fluid

The use of agitation to improve the productivity of a simple basin solar still in an active modification as additional energy is required to power the agitation tool. The purpose of the agitator is to increase the contact area of the water and the air, and to break the surface boundary layer. These result in an improved rate of evaporation. The slight vibration of the still can also increase the frequency at which condensate runs off the cover and collects as distillate. This could potentially reduce the number of droplets which fall back into the still by reducing the time that a drop spends on the cover surface. (Eltawil & Zhengming, 2009; Rajaseenivasan *et al*, 2017)

The most common way of agitating the fluid is with a rotating shaft (Eltawil & Zhengming, 2009; Kumar, Esakkimuthu & Murugavel, 2016; Abdel-Rehim & Lasheen, 2005) Comparison of a conventional still with a still modified to have a rotating shaft showed that the yield was increased by on average 25 % in the modified still (Abdel-Rehim & Lasheen, 2005). Rajaseenivasan *et al* (2017) achieved similar results and saw a 30 % increase in yield due to the addition of rotating shaft stirrers to the solar still.

There are other methods of achieving agitation within the still, an example of this is seen in the research done by Eldalil (2010) where the use of harmonic vibrations within the still was investigated. It was found that the yield was increased by 70 % when compared to a solar still without vibrations.

Agitating the fluid in the still is an effective modification but is more costly than passive modifications as it increases the operating costs of the still through the additional energy requirements. This modification is unlikely to be useful in an off grid system, and is beyond the scope of this work due to it being an active modification. However, the principle that by disturbing the boundary layer and increasing contact area between water and air the evaporation rate can be increased is relevant to the objective.

2.3.6 Reflectors

Reflectors are relatively cheap additions to solar stills which increase the incident solar radiation on the solar still which in turn improves the efficiency (Omara, Kabeel & Abdullah, 2017). Both external and internal reflectors can improve the production of a solar still. Internal reflectors help minimise the energy loss from the still and redirect some solar radiation onto the surface of the water (Omara, Kabeel & Essa, 2015), they are generally most useful when the solar radiation intensity is low (Omara, Kabeel & Abdullah, 2017). External reflectors are used primarily to change the direction of solar radiation in order to add flexibility to the still design. Compared to internal reflectors, external reflectors have the drawback of increasing the cover temperature simultaneously with the brine temperature which decreases the temperature difference between the brine and the cover and subsequently the driving force for evaporation (Estahbanati *et al*, 2016). External reflectors also increase the effective area of the still; this is not considered by most literature sources in the report of the yield and should be taken into account.

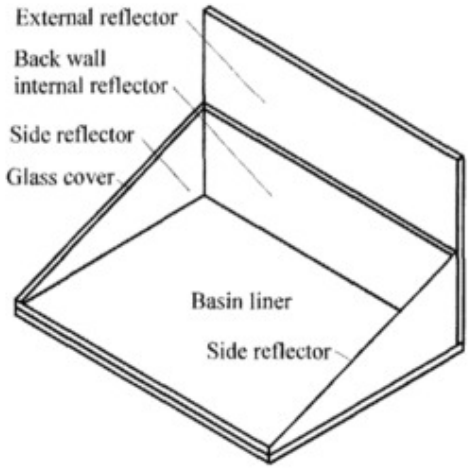

Figure 3: Typical reflector configuration for simple basin solar stills (Omara, Kabeel & Abdullah, 2017).

Figure 3 shows the typical configuration of both internal and external reflectors for a basin type solar still. The angle of the external reflector is of significant consequence to its performance and becomes most important as the angle of the sun changes. Tanaka (2009a) noted that in winter months when the sun is lower in the sky the reflector should be angled slightly forwards in order to ensure that reflected radiation enters the still. The opposite would then hold true for summer months; the reflector should be angled backwards due to the sun being higher in the sky. Care must be taken as the external reflector produces a shadow which can fall on the basin surface and result in a decrease in incident radiation entering the still. Tanaka (2009a) developed a model and

theoretically illustrated the aforementioned concept, showing that in summer the yield of distilled water can be increased by changing the inclination angle of the external reflector such that it is tilted slightly backwards. Similarly for winter months, Tanaka (2009b) experimentally showed that the productivity of the still could be increased by inclining the external reflector forwards. Shanmugan, Rajamohan & Mutharasu (2008) used an external reflector to increase the performance of a solar still and found that it increased the yield by approximately 30 % when compared to a conventional still.

Estahbanati *et al* (2016) investigated the use of internal reflectors. They observed a 16 % increase in yield in summer months in the still with the internal reflector compared to a still with no reflector, and a 41 % increase in yield in winter months. They also compared the use of front and side reflectors versus back wall reflectors and found that front and side reflectors increase the yield by approximately 18 % consistently while the effect of back wall reflectors varies greatly throughout the year but can be averaged to an increase in yield of 22 %. Internal reflectors were used by Abdallah, Badran & Abu-Khader (2008) and a 32 % increase in yield was obtained compared to a conventional still in summer.

The combination of reflector types is also effective: Monowe *et al* (2011) investigated a solar still with internal reflectors and an adjustable external reflector. Comparing the still with both sets of reflectors to a still with only internal reflectors resulted in an increase in yield of 43 %. This result is larger than the increase in yield obtained by using only a single reflector type.

Reflectors, especially internal reflectors, are worth considering as a modification to a basin solar still. The improved utilisation of solar irradiation can significantly improve the yield of the still for minimal additional cost.

2.3.7 Cover Surface

In a conventional solar still the cover of the still is the same surface on which condensation occurs. This results in a decrease in the amount of solar radiation entering the still as more condensate is generated due to increased reflection of the incident radiation. Reflection occurs on both the surface itself and the condensed water on the surface; characterising the amount of reflected radiation is non-trivial due to the dependence on the shapes of the water drops.

The material of the cover surface can have a significant effect on the productivity of the still. Studies up to now indicate that glass is preferential to other transparent plastics due to properties such as transmittance and roughness. Bhardwaj, ten Kortenaar &

Mudde (2013) investigated the effect of different cover materials on the yield of a solar still using glass and polyethylene terephthalate (PET). They achieved a yield of 27 % more in the glass covered still than in the PET covered still. The reasons for this are the droplet shapes on the respective materials; on glass the drops are flatter and more spread out which allows for more light to pass through compared to the drops on the PET. Additionally, the water vapour that collects on the PET remains in place for much longer than it does on the glass due to the higher contact angle of PET. This decreases the yield as the water fails to collect and allow additional condensation to occur. Glass is generally the preferred cover material due to its high transmittance for a wide range of angles of incidence (Murugavel *et al*, 2008).

The contact angle of a material is important to the condensation for more than the above mentioned reason; in the wetted condition materials with low contact angles allow more solar irradiation to pass through them than materials with high contact angles. The contact angle is therefore directly related to the production rate of distilled water. (Bhardwaj *et al*, 2013)

Another factor to consider with regard to the cover surface is the thermal conductivity. A higher thermal conductivity is better as it is easier for the cover to reject heat (Dimri *et al*, 2008). The thickness of the cover is also of concern, a thinner cover surface produces better yields than the same still with a thicker cover surface (Bhardwaj *et al*, 2013), this is again explained by the ability of the cover to lose heat to the surroundings (Dimri *et al*, 2008). Two glass covers of 3 mm thickness and 6 mm thickness were compared and it was observed that the thinner cover resulted in an increase in yield of 16.5 % (Murugavel *et al*, 2008).

Increasing the area of the cover can also affect the yield; an increase in area increases the amount of radiation which enters the still but also increases the area through which energy can be lost to the surroundings. Additionally, increasing the condensation surface area improves the yield of the still by providing additional area for the vapour to condense on, increasing the condensation rate results in a decrease in vapour pressure which consequently increases the rate of evaporation.

Bhardwaj, ten Kortenaar & Mudde (2015) increased the area for condensation without significantly increasing the entry area for solar radiation through the use of an irregularly shaped cover. They observed that as the area increased initially a large increase in yield was obtained but that after a point the effect of changing the area became less and a very large change in area was required for a small change in yield. Part of the reason Bhardwaj *et al* (2015) claimed for the increase in yield was that more heat was capable of leaving the still which increased the rate of condensation. Recall that a problem with

conventional solar stills is optimising the operating temperature between the optimum evaporation, and condensation, temperatures. Thus increasing the condensation surface area without increasing the area for incident radiation will result in a decrease in still temperature. This effect explains why Bhardwaj *et al* (2015) also observed that the yield of water versus condenser area went through an optimum, as there is an area above which too much heat is lost and there is insufficient energy for evaporation to proceed at a satisfactory rate.

There are many factors to consider regarding the cover surface of the still as it is responsible for both energy entering the system and energy leaving the system. It is not a simple parameter to optimise in the design of the still, and much work has been done on trying to understand the different ways it affects the still's performance. Modifying the cover surface is one of the few ways to directly influence the condensation rate in the system, either by changing the amount of time which drops spend on the cover, or by changing the amount of area available for drops to form on.

2.3.8 Insulation

Insulation is an important part of a basin solar still as it ensures that minimum amounts of heat are lost from the still to the surroundings. It is undesirable to lose heat and preferential that the energy be retained within the system and used to heat the water.

Basin type solar stills are typically insulated on both the sides and the bottom of the still. There are certain requirements that the insulating material must meet; it must be strong enough that the weight of the basin does not cause it to compress or deform, and it must be capable of withstanding high temperatures. (Khalifa & Hamood, 2009a)

Studies have been done on determining the degree to which the insulation improves the performance of the still, as well as determining the optimum thickness of the insulation material. Khalifa & Hamood (2009a) used polystyrene insulation and investigated three thicknesses: 3 cm, 6 cm, and 10 cm. The insulated stills were compared to a still with no insulation. They found that all the stills with insulation had a larger yield than the still without, and that the presence of insulation could improve the performance by more than 80 %. They also observed that the increase in yield from 3 cm insulation thickness to the 6 cm thickness was large, but that from 6 cm to 10 cm there was practically no change in the productivity of the still. This is in agreement with the results shown in Malik *et al* (1982 pp. 31) where the yield of the still increases rapidly up to an insulation thickness just larger than 4 cm, after which the effect the additional thickness has on the yield is minimal.

The above results can be generalised in terms of the thermal resistances. Polystyrene has a thermal conductivity of $0.04\,\mathrm{W \cdot m^{-1} \cdot K^{-1}}$ (Çengel & Ghajar, 2015 pp. 914), the thermal resistances calculated for a unit area of material and corresponding to thicknesses of 3 cm, 6 cm, and 10 cm are $0.75\,\mathrm{K \cdot W^{-1}}$, $1.5\,\mathrm{K \cdot W^{-1}}$, and $2.5\,\mathrm{K \cdot W^{-1}}$. It can now be suggested that around a thermal resistance of $1\,\mathrm{K \cdot W^{-1}}$ the insulation is at an optimum thickness.

There are many different types of insulating material that can be used and the thermal conductivity of the insulating material will determine how effective it is as an insulator. A material with a lower thermal conductivity will keep more of the heat inside the still than a material with a higher thermal conductivity. Madani & Zaki (1995) evaluated the effect of the presence of a 4 cm layer of glass wool insulation on the yield of the still and found that the presence of insulation resulted in approximately a 15 % increase in yield which appears low compared to the increases reported by Khalifa & Hamood (2009a) with polystyrene.

Adding insulation to the system seems like an obvious addition to the still in order to reduce energy losses from the system. It is, however, important to understand the effect which it has on the system in order to optimise the still economically as well as to obtain the maximum yield. Knowing that after a certain thickness the effect of adding additional insulation is negligible is of great benefit to the economic optimisation of the still.

2.3.9 External Condenser

The addition of an external condenser can be advantageous to the performance of the still. Based on one of the primary drawbacks of a simple solar still being that evaporation and condensation must occur in the same unit it is likely that using a separate condenser unit could be a key aspect to improving the performance. An external condenser acts as a heat and mass sink which results in a decrease in heat loss by convection from the water to the transparent cover, increases the condensation rate, and can theoretically increase the distillate yield by 56 % compared to a traditional solar still (Kabeel, Omara & Essa, 2017).

Rabhi *et al* (2017) compared a conventional unmodified solar still to a solar still with an external condenser, and an inlet to allow for air to move into the condenser. They observed that both the cover and absorber temperatures were lower in the still with the external condenser, and that the still with the condenser produced $3.15\,\mathrm{L \cdot m^{-2} \cdot day^{-1}}$ compared to the conventional still which produced $2.38\,\mathrm{L \cdot m^{-2} \cdot day^{-1}}$, a 32 % increase in yield.

Parameters such as the volume and area of the condenser are important to its performance. Al-Kharabsheh & Goswami (2003) found that varying the condenser area influenced the evaporation rate; doubling the fin area on the condenser increased the yield by 9 %.

In practice the use of an external condenser is usually combined with a vacuum fan to aid circulation of air from the still into the condenser. A study by Kabeel, Omara & Essa (2014a) investigated a basin still with an external condenser and a vacuum fan drawing the evaporated water from the still to the condenser. They tested the still with and without the vacuum fan and found that the presence of the fan increased the yield by up to 53 % depending on the power of the fan. Similarly Monowe *et al* (2011) investigated a solar still with an external condenser and a vacuum fan pulling humid air from the still into the condenser. The vacuum fan was powered by a PV panel of $1\,m^2$. They found that the presence of the vacuum fan increased the yield by 60 % compared to the still with just the external condenser.

If a vacuum fan is used in the still there are a few additional advantages. The vacuum fan can increase the turbulence of the air above the water which results in an improved evaporation rate (Omara, Kabeel & Essa, 2015), the reduction in pressure can decrease the operating temperature which can result in a decrease in losses (Ibrahim & Elshamarka, 2015; Al-Hussaini & IK Smith, 1995), and the movement of air within the still can also reduce the effect non-condensable gasses have on condensation (Al-Hussaini & IK Smith, 1995).

It is easy to understand how the use of vacuum and an external condenser in a solar still will increase the yield, research shows that it has a significant effect on the performance. Adding only an external condenser is a once off capital cost while the addition of a vacuum fan adds to the operating costs. It will be necessary to consider the economic implications of these modifications, but purely considering maximising the yield both are effective and worthwhile.

2.3.10 Brine Depth

The depth of water in the still has a large impact on the performance of the still. This is because the volumetric heat capacity of the still is largely determined by the volume of water available to absorb heat; if the incident radiation remains constant a larger volume of water will achieve lower temperatures than a smaller volume would. The depth of water is a parameter that is easily adjusted and is a cheap way to improve the performance of the still as it does not require additional components.

All literature indicates that increasing the depth of the water in the still decreases the yield. This has been observed by Badran & Al-Tahaineh (2005) who investigated water depths ranging from 2 cm to 5 cm and found a constant decrease in productivity as the depth increased, AK Tiwari & GN Tiwari (2006) who looked at larger water depths of 4 cm to 16 cm and observed approximately a 30 % decrease in the yield of the still, and Khalifa & Hamood (2009c) who found a linear relationship between the productivity of a solar still and the brine depth and found that reducing the depth of the brine can increase the productivity of the still by 33 % for depths between 10 cm and 1 cm. Feilizadeh, Estahbanati, *et al* (2016) investigated water depths of 2 cm, 4 cm, 8 cm, and 16 cm, while keeping the distance between the water and the cover constant, and found a 75 % decrease in yield as the depth increased from 2 cm to 16 cm in summer and 68 % decrease in winter. In general the relationship between water depth and still productivity is that as the depth increases the productivity decreases (Khalifa & Hamood, 2009b; Phadatare & Verma, 2007).

The studies mentioned above all focused on water depths larger than 1 cm and there are very few studies which have been done on fluid depth less than 1 cm. Sharshir, Peng, *et al* (2017) did a study on depths ranging from 0.25 cm to 5 cm and observed an optimum water depth within the still of between 0.5 cm and 1 cm. It is likely that below 0.5 cm dry spots develop in the still which negatively affect the yield of the still. (Sharshir, Peng, *et al*, 2017)

There is one advantage of a larger water depth; stills with a small depth of water are extremely sensitive to small changes in solar irradiation due to cloud cover or other fluctuations because of their low volumetric heat capacity, this can severely affect the yield. On the other hand, stills with more water are not as sensitive due to the higher thermal capacity of the system. (Murugavel *et al*, 2008)

The depth of brine in the still adds no significant cost to the still and is therefore an attractive way of optimising the yield. It is clear from the above discussion that it has a large impact on the performance of the still and is definitely worth careful consideration. Due to the varying volumetric heat capacity with varying depth, it is possible that the maximum temperature can be influenced thus affecting the evaporation rate.

2.3.11 Additives to Brine

In a conventional still the majority of the solar radiation is absorbed by the absorber plate and then transferred to the brine in the still as was discussed in Section 2.3.4. This is suboptimal as the water is heated from the bottom and must first rise to the top

before it can evaporate. Also, there are additional losses when the absorber plate is at elevated temperatures. For this reason the addition of nanoparticles or dyes to the brine is advantageous as it allows for a greater portion of the incoming radiation to be absorbed by the brine directly thus avoiding the heating of an absorber plate. (Malik *et al*, 1982 pp. 33)

Nanofluids are suspensions of nanoparticles in a fluid and are often characterised by their excellent thermal characteristics which can be used to improve the performance of other thermal systems (Mahian *et al*, 2013). Many studies have been carried out to determine how nanofluids affect solar collectors and to evaluate the possibility for their integration into solar energy.

Recently nanofluids have been used in conjunction with solar stills, instead of just solar collectors, and their effects evaluated. Kabeel, Omara & Essa (2014b) investigated the effect of different concentrations of metallic nanoparticles in the salt water. They found that as the nanoparticle concentration increased so did the yield, however, the increase in yield was asymptotic and after a certain concentration there appeared to be no additional effect on the performance of the still. This result corresponds to the trend observed when adding nanoparticles to solar collectors (Mahian *et al*, 2013).

A study done by T Elango, Kannan & Murugavel (2015) compared the use of three different nanoparticles: Al_2O_3, ZnO, and SnO_2, in simple basin solar stills. The concentrations of nanoparticles used was 0.1 % on a mass basis. They noticed a relationship between the still temperature and the thermal conductivity of the nanofluid; a higher thermal conductivity resulted in higher still temperatures and consequently higher production rates. Similarly, Gupta *et al* (2016) investigated the use of CuO nanoparticles at a concentration of 0.12 % on a mass basis. They achieved higher distillate yields when using the nanofluid than in the conventional solar still. The use of CuO and graphite nanoparticles was compared by Sharshir, Peng, *et al* (2017), they found that the graphite improved the performance of the still more than the CuO, likely due to the higher thermal conductivity and lower density of graphite which results in a better suspension. Furthermore, they observed the same asymptotic behaviour previously described.

Darkly coloured soluble dyes can also be used to increase the amount of solar radiation which the fluid absorbs which results in an increase in water temperature. The presence of a dye, specifically a black or violet dye, can improve the performance of the still greatly. The most significant improvement is seen when the water depth is large; at small depths the effect of the dye is mostly insignificant. (Malik *et al*, 1982 pp. 33-36) Akash *et al* (1998) observed a 60 % increase in yield in a still with black dye compared to a conventional still with only a steel absorber plate. They also used a black ink, this

resulted in only a 45 % in yield.

One problem with the use of brine additives in a simple basin still without other modifications such as an external condenser or cover cooling is that as the rate of evaporation increases due to increased heat capture the temperature of the cover also increases. This is undesirable as a large temperature difference between the water and the cover is necessary for optimal performance. The use of a nanofluid or dye does improve the yield of the still through an increase of evaporation rate, but the potential of the additive is not fully realised due to the heating of the cover.

2.3.12 Heat Storage

Heat storage is effective in improving the performance of a solar still partly because it increases the operating hours; a solar still is reliant on the presence of the sun to raise the temperature of the water, if sufficient energy is stored the system can operate for a period of time without the presence of the sun.

A possible heat storage method is using a sensible heat storage material such as sand or thermal fluids and to place this underneath the basin. Due to a significant portion of heat losses occurring through the bottom of the still this also serves to reduce those losses. This form of heat storage captures heat during daylight hours when there is an abundance of solar radiation, and releases the heat when the solar radiation is no longer present.

Deshmukh & Thombre (2017) did an investigation on solar stills with and without sensible heat storage. The thicknesses of heat storage material were 0.5 cm, 1 cm, and 1.5 cm and two different types of heat storage material were investigated, sand and servotherm medium (SM) oil. The different thicknesses corresponded to 4.1 kg, 8.2 kg, and 12.3 kg of sand and 2.1 kg, 4.2 kg, and 6.3 kg of SM oil. They found that the temperature of the sand was significantly lower than the water temperature likely due to poor contact between the sand and the basin bottom while the SM oil temperature was nearly identical to the water temperature due to convection improving the heat transfer between the basin and the heat storage medium. They observed the following trends: the daylight yield decreased with increase in mass of sensible heat storage and the overnight yield increased with the addition of heat storage but then remained approximately constant for the different masses. The total yield combining overnight and daylight experienced an optimum around 0.5 cm of sensible heat storage material.

Other heat storage methods include the addition of black rubber or black gravel to the still. Experimental results have shown that they both increase they yield by approxi-

mately 20 % (Murugavel *et al*, 2008). Abdel-Rehim & Lasheen (2005) investigated the use of glass balls as thermal storage; they covered the basin surface with glass balls of a 13.5 mm diameter and compared the operation of the modified still to that of a conventional still. They found that the packing allowed for basin temperatures to remain elevated as the incident radiation decreases towards the end of the day. The modified still showed on average a 45 % increase in yield.

Heat storage is most useful if the still is to be run during the night when there is no solar radiation available. However, results indicate that the addition of small amounts of heat storage can increase the yield during daylight hours. The cost of adding heat storage material versus the additional water produced must be carefully considered.

2.4 Summary of Literature

As the demand for water increases it is necessary to find alternative sources of water. Desalination is a viable method of producing distilled water to supplement the existing fresh water reserves.

There are many desalination techniques which are suited to different situations; considering a rural community without access to the electric grid a simple solar still is the recommended desalination method due to its low maintenance requirements, ease of construction and operation, and low cost. Solar stills have low daily yields and much research has been done on ways to improve the yield of the still, these include:

- Decreasing the height of the basin to improve the yield due to a reduced distance for vapour to travel before condensation as well as a smaller volume which must become saturated.
- Increasing the ratio of length to width to increase the yield due to more solar radiation reaching the water for a given orientation.
- The inclination angle of the cover should be equal to the latitude of where the still is located.
- Increasing the area of the absorber surface through the use of corrugation, wicks, fins, pins, or the addition of a porous medium to improve the yield of the still. This results in an improved rate of heat transfer from the absorber to the water and a subsequent increase in evaporation rate.
- Using a suspended absorber surface to increase the yield by reducing the amount of convective heat transfer that must occur in order for the heated water to reach

the surface. This also causes a decrease in the conductive losses from the base of the still due to lower base temperatures.

- Agitating the fluid within the still to disrupt the surface boundary layer and consequently increase the yield through an increase in evaporation rate.
- The use of internal and external reflectors to improve the yield by reducing the amount of energy lost to the sides of the still.
- The correct selection of cover material and thickness; thinner cover materials appear to improve the yield by improving the rate of condensation.
- Addition of an external condensing unit can also significantly improve the yield of the still by influencing the condensation rate.
- Using the correct depth of water in the still to reach higher temperatures and increase the evaporation rate.
- Adding nanoparticles or dyes to the water in the still to increase the yield by increasing the thermal properties of the water and modifying the evaporation rate.
- Adding small amounts of heat storage such as sand to improve the yield of the still by reducing heat loss.

As can be seen there is extensive literature available regarding parameters affecting the performance of a simple basin solar still. If correctly implemented these modifications and combinations of them will result in an improved yield from the solar still thus increasing its potential for use in rural communities.

Based on the operating principles of a simple basin solar still the variables deemed most likely to have the largest effect on the performance of the still are the temperature of the water, the temperature of the cover surface, the area available for evaporation, and the area available for condensation. The latter two variables can be directly changed by adding area to one of the two surfaces, while the first two variables require more indirect methods to effect a change in the desired variable. These can be grouped into two categories; condensation rate which includes the cover surface temperature and the area available for condensation, and evaporation rate. These two categories combined with heat losses from the still were investigated in this work.

3 Experimental

3.1 Apparatus

3.1.1 Configuration of Basin Solar Still

The basin solar still was designed using as far as possible the optimum geometric parameters obtained in literature. In specific:

- The ratio of length to width was designed to be 2, as recommended by Feilizadeh, Soltanieh, *et al* (2017) and El-Swify & Metias (2002).
- The average height of the still was minimised within practical constraints; primarily the need for a water catchment system with sufficient angle to allow flow of condensed water (Feilizadeh, Soltanieh, *et al*, 2017; Rajaseenivasan *et al*, 2017; Jamil & Akhtar, 2017).
- The inclination angle of the cover was designed to be 25°; the latitude of Pretoria, South Africa, the location where the experiments would be run (GN Tiwari, Thomas, *et al*, 1994; Singh & GN Tiwari, 2004).

The stills were designed to have a cover area of $0.5\,\mathrm{m}^2$, this being the area through which solar irradiation enters the still.

The stills were raised in order to prevent conduction to the ground from the base of the still as well as to allow for the condensate collection system to be mounted on the frame. Photographs of the stills during operation can be seen in Figure A.1 and Figure A.2 in Appendix A.

The still body was made of 18 mm ShutterPly, a type of plywood. It was chosen as it is cheap, strong, and readily available. The still body needs to be rigid and sufficiently durable to withstand exposure to ambient conditions. Wood is not the best solution as it must be maintained when left outdoors for extended periods of time, the cost constraints were the deciding factor. The plywood has an approximate thermal conductivity of $0.12\,\mathrm{W}\cdot\mathrm{m}^{-1}\cdot\mathrm{K}^{-1}$ (Çengel & Ghajar, 2015 p. 912). The wood was coated on the inside with black Duram© Durapond which is a non-toxic, polyurethane waterproofing with a service temperature range of $-44\,^{\circ}\mathrm{C}$ to $120\,^{\circ}\mathrm{C}$ making it suitable for the use in the solar still (*Data Sheet: Waterproofing, Durapond* 2014). The absorber, as mentioned in Section 2.3.4, must have a high absorptivity, be resistant to corrosion, non-toxic, and able

to handle the high temperatures which the still experiences. Durapond was selected for its ability to act as both the waterproofing and the absorber surface. Due to a lack of available data for the emissivity of Durapond a value of 0.97 was used in later analysis, as this is the commonly used emissivity of black paint, the corresponding absorptivity for black paint is also taken as 0.97 (Çengel & Ghajar, 2015 p. 743).

The stills were later coated with polyvinyl chloride (PVC) coated textiles, such as those used in dam linings, to replace the Durapond absorber. The Durapond proved to be unreliable and the quality of the waterproofing deteriorated over time, it is uncertain if this was due to an incorrect service temperature range of the Durapond or if there were unfavourable interactions between components of the still (This is discussed further in Section 4.1). The PVC is a black coated fabric which is UV stabilised to discourage degradation of the polymer.

The cover material was chosen with the aim being to use cheap and robust materials in order to make the design practical. This eliminated glass as it is more likely to break. The cover must have high transmittance, be smooth, retain structural integrity at elevated temperatures, and be stable in UV. The comparison in Table 1 led to the selection of polymethyl methacrylate (PMMA) as the cover material. A sheet thickness of 5 mm was used.

Table 1: Comparison of relevant material properties for common transparent polymers. (Wypych, 2016)

	PMMA	PC	PS
Thermal conductivity [$\mathrm{W \cdot m^{-1} \cdot K^{-1}}$]	0.19	0.22	0.128
Transmittance [%]	92	82-91	89-90
Refractive Index	1.49	1.58	1.6
Contact Angle of water	69.1-74.7	81.3-84	85.3-88.5
UV Stability	yes	limited	limited
Flexural Strength [MPa]	107-117	94-120	66-95

Two of the stills were insulated using two layers of 13 mm Armaflex® sheet, which is a foamed nitrile rubber, and has a thermal conductivity of $0.035\,\mathrm{W \cdot m^{-1} \cdot K^{-1}}$ at 0 °C increasing to $0.039\,\mathrm{W \cdot m^{-1} \cdot K^{-1}}$ at 40 °C and a service temperature range of −40 °C to 105 °C (*Class O Armaflex®* 2013).

The third still was insulated using 50 mm of a polyurethane foam, with a thermal conductivity of $0.026\,\mathrm{W \cdot m^{-1} \cdot K^{-1}}$ (Çengel & Ghajar, 2015 p. 914). It should also be noted that the outside of stills 1, 2, and 3 were coated with a reflective aluminium tape.

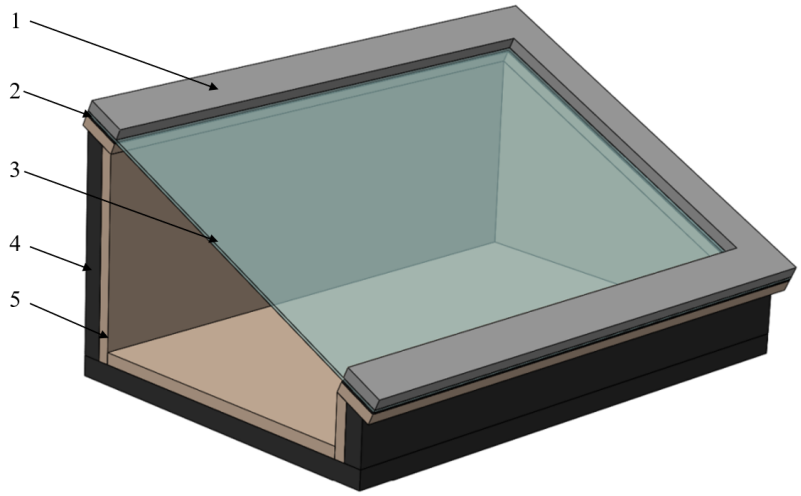

Figure 4: A section view of the basin still that was designed and constructed for this project.

The schematic in Figure 4 shows the following components of the still.

1. The aluminium frame that was used to seal the still. It was hinged at the top of the wooden structure, riveted to the PMMA cover sheet, and had clasps at the bottom to hold it shut. The hinged cover was necessary to allow for ease of maintenance.
2. The neoprene seal to ensure the still was properly closed.
3. The cover plate.
4. The Armaflex® insulation.
5. The wooden body of the still.

What was not shown in Figure 4 is the condensate collection channel which was mounted to the front wall of the still. Figure 5 shows the two cross sections of the different collection channels. The U-channel, on the right, was used in Still 1 and Still 2 while the angled channel pictured on the left was used in Still 3. The channel was raised in the middle slanting down towards the sides of the still in order to allow for water to move easily.

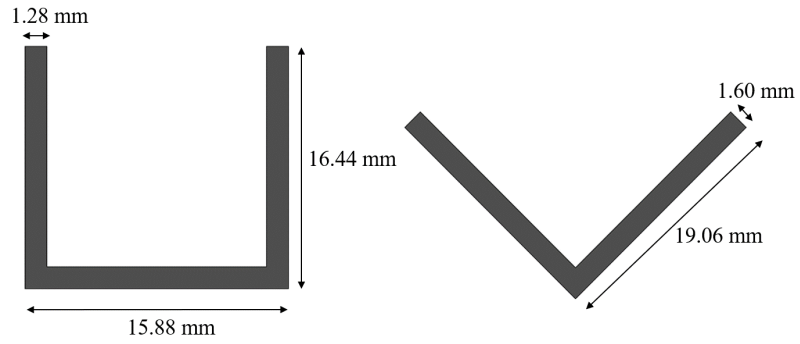

Figure 5: A cross section view of the two channel shapes used for water collection in the stills.

Figure 6 shows the internal dimensions of the basin stills that were built. All stills had identical internal dimensions.

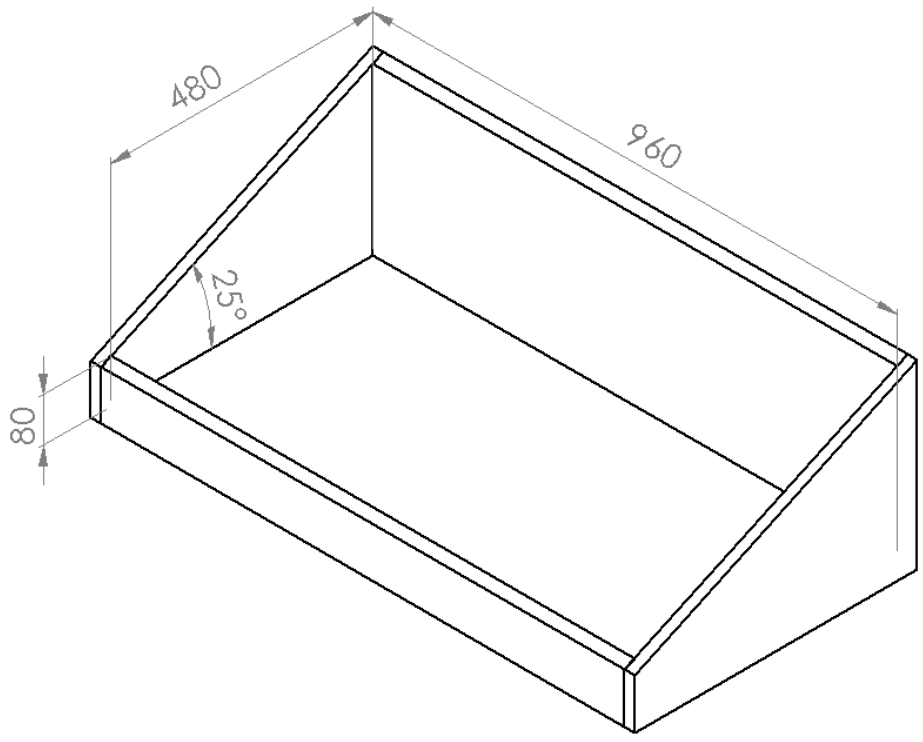

Figure 6: Schematic showing dimensions of the constructed basin stills, all lengths in mm.

One additional still was built at the end of the project, the still had the same dimensions, used PVC as the absorber surface, used the angled channel from Still 3 but was raised on the sides sloping down towards the middle. The main difference with this still, Still 4, was that the body of the still was built from 40 mm Isoboard extruded polystyrene insulation and the outside of the still was painted black. The Isoboard insulation has a thermal conductivity of $0.024\,\mathrm{W}\cdot\mathrm{m}^{-1}\cdot\mathrm{K}^{-1}$ (IsoBoard, 2018). The plywood was built around the Isoboard to act as structural support but was not in contact with the water.

3.1.2 Data Acquisition

In order to monitor the performance of the stills it was necessary to carefully monitor temperatures of water, air, and surfaces inside the still, humidity inside the still, mass of water produced by the still, as well as the ambient conditions. An Arduino™ MEGA 2560 microcontroller with a data logging shield was used for all data capture within the still, measurements were logged to the SD card every minute.

DS18B20 temperature sensors were used for the temperature measurements in the still. The waterproof version of the sensor was used for liquid temperature measurements while the chip version was used for all surface temperatures. The DS18B20 temperature sensors are addressable allowing for multiple sensors to be connected in series using a single data pin on the Arduino for communication with the microprocessor. The sensors are capable of measuring temperatures in the range of $-55\,°C$ to $125\,°C$ and have an accuracy of $\pm 0.5\,°C$ for temperatures above $-10\,°C$ and below $85\,°C$. The resolution of the measurements is either 9-bit or 12-bit. Each sensor has a ground, live, and data pin and makes use of a pullup resistor of $4.7\,k\Omega$ connecting the live and data pins. (*DS18B20 - Programmable Resolution 1-Wire Digital Thermometer* 2018)

DHT22 temperature and humidity sensors were used for humidity measurements and measuring the air temperature within the still. The humidity sensor has a resolution of $0.1\,\%$ with a range of $0\,\%$ to $99.9\,\%$ and an accuracy of $\pm 2\,\%$. The temperature sensor has a resolution of $0.1\,°C$, or 16-bit, with an accuracy of $\pm 0.5\,°C$ and a range of $-40\,°C$ to $80\,°C$. (*Temperature and Humidity Module - AM2302 Product Manual* 2018)

To measure the amount of water produced over the course of the day a TAL220, $10\,kg$ load cell, and a HX711 load cell amplifier was used. The load cell was observed to be accurate to $0.1\,g$ after calibration.

Apogee SP-215 silicon-cell pyranometers were used to monitor the intensity of solar irradiation. The pyranometer has a range of $0\,W \cdot m^{-2}$ to $1250\,W \cdot m^{-2}$ and measures global short-wave radiation, not direct normal radiation (*Owner's Manual, Pyranometer, Models SP-212 and SP-215* 2018). The pyranometer was mounted on the cover plate of the still, perpendicular to the cover.

A Microbit Weatherbit was used for measuring all ambient conditions; wind speed and direction and ambient temperature and humidity.

Figure 7 shows the locations of the various sensor types inside the stills and Figure 8 shows the sensors on the cover plate as well as on the outside of the still. The only

sensors not shown in these figures are the load cell and temperature sensor measuring the temperature of the collected condensate.

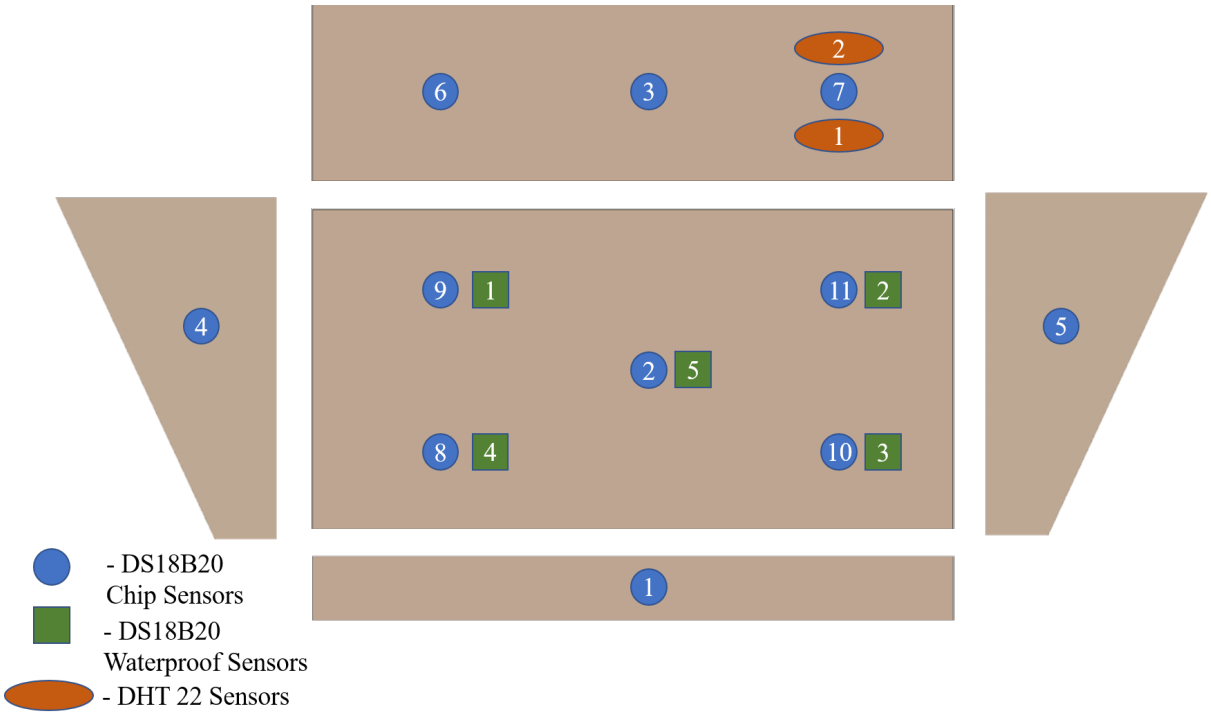

Figure 7: The location of sensors on the inside of the basin still.

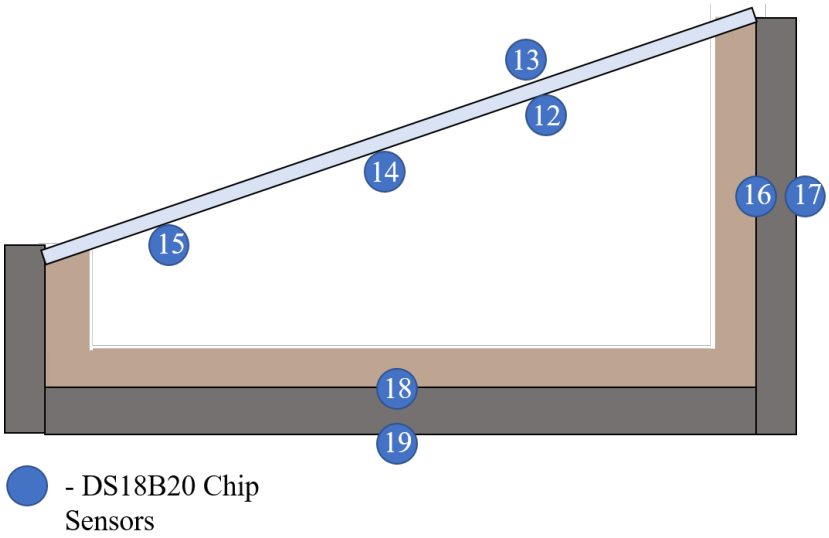

Figure 8: The location of sensors on the cover and on the outside of the basin still.

Note that not all sensors were present in all of the stills, Table 2 shows which sensors were in which of the four stills.

Table 2: Summary of which sensors, shown in Figure 7 and Figure 8, were in which of the four basin stills.

Sensor Type	Sensor Number	Still 1	Still 2	Still 3	Still 4
DS18B20 Chip	1	✓	✓	✓	
	2	✓	✓	✓	✓
	3	✓	✓	✓	
	4	✓	✓	✓	
	5	✓	✓	✓	
	6			✓	✓
	7			✓	✓
	8		✓	✓	
	9		✓	✓	
	10		✓	✓	
	11		✓	✓	
	12	✓	✓	✓	
	13	✓	✓	✓	✓
	14		✓		
	15		✓		
	16		✓		✓
	17		✓		✓
	18		✓		✓
	19		✓		✓
DS18B20 Waterproof	1	✓	✓	✓	
	2	✓	✓	✓	
	3	✓	✓	✓	
	4		✓	✓	✓
	5			✓	
	6	✓	✓	✓	
DHT 22	1		✓	✓	✓
	2	✓	✓	✓	✓

3.2 Experimental Design

Considering the physical phenomena occurring within the system, discussed in Section 2.2, certain variables can be identified as those likely to improve the performance of the still the most significantly. These were covered in Section 2.2 and decided to be

the temperature of the water, the temperature of the inside cover surface, the area for evaporation, and the area for condensation. This work was focused on decreasing heat losses to the surroundings as well as favourably changing the aforementioned variables.

3.2.1 Baseline Experiments

Due to inherent variations between the different stills it was important to perform experiments where all of the stills would run with the same conditions in order to characterise the difference between the stills due to variability in materials and construction. This was done for ten days initially and repeated sporadically throughout the experiments to ensure repeatability.

All variables were monitored during these baseline tests and the differences between the stills observed. An average difference in yield between each still and the reference still was determined in order to correct for the inherent variability when evaluating the effects of modifications made to the stills.

In all experiments done Still 2 acted as the reference still, Still 1 and Still 3 were modified over the course of the project, and Still 4 was built near the end of the project taking into account the information that was gathered during the duration of the project.

3.2.2 Reducing Energy Loss

In reducing energy losses from the system two modifications were made. The first involved testing various insulation thicknesses to minimise losses. This was discussed in Section 2.3.8 and is a vital part of the basin still.

There were six different configurations of insulation that were tested, listed below are the configurations as well as the corresponding thermal resistances of the still calculated for a unit area of the still:

1. No additional insulation (only the ShutterPly still body), thermal resistance of $0.16\,\mathrm{K}\cdot\mathrm{W}^{-1}$.
2. 13 mm of Armaflex® insulation, thermal resistance of $0.49\,\mathrm{K}\cdot\mathrm{W}^{-1}$.
3. 13 mm of Armaflex® insulation and 10 mm of polystyrene, thermal resistance of $0.74\,\mathrm{K}\cdot\mathrm{W}^{-1}$.
4. 26 mm of Armaflex® insulation, thermal resistance of $0.83\,\mathrm{K}\cdot\mathrm{W}^{-1}$.

5. 26 mm of Armaflex® insulation and 10 mm of polystyrene, thermal resistance of $1.1\,\mathrm{K}\cdot\mathrm{W}^{-1}$.

6. 50 mm of polyurethane expanded foam insulation, thermal resistance of $2.1\,\mathrm{K}\cdot\mathrm{W}^{-1}$.

While the final still design made use of 40 mm Isoboard insulation, which when applied to the still has a thermal resistance of $1.5\,\mathrm{K}\cdot\mathrm{W}^{-1}$ calculated for a unit area of the still, the results could not be compared to the experiments described here due to the difference in the material of construction of the still body.

Table 3 shows the experiments done with different insulations where the configuration number refers to the list above.

Table 3: A summary of the experiments done with varying insulation thicknesses and types.

	Configuration	1	2	3	4	5	6
Experiment 1	Still 1	✓					
	Still 2		✓				
	Still 3						
Experiment 2	Still 1			✓			
	Still 2		✓				
	Still 3						
Experiment 3	Still 1					✓	
	Still 2		✓				
	Still 3						
Experiment 4	Still 1				✓		
	Still 2				✓		
	Still 3						✓

Each experiment was run for a minimum of five days in order to ensure repeatability of results.

The second set of tests done to reduce energy losses was the redirection of energy from the sides of the still to the water using 2 mm aluminium sheets as internal reflectors. In Section 2.3.6 internal reflectors are discussed with their primary purpose being to direct more solar irradiation onto the water. However, in the experiments done the main intention of utilising the aluminium as an internal reflector was to lower the temperature of the sides of the still by redirecting the energy to the water. This was in order to reduce conductive losses from the sides and better utilise the energy.

Still 2 was the reference still and remained unmodified in these experiments while Still 1 ran for five days with the aluminium added only to the back wall, and five days with the aluminium added to the sides and back of the still.

It should be noted that throughout all of the experiments described in this section the absorber surface of all three stills was the Durapond waterproofing.

3.2.3 Increasing Evaporation Rate

In order to increase the evaporation rate different materials were added to Still 1 to modify the amount of solar irradiation which would be absorbed by the water, Still 2 was the reference still and remained unchanged throughout the experiments.

The first test which was done was changing the absorber in Still 1 to black PVC tarpaulin. This material is less reflective than the Durapond waterproofing and was expected to improve the performance. Experiments were run comparing Still 1 and 2 for four days sequentially, and repeatedly between each additional modification that was made resulting in a total of twenty days comparing the two different absorber materials. The PVC tarpaulin was also added to Still 3 at a later point in time. Still 4 was built with the PVC tarpaulin as the absorber material from the beginning as a result of the observations made in the previous experiments.

The second test involved the addition of a carbon black nanofluid. The nanofluid was tested previously by Bester (2017) and the method of preparation described by Bester (2017) was used. As discussed in Section 2.3.11 nanofluids have been shown to have a positive effect on the performance of basin solar stills due to the improved rate of heat capture and absorbance. Based on the work done by Bester (2017) a nanofluid with a 0.005 % volume concentration of carbon black was selected for testing.

The nanofluid was prepared by coating the carbon black, REGAL® 400R carbon black sourced from CABOT, nanoparticles with TWEEN-20, a non-ionic surfactant, in a 1:2 carbon black to surfactant mass ratio. These particles were then added to a synthetic sea water solution of $35\,\mathrm{g}\cdot\mathrm{L}^{-1}$ of NaCl in water and sonicated for 60 min. A concentrated masterbatch was produced like this and was later diluted to the required concentration. Reference samples were left in the laboratory under approximately constant temperature conditions to observe the nanofluid over time, specifically watching for settling of particles. This was the control to compare the nanofluid behaviour against.

The nanofluid was analysed using particle size analysis in a Mastersizer Hydrosizer 3000 (Malvern Instruments, Malvern, UK) before and after being used in the still in order to

determine the presence of agglomerates in the fluid as well as variations in the particle size distribution over time. Agglomerate formation is the primary indicator of nanofluid degradation and a good indicator of the stability of the fluid. The nanofluid was also analysed in a T60 UV-VIS spectrophotometer (PG Instruments Limited, Leicestershire, UK) to observe the absorbance of the fluid. This was done using a spectral scan between the wavelengths of 190 nm and 1100 nm, a blank was run simultaneously with the samples to correct for the instrument background. Changes in absorbance could also be used give an indication of the stability of the fluid; whether or not the particles remained dispersed.

The required volume of nanofluid was added to Still 1 and experiments run for three days sequentially.

The third test involved the addition of activated charcoal to Still 1. Activated charcoal has a large surface area which aids absorbance of solar irradiation, and increases the rate of heat transfer from the absorber to the water. The irregular shape and surface can also reduce reflection back out of the still. A mass of 1 kg of activated charcoal particles, varying in size and shape, were added to the still. The experiments were run for five days sequentially.

The final test was the addition of a 12.7 mm carbon felt to Still 1. The felt floated beneath the surface of the water increasing the area for evaporation as the surface of the felt was coated by a very thin layer of water and the fibrous nature of the material still visible. This test was run for four days comparing Still 1 and 2. This utilises the ideas behind a suspended absorber mentioned in Section 2.3.4.

3.2.4 Increasing Condensation Rate

The experiments focused on improving condensation were performed in Still 3. The experiments focused on increasing the area for condensation as well as improving the driving force for condensation by decreasing the cover temperature.

The first test involved increasing the internal area of the cover by milling grooves into the PMMA. The grooves are shown in Figure 9. The grooves were semi-circular with a diameter of 3 mm, each groove had a length of 480 mm and 24 grooves were milled in total. This resulted in an increase in internal area of 0.02 m^2, a 4 % increase in area.

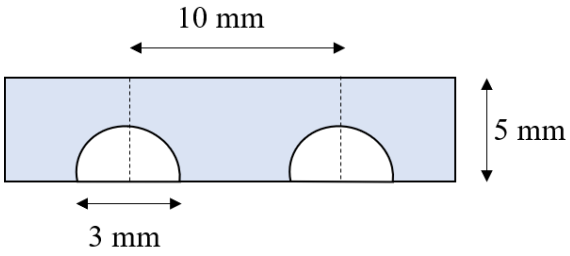

Figure 9: A cross section of a portion of the cover plate showing the dimensions of the grooves which were milled into the cover plate.

It was unknown whether or not the grooves would have a negative effect on the still, possibly due to increased reflectance of incident radiation. Possible advantages, additional to the increased area, were the increased scattering of light expected on the inside of the still as well as increased adhesion of drops which formed in the grooves. These experiments were run for nine days and the performance of Still 2 and 3 compared.

The following test involved the addition of two aluminium heat sinks to a portion of the top of the cover. The geometry of the heat sink can be seen in Figure 10. The contact area between each heat sink and the cover was $0.0105\,\mathrm{m}^2$, making the total contact area $0.021\,\mathrm{m}^2$. The heat sinks were partially shaded to reduce the temperature of the metal. This was added to the same cover plate that had been milled, after the previous set of experiments had concluded. Tests were run for thirteen days in this configuration.

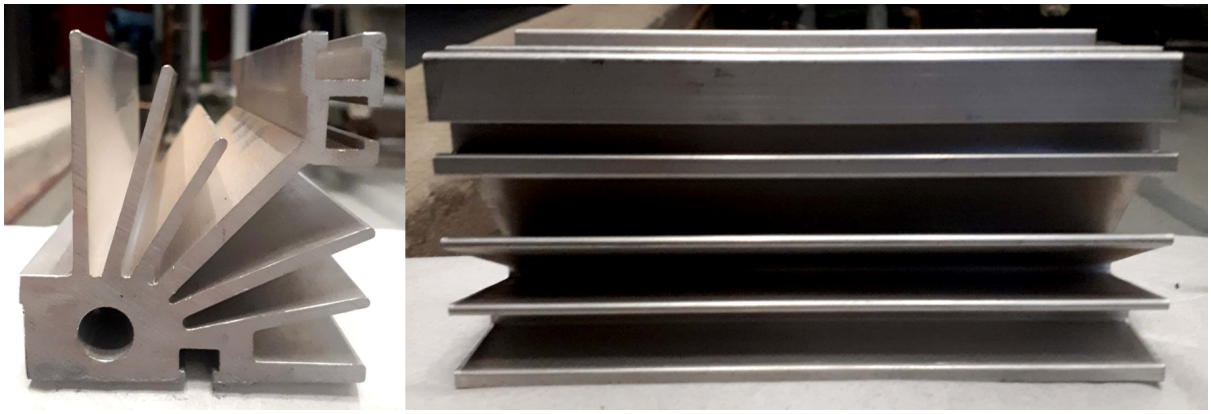

Figure 10: The geometry of the heat sinks that were added to the cover, length of a single heat sink was 150 mm, height and width both 70 mm.

A crude test was done by manually tapping the cover to force drop movement. The cover was tapped approximately every 30 minutes when possible, hourly otherwise, from the time that the surface was covered with water droplets. This was done for three days intermittently during the experiments with the heat sink added to the cover.

To increase the external condensation area two aluminium tubes, each of length 840 mm and internal diameter of 12.7 mm, were added to the back of the still. The tubes had an inlet and outlet at the top and bottom of the still, with an additional pipe draining to the condensate collection. This is shown in Figure 11.

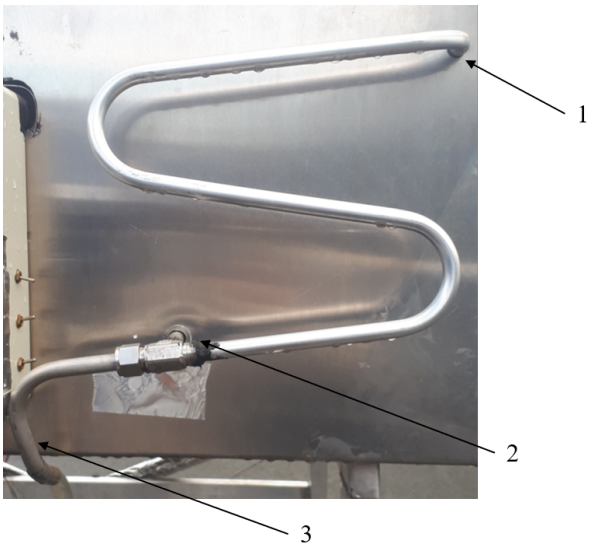

Figure 11: Picture showing one of the external tubes added to the still. The outlet from the still is shown at 1., 2. shows the inlet to the still, and 3. is the pipe collecting the condensate.

3.2.5 Revised Design

As mentioned, Still 4 was designed using information gained over the duration of the project. Still 4 was run for several days and its performance compared to that of the existing stills to evaluate the effect which the design modifications had.

3.2.6 Summary of Experiments

All four stills were built with the same internal dimensions, the differences in base designs of the still are shown in Table 4.

Table 4: A summary of the differences between the base designs of the four stills.

		Still 1	Still 2	Still 3	Still 4
Still body	18 mm ShutterPly	✓	✓	✓	
	40 mm Isoboard				✓
Cover	5 mm PMMA	✓	✓	✓	✓
Absorber	Durapond waterproofing	✓	✓	✓	
	PVC Tarpaulin	✓[a]		✓[a]	✓
Insulation/	26 mm Armaflex®	✓	✓		
Outer Layer	50 mm Polyurethane foam			✓	
	18 mm ShutterPly				✓

[a] Due to deterioration of the Durapond, the Durapond in Still 1 was replaced with PVC Tarpaulin after the first set of tests involving the carbon black nanofluid and in Still 3 at the start of the tests involving external tubes for condensation.

In all experiments done, aside from the insulation experiments detailed in Table 3, Still 2 remained unchanged from the base design summarised in Table 4. The list below summarises the changes made to the remaining stills for each of the experiments described in Section 3.2.1 to Section 3.2.5.

1. Baseline Experiments
   Stills 1, 2, and 3 used for comparison. Stills were run with the base designs as given in Table 4.

2. Reducing Energy Loss

   2.1 Insulation: Stills 1, 2, and 3 used for comparison. See Table 3 for detailed summary of changes.

   2.2 Internal Reflectors: Still 1 and Still 2 were compared. Still 1 had aluminium sheeting added first to the inside back wall, and then to the side walls.

3. Increasing Evaporation Rate

   3.1 PVC Tarpaulin: Still 1 and Still 2 were compared. Still 1 had the Durapond absorber replaced with PVC tarpaulin.

   3.2 Carbon Black Nanofluid: Still 1 and Still 2 were compared. Still 1 effective absorber material was the carbon black nanofluid.

3.3 Charcoal: Still 1 and Still 2 were compared. Still 1 effective absorber material was the activated charcoal.

3.4 Carbon Felt: Still 1 and Still 2 were compared. Still 1 effective absorber material was the carbon felt.

4. Increasing Condensation Rate

4.1 Grooved Cover: Still 2 and Still 3 were compared. Still 3 had grooves milled into the cover plate.

4.2 Heat Sink: Still 2 and Still 3 were compared. Still 3 had heat sinks added to the top of the milled cover plate.

4.3 Tapping on Cover: Still 2 and Still 3 were compared. Still 3 had the cover (with grooves and heat sinks) tapped regularly.

4.4 External Tubes: Still 2 and Still 3 were compared. Still 3 had tubes attached to the back of the still creating external condensation area.

5. Revised Design
Still 2 and Still 4 were compared. Stills were run with the base designs as given in Table 4.

3.3 Methods

3.3.1 Experimental Procedure

All experiments were carried out on the roof of Engineering Building 2 at the University of Pretoria, the different stills were placed next to each other, all facing the same direction. The stills were always run in parallel to allow for comparison between the stills using data collected on the same day. The stills were started each morning as early as possible, the start up procedure was as follows:

1. Begin the logging of weather data using the microbit-weatherbit.
2. Clean the inside and outside of the cover plates.
3. Fill each still with the required 9.2 kg of water and close the stills.
4. Calibrate the load cells on each still with a 4 kg calibration mass and the respective zero weights.
5. Begin logging data for the stills.

6. Add 0.2 kg of water to each collection container to act as a baseline measurement.

It should be noted that the stills were not emptied and filled with the complete 9.2 kg every single day, this happened every week or two, or when changes were made to the still. Instead, the stills were filled each day with the required amount to make up for the water lost, they were simply topped up to the 9.2 kg. A mass of 9.2 kg was selected as this results in a water depth of 20 mm in the still which was the minimum practical depth to ensure accurate measurements of water temperatures in the still.

Before start up, the data from the previous day would be collected from the SD cards and the final volumes of condensate measured to check accuracy of the load cells.

3.3.2 Data Analysis

Analysis and post processing of the measured data was done using Python.

The load cell data was adjusted, using the baseline measurement, and any spikes in the data that occurred due to wind or sensor noise removed. These points were found by checking the difference between sequential data points and setting the point to the previous value if the difference exceeded 20 g (Differences between load cell readings do not typically exceed 3 g, points with a large difference were due to external interference in the measurement). Due to the instantaneous nature of the erroneous values, the frequency at which measurements were taken, and the slow rate of change of the load cell date, this was an acceptable technique to apply. This data was also smoothed using a moving average smoothing technique, the smoothed data was only used in locating the point at which the curvature of the graph changes significantly indicating an effective onset of condensate collection. The change in curvature was found by calculating the second derivative of the curve, starting at a guess value and moving both forwards and backwards in increments to find the point with the highest second derivative; this approach proved to be robust for variability in the data sets and was accurate to within 10 min on average.

Rates of change of the condensate mass (which can be considered to be the rate of condensation) as well as of various temperature measurements were calculated. This was done by taking a time increment, assuming a linear change in the variable of interest during the increment, fitting a straight line to the data points in that increment using least squares linear regression techniques, and obtaining the slope of that line. Different increment sizes could be used to ensure linearity within the range. The reason for not using a common numerical differentiation method such as Newton's method was that noise in the data made taking discrete points difficult as one erroneous point would have

a huge effect on the derivative, using a regression technique to reduce the effect of noise was preferable.

All integrals were calculated numerically using the midpoint rule; due to the small time steps it was deemed sufficiently accurate and its simplicity made it an attractive solution. Integrals were used to determine total energy content of incident radiation as well as the totals for the various losses that were calculated at discrete time points over the course of the day.

Certain of the DS18B20 chip sensors gave erratic errors during operation due to corrosion of the soldered joints or simply damaged or wet connections. These errors could be dealt with by predicting the correct value using asymmetric least squares signal correction algorithms (Eilers, 2003). For days where certain sensors were completely non-functional, some of the values could be predicted using relationships between variables that were observed in the system. For example, it was observed that a linear relationship exists between the air temperature within the still and the temperature of the cover plate. Using days where the cover plate sensors were operating correctly an equation for this relationship could be obtained using linear regression techniques and used to predict the temperature on other days. This relationship can be observed in Figure A.3 in Appendix A for a selection of days.

Each day was assigned a numerical value representing the amount of incident solar irradiation that it received. This fraction could be used to compare yields across vastly different days by dividing the mass produced by the fraction of irradiation for that day. This was to ensure that results for varying amounts of incident irradiation could be compared, within reason, and the results would not be biased.

Where percentage increases in yield were calculated the following equation was used:

$$Yield\ Increase = \frac{Yield_{(still\ i)} - Yield_{(reference\ still)}}{Yield_{(reference\ still)}} \tag{22}$$

In Section 4, all data labelled corrected yield increase was calculated according to the following method.

1. The baseline yield increase for the relevant still was obtained.
2. The predicted yield of Still i was calculated using the baseline yield increase and the yield of the reference still.
3. The corrected yield increase was calculated according to Equation 23.

$$Corrected\,Yield\,Increase = \frac{Yield_{(still\,i)} - Predicted\,Yield_{(still\,i)}}{Predicted\,Yield_{(still\,i)}} \tag{23}$$

3.3.3 Energy Balance Analysis

It is necessary to explicitly define the control volume selected for the energy balance. This is shown in Figure 12 where the dotted red line indicates the boundary of the control volume. As can be seen in Figure 12, the cover, and the body of the still are included in the control volume while the insulation material is not.

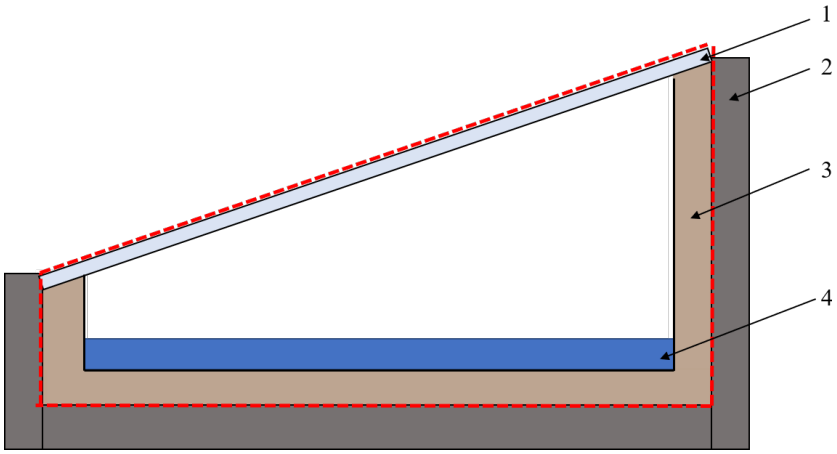

Figure 12: A cross section view of the basin still showing the control volume for the energy balance. 1. is the cover plate, 2. the insulation, 3. the wooden still body, and 4. the water in the still.

As data was collected minutely, the energy balance as shown in Equation 17 could be solved in the following way:

$$\int_{t_0}^{t_n} d(mU)_{cv} = \int_{t_0}^{t_n} \left(\dot{Q}_{net} - \dot{m}_{out}H\right) dt \tag{24}$$

$$\Delta(mU)_{cv} = \sum_{i=0}^{n-1} \left[\frac{\dot{Q}_{net}^{(i)} + \dot{Q}_{net}^{(i+1)}}{2}(t_{i+1} - t_i) + \frac{\left(H^{(i)} + H^{(i+1)}\right)}{2}\left(m^{(i+1)} - m^{i}\right)\right] \tag{25}$$

where t_n refers to the time at the end of the experiment and t_0 to the beginning. The internal energy, $\Delta(mU)_{cv}$, was separated into its various components and each one calculated as follows:

$$\Delta(mU)_{water} = {m_{water}}^{(n)}{U_{water}}^{(n)} - m_{water}^{(0)}U_{water}^{(0)} \tag{26}$$

$$\Delta(mU)_{air} = m_{air}C_{v_{air}}\left(T_{air}^{(n)} - T_{air}^{(0)}\right) + m_{air}\left(\mathcal{H}_{abs}^{(n)}U_{water}^{(n)} - \mathcal{H}_{abs}^{(0)}U_{water}^{(0)}\right) \tag{27}$$

$$\Delta(mU)_{cover} = m_{cover}C_{p_{cover}}\left(T_{cover}^{(n)} - T_{cover}^{(0)}\right) \tag{28}$$

$$\Delta(mU)_{wood} = m_{wood}C_{p_{wood}}\left(T_{wood}^{(n)} - T_{wood}^{(0)}\right) \tag{29}$$

Due to the fact that the mass of air, essentially, remains constant, the mass of wood is constant, and the mass of the cover is constant, the (ΔmU) terms could be solved without difficulty.

The internal energy change of the system when the energy balance is applied over the whole day is rarely significant when compared to the other terms present in the energy balance. This is due to the start and end temperatures being almost the same, internal energy is a state variable so if the change in temperature over the whole process is negligible the change in internal energy will be negligible too. A positive value for the internal energy change indicates that energy was accumulated in the wood, water, cover, or air and not released to the surrounding environment. This accumulated energy is not useful energy as it could not be used to produce condensate. If the change in internal energy is negative then that energy can be considered as energy that was made available to contribute to condensate production. The values for U_{water} and H were obtained from Lemmon, McLinden & Friend (2018). The condensate leaving the system is assumed to leave the system at the temperature of the cover, this is a good assumption as the air temperature in the still is higher than the cover temperature so it is unlikely that the condensate will be at a lower temperature, it is a conservative value for the energy of the condensate.

The $\dot{Q}_{out}$ term included in $\dot{Q}_{net}$ considered the reflection of incident irradiation from the cover, the radiative and convective losses from the cover, conductive losses from the still body, and radiative losses from the still base. This is shown in Equation 30. Radiative losses from the inside walls of the still were not considered.

$$\dot{Q}_{out} = \dot{Q}_{ref,cover} + \dot{Q}_{rad,cover} + \dot{Q}_{conv,cover} + \dot{Q}_{cond,body} + \dot{Q}_{rad,base} \tag{30}$$

Based on the defined boundaries of the control volume the conductive losses from the cover were not required, nor were convective or radiative losses from the outside of the still body. It should further be noted that the cover losses were calculated based on the internal surface temperature of the cover which is a few degrees warmer than the outside surface, this results in the cover losses being slightly overestimated. The cover temperature is remarkably difficult to measure accurately as it is in direct sunlight. The cover sensors were covered with a reflective tape to try and reduce the amount of sunlight

heating up the sensor directly, however this is not a perfect solution as the tape heats up due to not being perfectly reflective. Additionally, poor contact between the sensor and the cover surface can result in a higher temperature being measured.

The conductive losses were obtained using Fourier's law in Equation 1 with the correct thicknesses, areas, and thermal conductivities. A linear temperature gradient was assumed through the insulation in order for the equation to be simplified to

$$\dot{Q}_{cond} = \frac{-kA\Delta T}{x} \tag{31}$$

where x is the thickness of the material. All conductive losses were calculated using this equation.

The convective losses were found from Equation 2 obtaining h_{conv} from the relevant Nusselt relation using the temperatures and wind speed. The cover surface was assumed to be a flat plate to simplify the solution of the convective heat transfer coefficient. As a consequence of the flat plate assumption it was necessary to modify the wind speed, based on the wind direction, to account for the actual geometry of the system. If the direction of the wind was such that it would hit the back wall of the still first the wind speed was multiplied by a factor between 0.5 and 0.75, depending on if it was perpendicular to the back or at a slight angle. This was to compensate for the flat plate equations not considering how the wind speed would change if it were to hit the back of the still and be redirected downwards over the cover.

The radiative losses were calculated using the Stefan-Boltzmann law for radiation in Equation 9. The temperature of the sky was taken to be 6 °C below the ambient temperature (C Elango *et al*, 2015). For the radiation from the base of the still, the base and cover were assumed to be parallel surfaces and the transmittance of the cover was taken into account.

In the energy balance analysis, an unaccounted energy term was calculated as

$$E_{un} = \int_{t_0}^{t_n} \left(\dot{Q}_{net} - \dot{m}_{out} H \right) dt - \int_{t_0}^{t_n} d(mU)_{cv} \tag{32}$$

A positive value for the unaccounted energy could mean that the losses are underestimated (larger losses reduce the value of $\dot{Q}_{net}$), while a negative value could mean the reverse, an overestimation of the losses. Possible explanations for unaccounted energy include the radiative losses from the sides of the still which are excluded from the calculations, the overestimation of losses from the cover due to using the higher temperature to calculate these terms. Re-evaporation from the collected condensate could contribute to the unaccounted energy as this would mean an underestimation in condensate energy.

And finally the assumptions made in calculating the loss terms: no temperature gradients across the surfaces in the still, a linear temperature gradient through the walls, cover, and insulation, and the flat plate assumption and wind speed modifications for the convective losses.

The different loss terms, energy of condensate, and unaccounted energy were expressed as percentages of the total energy where the total energy was calculated as

$$E_{total} = \int_{t_0}^{t_n} \dot{Q}_I dt - \int_{t_0}^{t_n} d(mU)_{cv} \tag{33}$$

These percentages were used in the discussion to discuss the different losses on different days.

The efficiency was calculated slightly differently from Equation 21 which only considers the incident irradiation as energy which can be utilised to produce condensate. The efficiency of the still was calculated as

$$\eta = \frac{\sum_{i=0}^{n-1} \left[\left(m^{(i+1)} - m^i \right) \lambda_{vap} \right]}{E_{total}} \tag{34}$$

in order to account for the production of water overnight due to energy stored in the system.

4 Results and Discussion

4.1 Observations from Experiments

During the several months of experimental work there were various observations made during the operation of the stills that are necessary to note.

Condensate began forming on the covers within minutes of closing the stills. The droplet size increased until the drops began running consistently down the cover every few seconds. As soon as a drop had run and cleared the area in its path, condensate reformed on this area immediately, drop formation could be observed in real time.

All of the stills had problems with drops dripping back into the stills from the cover. If the drop began to run from the top half of the cover it would become too large to adhere to the cover and would fall back into the still before reaching the channel where condensate was collected. Counting, for a few minutes, the drops that ran all the way to the bottom and the drops that fell into the still indicated that for every drop collected a portion of another drop could be lost. This was for the period of time when the cover was most saturated with large drops, when smaller drops exist on the cover there is less water for them to collect as they run down and fewer drops are lost in this manner.

The Durapond sealant caused numerous problems. The surface looked like the sealant had bubbled (See Figure A.4 in Appendix A). It is unclear if this was due to poor adhesion of the sealant to the wood, the temperatures experienced inside the still causing degradation of the polyurethane sealant, air pockets trapped beneath the sealant, or solvent which had not evaporated properly when the sealant was drying. Regardless of the reason, the Durapond sealant began to leak at some point in time and had to be replaced with the PVC tarpaulin used in the later experiments. Due to the design of Still 3 the leak was not noticed until much later, this resulted in the polyurethane foam becoming wet and inconsistent results being obtained from a selection of experiments done in that still.

The collection channel in Still 1 and Still 2 was the aluminium U-channel shown in Figure 5. This channel did not allow for quick enough movement of water, a significant number of drops had to collect for the water to run properly through the pipes and to the collection system. This delayed movement of water could have resulted in a small portion of re-evaporation from the collection channel.

4.2 The Energy Balance

The energy balance analysis was used to understand the operation of the still and wherever possible to evaluate changes in performance when modifications were made.

Shown in Figure 13 is the energy balance analysis for a selection of days considering both sunny and cloudy days. The energy balance and energy term percentages were calculated as described in Section 3.3.3.

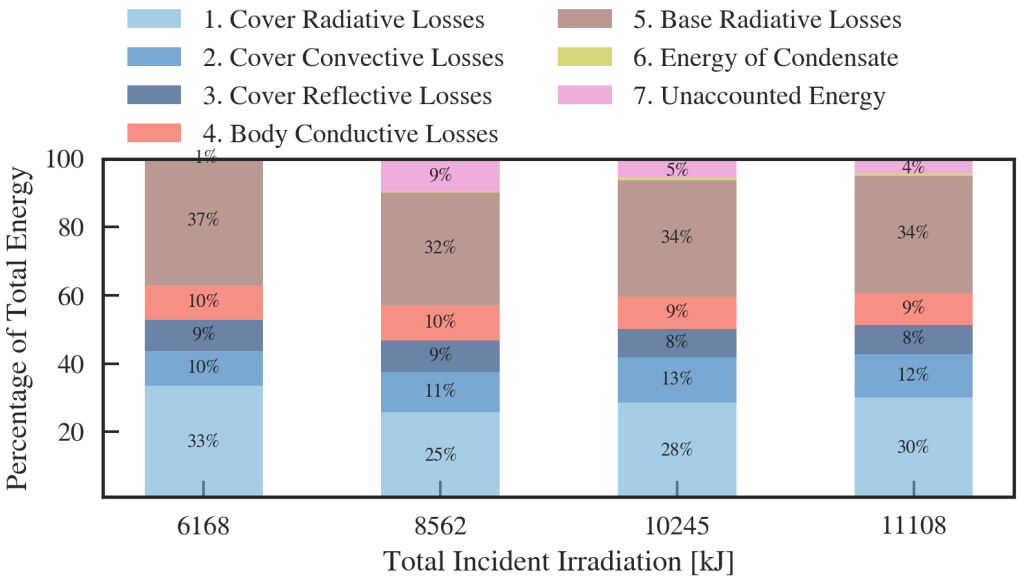

Figure 13: Energy balance analysis for Still 2 versus total daily solar irradiation seen by the still, considering the $0.5\,\mathrm{m}^2$ area, for a selection of days where the first two columns represent cloudy days and the last two show sunny days.

Immediately evident is the large portion of energy lost through radiation from the inside of the still, in excess of 30 %. As the base of the still is black to allow for maximum absorbance it has a correspondingly high emissivity, as discussed in Section 3.1.1, it is also one of the hottest surfaces in the system commonly reaching temperatures higher than 60 °C. It is not unexpected that it would account for such a large portion of the energy. Large improvements could be made if this radiation leaving the still could be blocked by the cover.

The cover losses consist of three parts and sum to around 50 % of the total energy on average. Excluding the reflective losses, a portion of this energy lost from the cover is necessary in order for condensation to occur. The heat transfer coefficients for condensation are in the order of magnitude of $200\,000\,\mathrm{W}\cdot\mathrm{m}^{-2}\cdot\mathrm{K}^{-1}$ for drop-wise condensation and $10\,000\,\mathrm{W}\cdot\mathrm{m}^{-2}\cdot\mathrm{K}^{-1}$ for film condensation (Çengel & Ghajar, 2015 pp. 618–627),

huge amounts of energy are transferred to the cover during condensation and must be removed from the cover for there to be a continued driving force for condensation.

The importance of being able to lose energy through the cover is illustrated in Figure 14. This Figure shows the condensate produced in Still 3 for two days, on day number 288 the still was left to operate normally, on day 289 the cover plate was insulated with 40 mm of Isoboard insulation after the sun had set. From the graph the absence of any condensate formation after the addition of the Isoboard is easy to see by the negligible slope from the point at which the Isoboard was added. This small slope indicates a negligible rate of condensation.

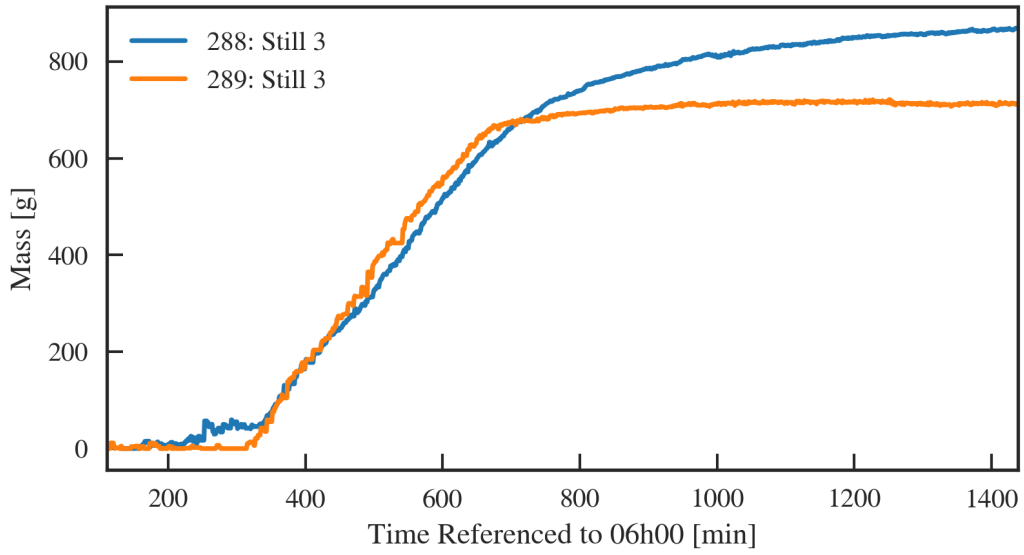

Figure 14: Mass of condensate produced in Still 3 on two consecutive days showing the importance of cover losses. The x-axis shows the minutes that have passed since 06h00; e.g. 200 correspond to a time of 09h20, 400 to a time of 12h40, and 600 to a time of 16h00.

However, trying to characterise the useful portion of the cover losses is not trivial. The efficiency, calculated as described in Section 3.3.3, can be considered a rough descriptor of the amount of useful cover losses. For the four days shown in Figure 13 the efficiencies were 9.2 %, 8.5 %, 12.3 %, and 10 %. With the cover losses ranging from 36 % to 43 % (excluding reflection) it is clear that only a small portion of the cover losses was efficiently utilised in the system. The note made in Section 4.1 regarding condensate dripping back into the still should be kept in mind when comparing the efficiency and the cover losses; to produce condensate the energy must be lost from the cover, if the water is not recovered the calculated efficiency is lower than it could be if all the condensate had been collected.

It should be noted that the reflective losses are an underestimate. They are calculated

theoretically, as described by Kalogirou (2014 pp. 83–85), and only consider the reflection from the PMMA cover plate, it excludes the water droplets that collect on the cover. Early during the experiments an additional pyranometer was placed inside the still and the amount of radiation received on the inside and outside were compared. It was found that on average the total irradiation on the inside of the still was 21.5 % less than the irradiation incident on the outside of the still. This is significantly larger than the theoretical reflectance values seen in Figure 13 of 8 % and 9 %.

In Figure 15 the cover and base losses are shown for the course of the day. The convective losses are erratic due to the variation in wind speed, it is clear that larger wind speeds can greatly increase the convective losses from the still cover. The radiative losses from both the cover and the base of the still are high, reaching maximums near 100 W, and remaining consistently high due to the high system temperatures. The losses via reflection are significantly lower than both the radiative and convective losses, however, if these losses could be reduced further it could improve the performance of the still.

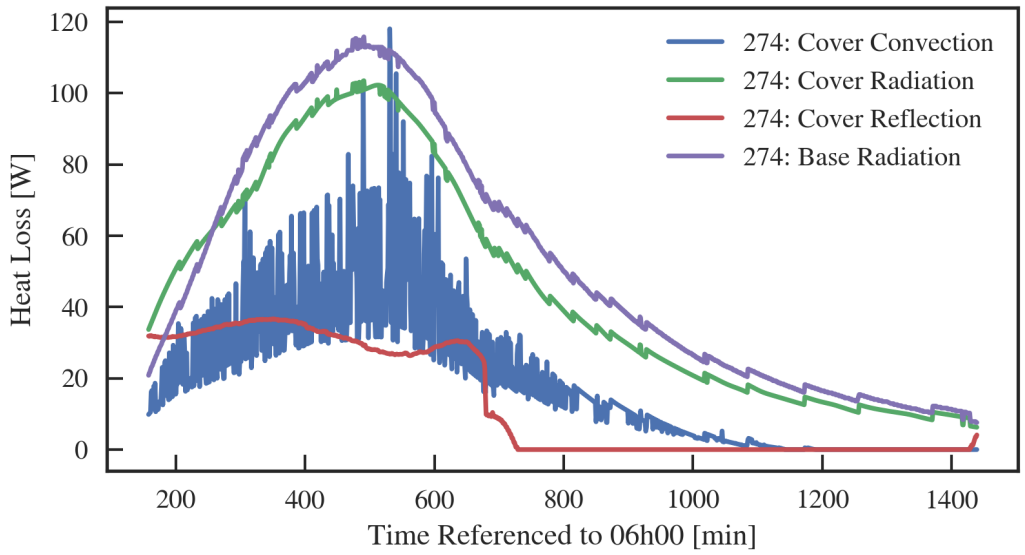

Figure 15: Losses from the cover plate plotted against time, for day number 274, a day representative of normal operation.

In Figure 13 the conductive losses are seen to remain relatively constant around 10 % of the total energy, there is little improvement that can be made on this that is cost effective and is discussed further in Section 4.5.1. Figure 16 shows the conductive losses from the still body for day 274, the last column in Figure 13. The conductive losses reach a maximum around 13 W, a near negligible value in comparison to the other energy terms. The back conductive losses could be reduced by reducing the area of the back wall or directing the energy away from the surface, but additional insulation on the still

body is not a cost effective solution considering the small amount of energy that could be gained.

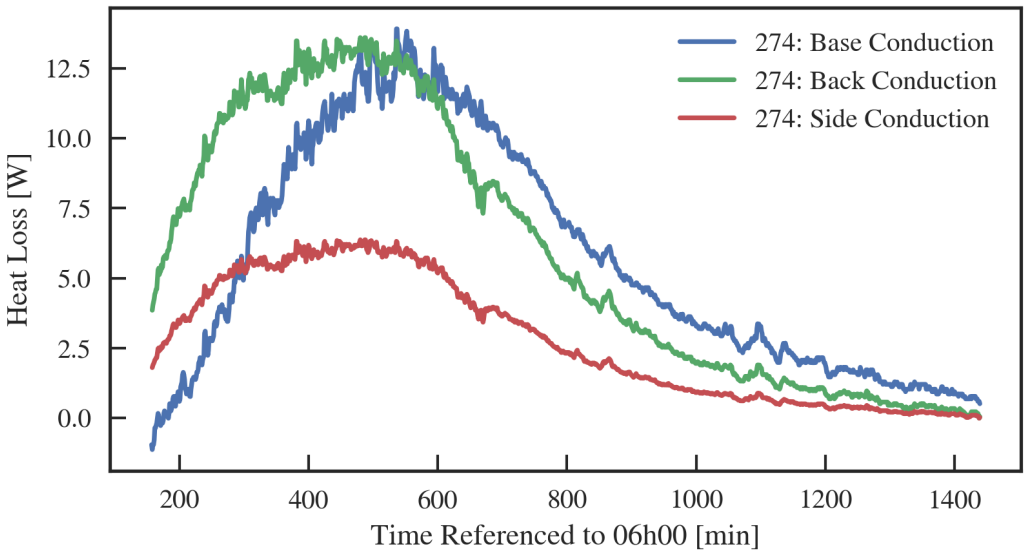

Figure 16: Losses from the still body plotted against time, for day number 274, a day representative of normal operation.

The energy removed from the system by the collected condensate is minuscule in comparison to the other loss terms and the total incident radiation.

Energy enters the system as solar radiation, and is lost through several surfaces through convection, conduction, and back-radiation. The energy that is absorbed by the water and which causes vaporisation is then transferred to the cover (and other surfaces of the interior of the still if condensation occurs there) when droplets form. The vast majority of this energy is then lost through radiation and convection from the cover. The fact that energy is only used once to vaporise a mass of water and then removed through losses from the cover is the reason that the total energy extracted in the form of condensate is so small.

Ideally, one would want the energy released during condensation to be re-used to evaporate more water. However, as the energy is at a lower quality (at a lower temperature) than the water in the still it cannot be re-used efficiently. Storing the energy and using it to reduce the heat loss of the still during the night is a potential method of re-using the energy released in condensation.

The unaccounted energy seen in Figure 13 is relatively small and can be explained with the various suggestions made in Section 3.3.3.

Figure 17 shows the incident solar irradiation over the course of the day. The maximum value nears 500 W on the 0.5 m^2 cover surface which is more than four times larger than any of the individual loss terms, there is more than enough energy available to produce water should the losses be efficiently managed.

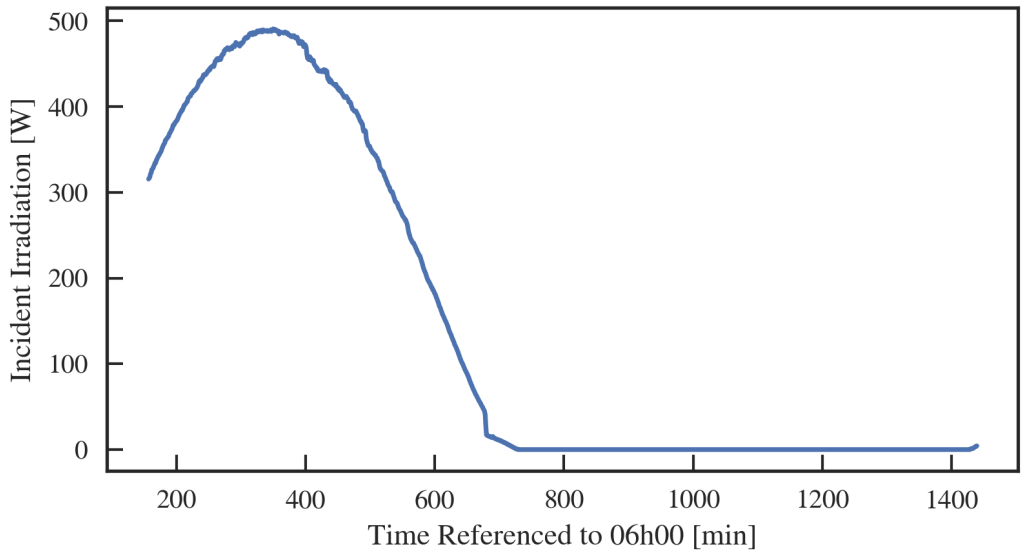

Figure 17: Incident irradiation, considering the 0.5 m^2 area, plotted against time, for day number 274, a day representative of normal operation.

The total efficiency for the day under consideration, was 9.95 %, calculated as described in Section 2.2 and Section 3.3.3. Figure 18 shows the efficiency for each 30 minute interval over the course of the day. The efficiencies during the night time period are significantly higher due to the lack of incident irradiation but continued production of water. This suggests that heat storage could greatly improve the performance of the still; the energy received during the day that cannot be efficiently used could be released back into the system over night to increase the production of water.

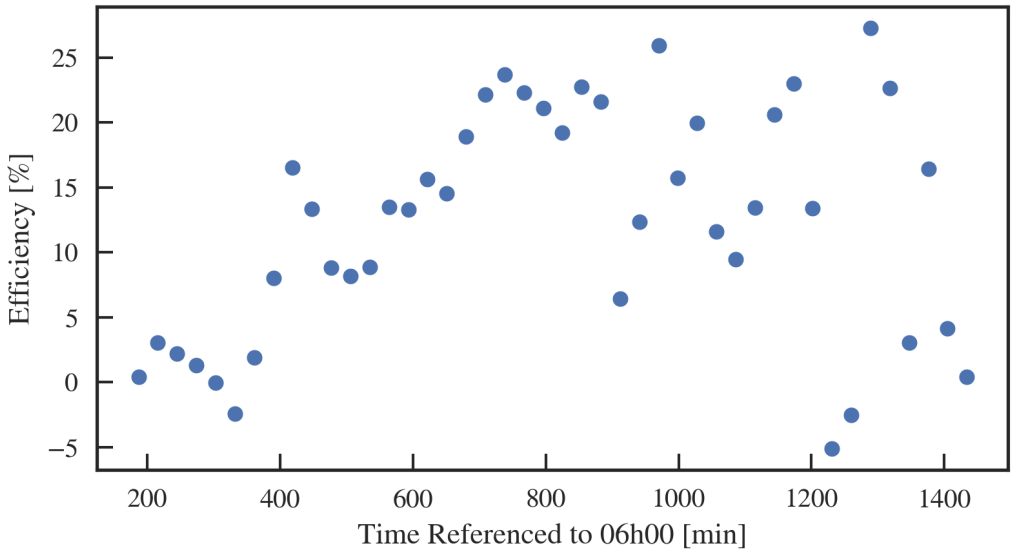

Figure 18: Efficiencies calculated for 30 minute intervals for day number 274, a day representative of normal operation.

4.3 Effects of Disturbance Variables

It is necessary to understand the effects which disturbance variables have on the performance of the still. These variables are the wind speed, wind direction, ambient temperature, and intensity of solar irradiation. Many of the independent variables in the system can be classified as disturbance variables making it even more important to understand their effects. The discussion in this section will focus primarily on the results from Still 2 as it remained unmodified throughout the entirety of the project and for that reason its results can easily be compared.

4.3.1 Ambient Conditions

Theory suggests that the wind speed will affect the convective heat losses from the cover plate and change the temperature of the cover. Wind speed and direction changes erratically during a day and characterising the wind behaviour over a day using simple averages or variances did not yield any direct observable correlations with still performance.

Figure 19 shows the amount of water produced in Still 2 as a function of the total solar irradiation received by the still in that day. The data points in Figure 19 are coloured based on the average daily ambient temperature with the dark red dots representing the warmest temperatures and the dark blue dots the coldest. The points with incident irradiation values in the excess of 14 000 kJ are possibly anomalies; the irradiation

measurements for several consecutive days was abnormally high, the measured values decreased again after this period. However, the linear relationship observed would support the validity of the points despite their large irradiation intensities.

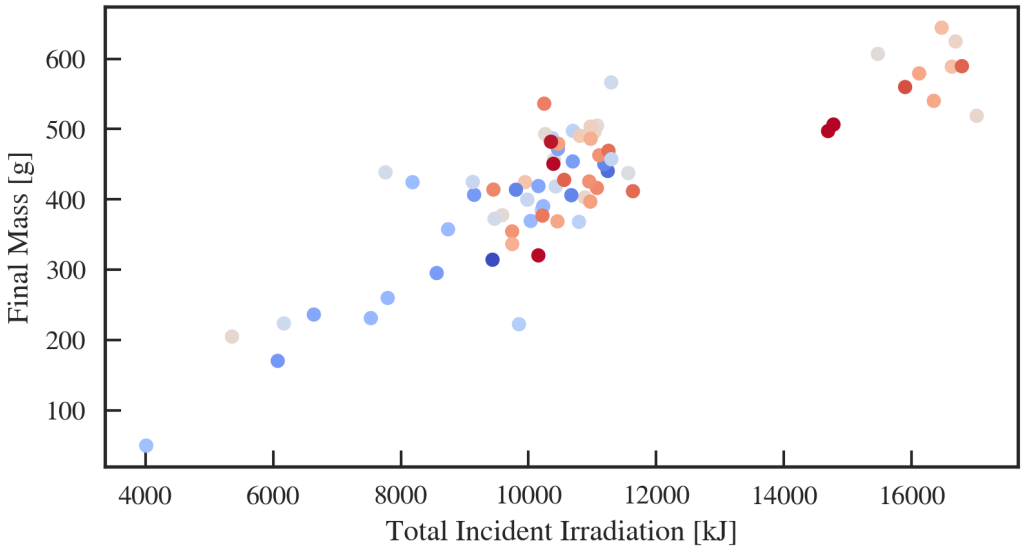

Figure 19: Mass of condensate versus total daily solar irradiation seen by the still, considering the 0.5 m^2 area, with dots coloured based on average daytime ambient temperature.

The data strongly suggests a linear relationship between the incident solar irradiation and the yield of the still. Considering the energy balance, the only energy that is added to the system is due to solar irradiation in the $\dot{Q}_{net}$ term, or a negative change in the internal energy of the system, hence the large effect which this variable has on the system. While Figure 19 shows that the days with the lowest yields experienced cooler temperatures than the days with the highest yields, there is no clear relationship that can be seen between the yield of the still and the ambient temperature. This is perhaps better illustrated in Figure 20.

In Figure 20 the yield of Still 2 is plotted against the average ambient temperature during daylight hours. A weak linear relationship between the two variables might be suggested, this would be in agreement with theoretical predictions. The ambient temperature is expected to have an effect on the heat losses included in $\dot{Q}_{net}$. These losses are functions of the ambient temperature, wind speed, and wind direction.

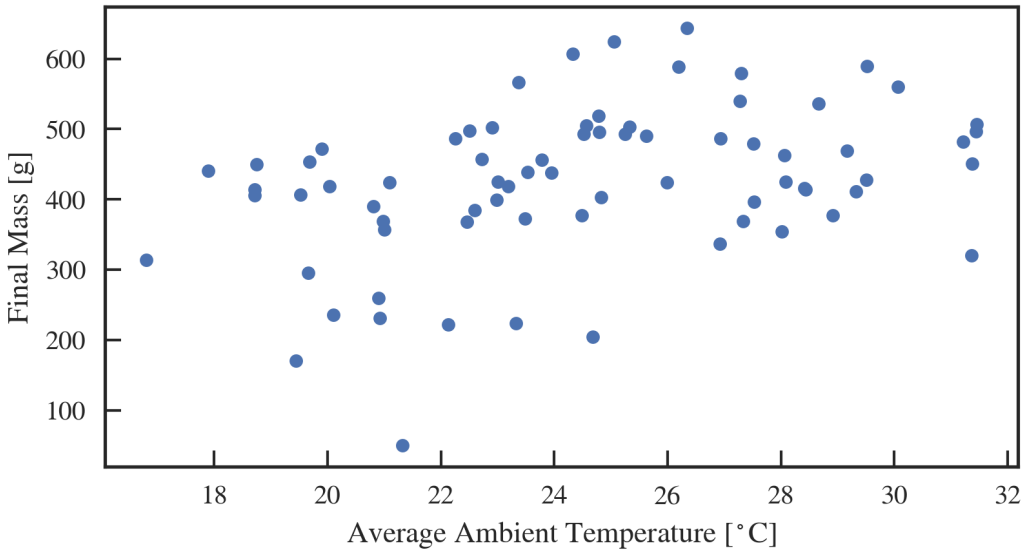

Figure 20: Mass of condensate versus average daytime ambient temperature.

Figure 21, shows that the radiative losses from the cover plate, as a percentage of the total energy, are also weakly influenced by the ambient temperature. This would be better seen by neglecting the outliers, the two points between 32 % and 34 % as well as the point around 20 %. A small upward slope in the radiative losses is seen as the average temperature increases. The radiative losses are the largest loss from the system and vary between 26 % and 32 % on average. Figure 22 suggests that the conductive losses from the still body may decrease as the average ambient temperature increases.

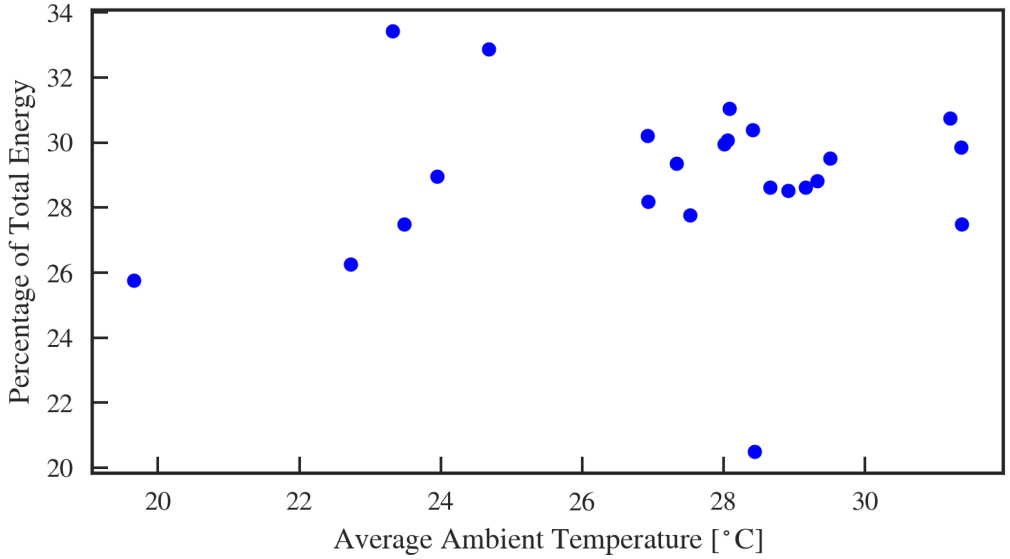

Figure 21: Radiative losses from the cover expressed as a percentage of the total energy entering the system, plotted as a function of the average daytime ambient temperature.

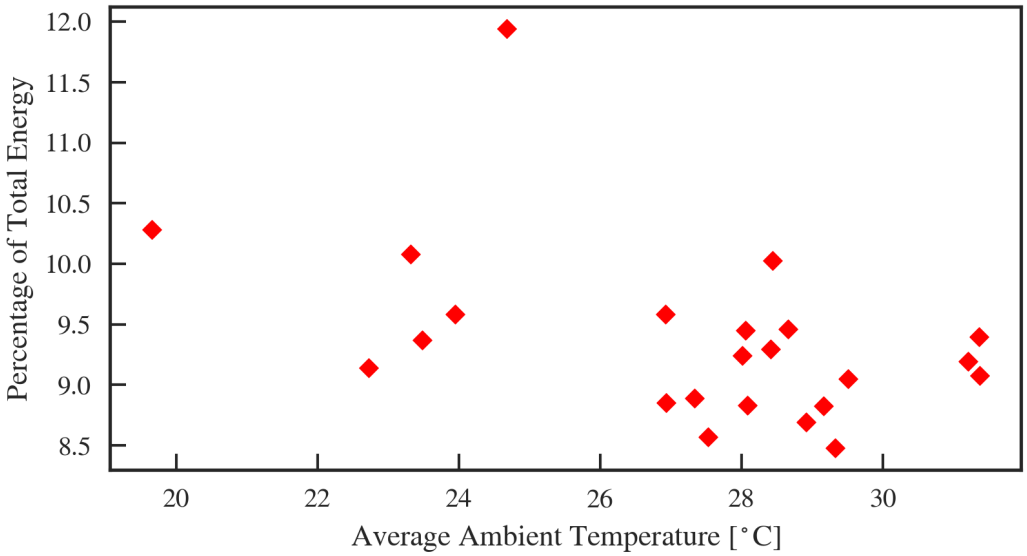

Figure 22: Conductive losses from the still body expressed as a percentage of the total energy entering the system, plotted as a function of the average daytime ambient temperature.

The other losses to consider are the convective losses from the cover plate as well as the reflective losses. The reflective losses are purely dependent on the intensity of incident irradiation, they are independent of ambient conditions, and the convective losses are likely to be strongly dependent on the wind speed and direction as previously mentioned.

Figure 23 shows the efficiency, calculated as described in Section 2.2, for the varying ambient temperatures. While the various loss terms are weakly dependent on the average ambient temperature, the effect which they have on the efficiency is insufficient for the efficiency to express any observable dependence on the temperature, this is seen in Figure 23. Due to the linear relationship between the amount of water produced and the amount of incident irradiation, the efficiency is seen, in Figure 24, to be mostly independent of the amount of incident irradiation seen by the still. It should be noted that there are limits to this independence. The outliers in Figure 23 and Figure 24 are from days where unusually low amounts of solar irradiation were present.

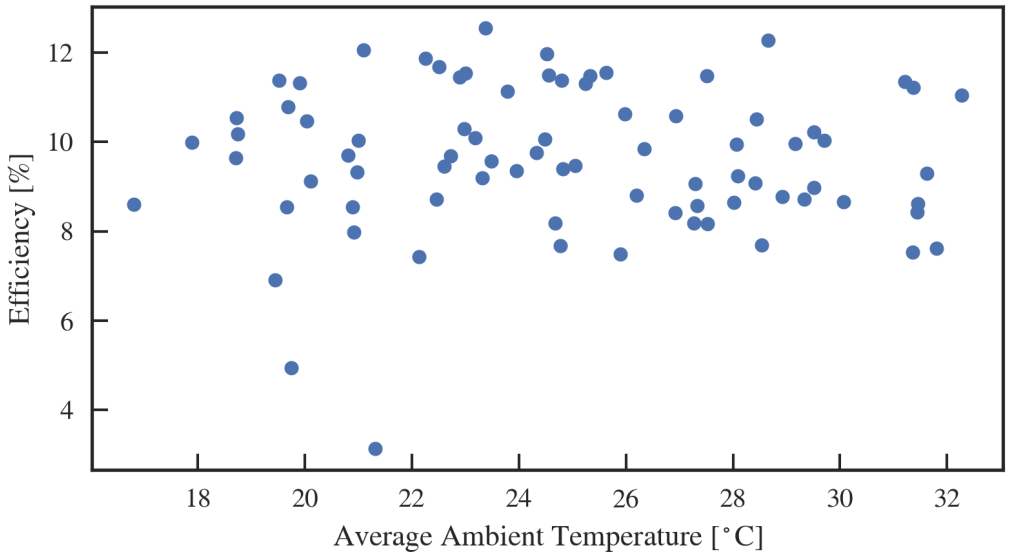

Figure 23: Efficiency of the still plotted as a function of the average daytime ambient temperature.

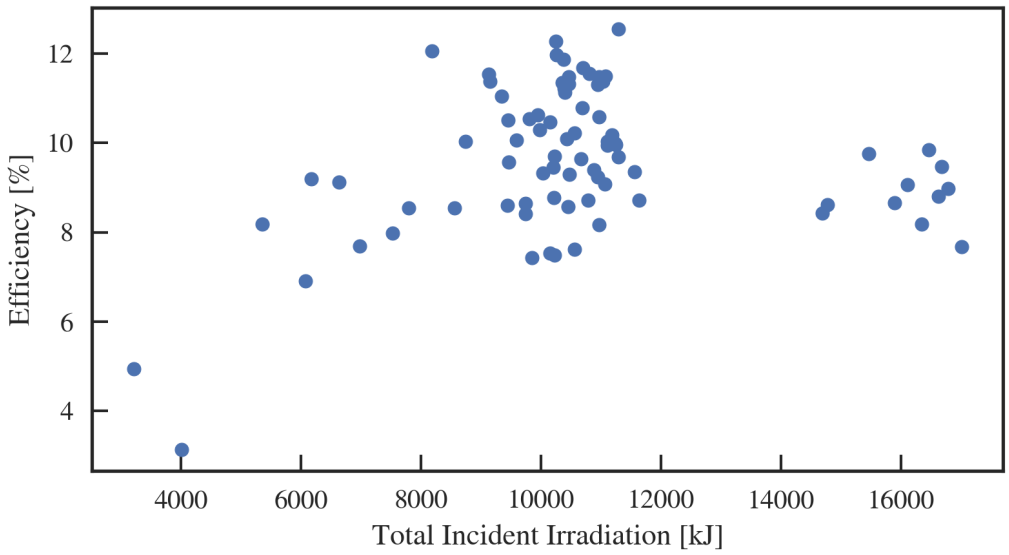

Figure 24: Efficiency of the still plotted as a function of the total incident irradiation, considering the $0.5\,\mathrm{m}^2$ area.

4.3.2 Seasonal Variation

Experiments were run from the 30^{th} of May up until the 2^{nd} of November. This spans the South African autumn, winter, and spring in that order. For this reason it is important to observe the effect of seasonal variation on the performance of the still.

Figure 25 shows the change in average daytime ambient temperature over the course of the year. The gradual change in season is immediately evident from the roughly 15 °C increase in temperature that can be observed.

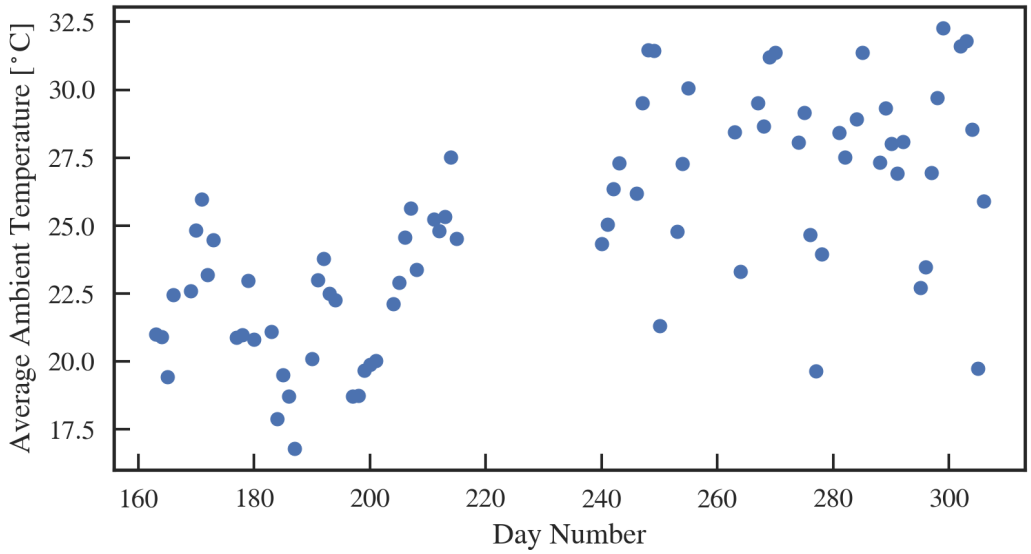

Figure 25: Average daytime ambient temperature plotted against day number to observe the change in season.

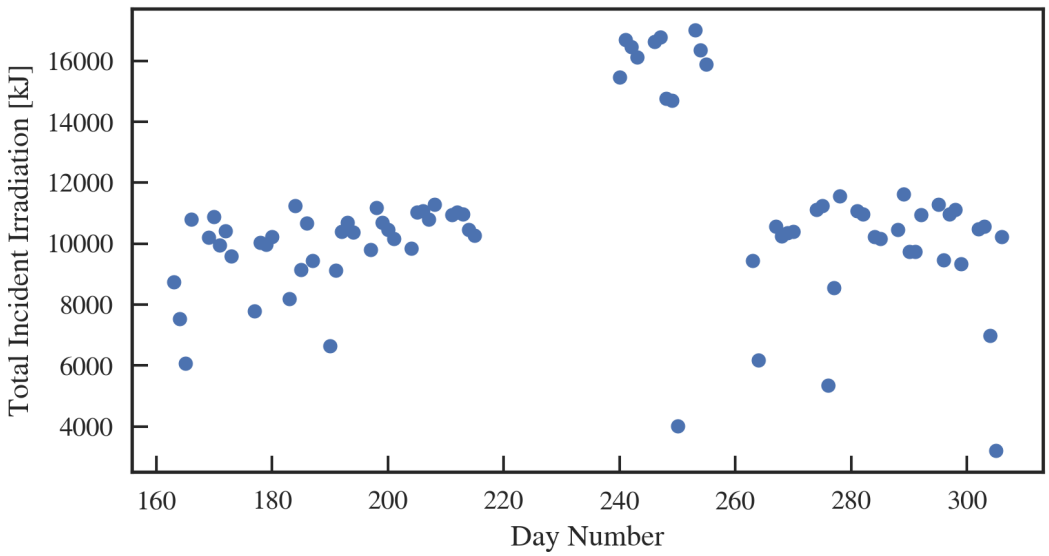

Figure 26: Total daily solar irradiation seen by the still, considering the 0.5 m^2 area, plotted against day number to observe the change in season.

Figure 26 however, does not show a strong correlation between the day of the year and the intensity of solar irradiation, this is expected as the pyranometer measures global short-wave radiation. The abnormally large amounts of radiation can be seen again between

days 239 and 254; clear anomalies in the amount of energy received by the stills, but producing results agreeing with the measured intensity as seen in Figure 19. In South Africa the winters are usually less cloudy while the summers are often very sunny which can account for the little seasonal variation in intensity of irradiation. Finally, Figure 27 shows the amount of condensate produced in Still 2 over the course of the year. Very little correlation is seen as is expected given the minimal change in incident irradiation and the strong relationship between the incident irradiation and the mass of water produced.

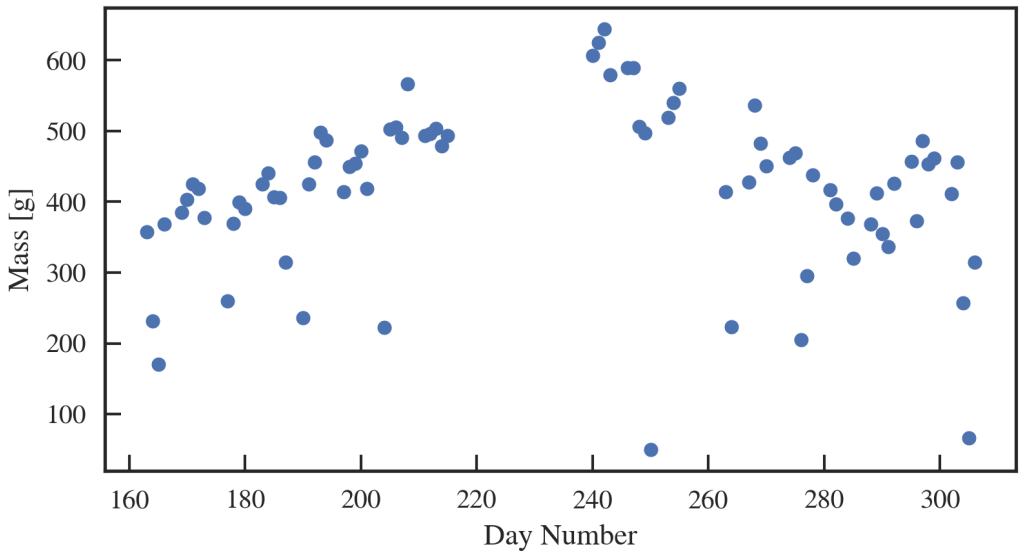

Figure 27: Mass of condensate plotted against day number to observe the change in performance over the change in season.

4.4 Baseline Experiments

Inherent differences exist in the stills as a result of small differences in materials of construction or inaccuracies introduced during construction. Baseline tests were run to determine the extent of these differences and to quantify the effect which they have on the performance of the stills to allow for comparison of results.

4.4.1 Still 1 Baseline

Early in the project the baseline tests were run for Still 1 and 2, as described in Section 3.2.1. Table 5 shows the final masses of water produced by each still as well as the improvement in yield when comparing Still 1 to Still 2.

Table 5: Efficiencies and Water Produced in Still 1 and 2 in the Still 1 Baseline Experiments.

Day Number	Still 2 Yield	Still 1 Yield	Increase in Yield	Still 2 Efficiency	Still 1 Efficiency
204	0.222 kg	0.250 kg	12 %	7.4 %	8.4 %
205	0.502 kg	0.587 kg	17 %	11.4 %	13.5 %
206	0.504 kg	0.595 kg	18 %	11.5 %	13.6 %
207	0.490 kg	0.562 kg	14 %	11.5 %	13.2 %
208	0.566 kg	0.586 kg	3 %	12.5 %	13.0 %
211	0.493 kg	0.571 kg	16 %	11.3 %	13.1 %
212	0.495 kg	0.571 kg	15 %	11.4 %	13.1 %
213	0.503 kg	0.594 kg	18 %	11.5 %	13.6 %
214	0.479 kg	0.586 kg	22 %	11.5 %	14.1 %

The difference remains within a reasonable tolerance and the average increase in yield was 17 % with a standard deviation of 3 %, excluding the outlier on day number 208. This difference was used when analysing future results to correct for the variations between the stills when they operated under the same conditions.

Figure 28 shows the energy balance analysis for Still 1 and 2 for a selection of days from the baseline experiment.

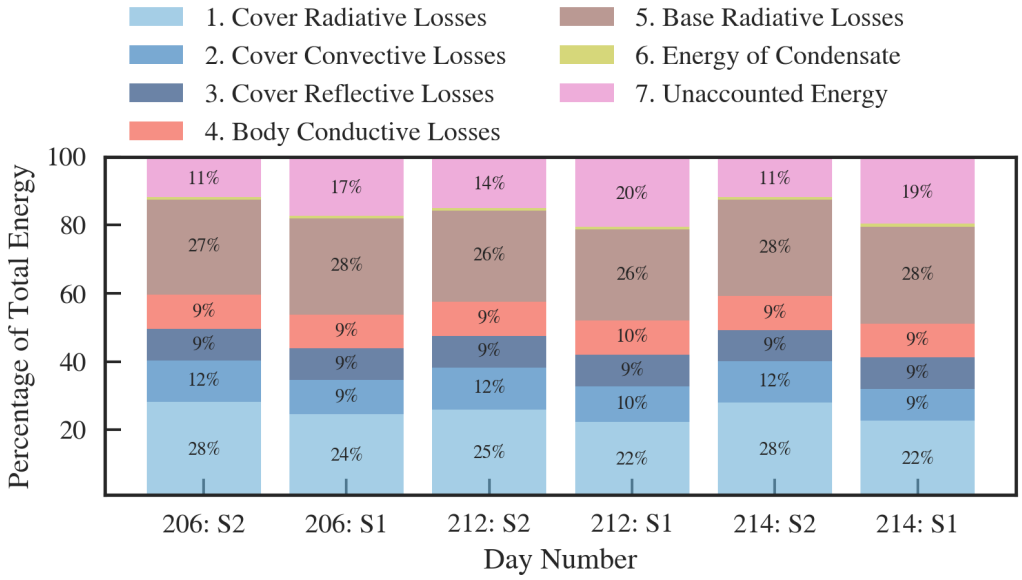

Figure 28: The energy balance for both Still 1 and Still 2 for a random selection of days during the baseline experiments.

The conductive losses do not appear to vary significantly between the two stills, and the reflective losses are calculated theoretically and cannot vary as they do not consider the condensate on the cover. The cover convective losses and radiative are slightly lower in Still 1 which is likely the reason for Still 1 producing more water. Figure 29 shows the cover temperatures for the two stills, Still 1 is seen to have a slightly lower cover temperature than Still 2 which explains the reduced cover losses seen in Figure 28. The difference in the maximum cover temperature ranges between 2 °C and 4 °C. An increased driving force for evaporation and condensation is present when the cover temperature is lower.

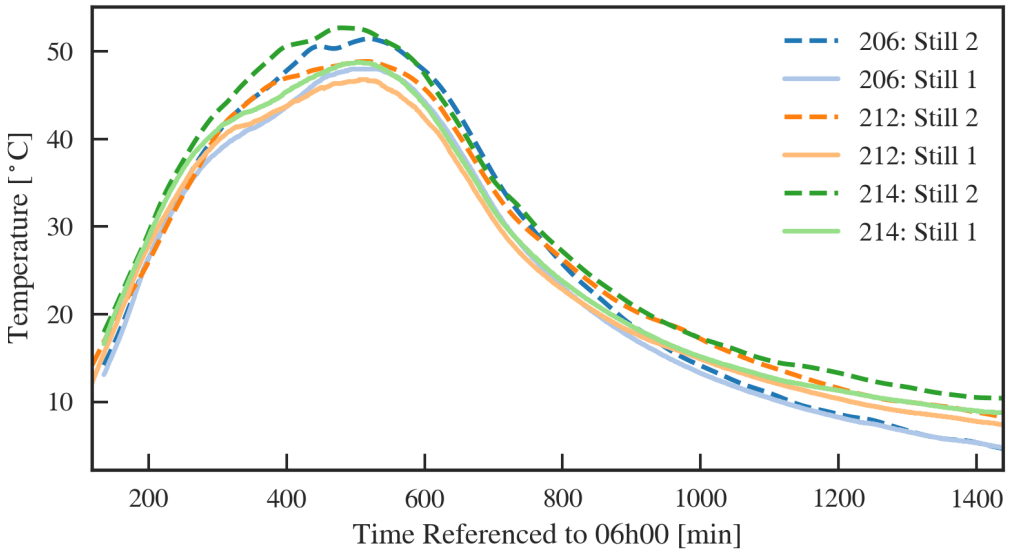

Figure 29: Cover temperatures for both Still 1 and Still 2 for a random selection of days during the baseline experiments.

Figure 30 shows that the water temperature in each still is nearly identical, this is important as many experiments done were focused on increasing the water temperature in the still. The similarity in water temperature explains the similar values for base radiation seen in the energy balance. If the water in each still is at the same temperature the base temperatures are approximately the same as well. Furthermore Figure 31 makes it clear that despite Still 1 producing more water than Still 2 the time at which the rate of condensate collection increases significantly remains approximately constant in both stills around 420 minutes after 06h00, at 13h00.

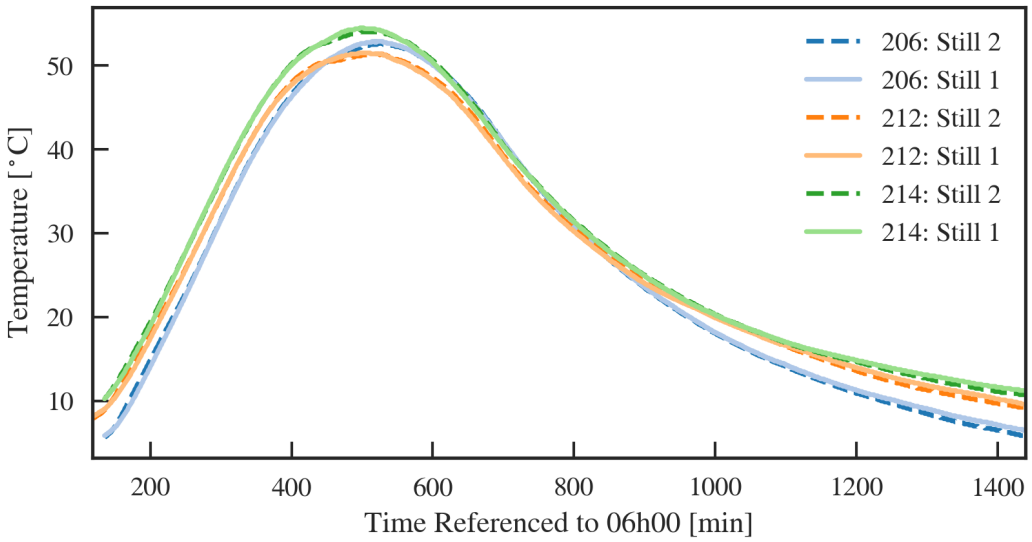

Figure 30: Water temperature for both Still 1 and Still 2 for a random selection of days during the baseline experiments.

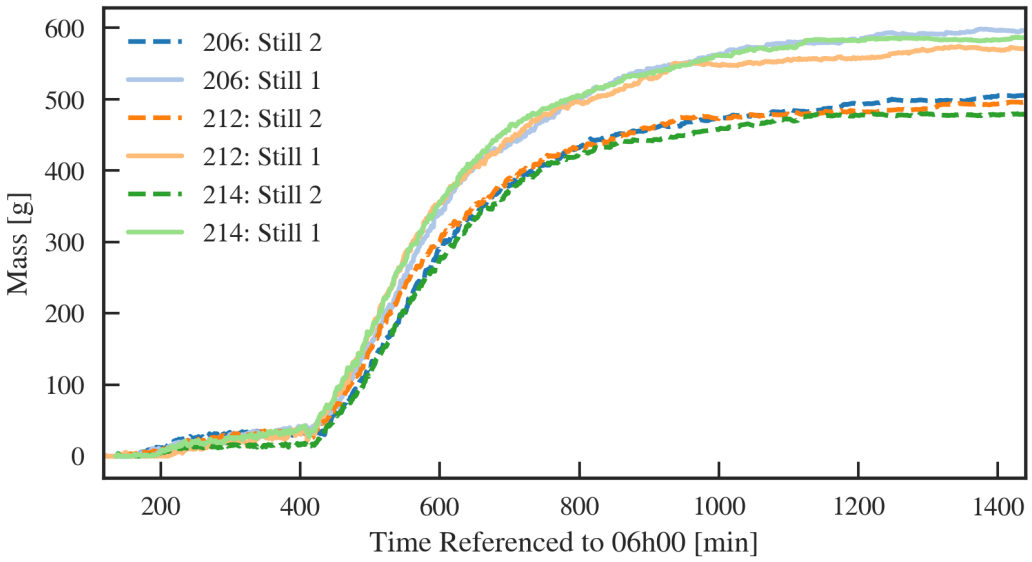

Figure 31: Mass of condensate versus time for both Still 1 and Still 2 for a random selection of days during the baseline experiments.

4.4.2 Still 3 Baseline

As described in Section 3.1.1, Still 3 differs from Still 2 in its insulation; while Still 2 uses 26 mm of Armaflex foamed Nitrile rubber insulation Still 3 is insulated with 50 mm of polyurethane foam. This affects the conductive losses from the still and the overall

performance. The effect of the insulation is discussed in detail in Section 4.5.1 but a brief discussion of the differences between stills 2 and 3 is included here.

Table 6: Efficiencies and Water Produced in Still 2 and 3 in the Still 3 Baseline Experiments.

Day Number	Still 2 Yield	Still 3 Yield	Increase in Yield	Still 2 Efficiency	Still 3 Efficiency
206	0.504 kg	0.744 kg	47 %	11.5 %	16.5 %
207	0.490 kg	0.657 kg	34 %	11.5 %	15.5 %
208	0.566 kg	0.694 kg	22 %	12.5 %	15.4 %
211	0.493 kg	0.670 kg	35 %	11.3 %	15.4 %
212	0.495 kg	0.648 kg	30 %	11.4 %	14.9 %
213	0.503 kg	0.661 kg	31 %	11.5 %	15.0 %
214	0.479 kg	0.628 kg	31 %	11.5 %	15.1 %
215	0.492 kg	0.606 kg	23 %	12.0 %	14.7 %

From the data in Table 6 an average improvement in yield of 32 % when comparing Still 3 to Still 2 is observed, with a standard deviation of 2 % when excluding the following outliers. Day 208, as mentioned previously, is an outlier in the data due to the unusually high yield of Still 2. The reasons for this are uncertain as the starting conditions in Still 2 were comparable with the other stills. Additionally day 206 saw a larger yield from Still 3 than on the other days; Still 3 had been freshly filled with water while Still 2 had been running an experiment the previous day, this resulted in the water temperature in Still 3 being roughly 6 °C higher than in Still 2 to begin with and can explain the high yield. Day 215 saw an unfortunate combination of higher than normal yield in Still 2 and lower than normal yield in Still 3 which caused an unusually low difference between the stills.

Figure 32 shows that the maximum water temperature in Still 3 is slightly higher than in Still 2, by approximately 2 °C, and Figure 33 shows the difference in condensation rate; the onset time for condensate collection did not vary by more than 10 minutes between the two stills.

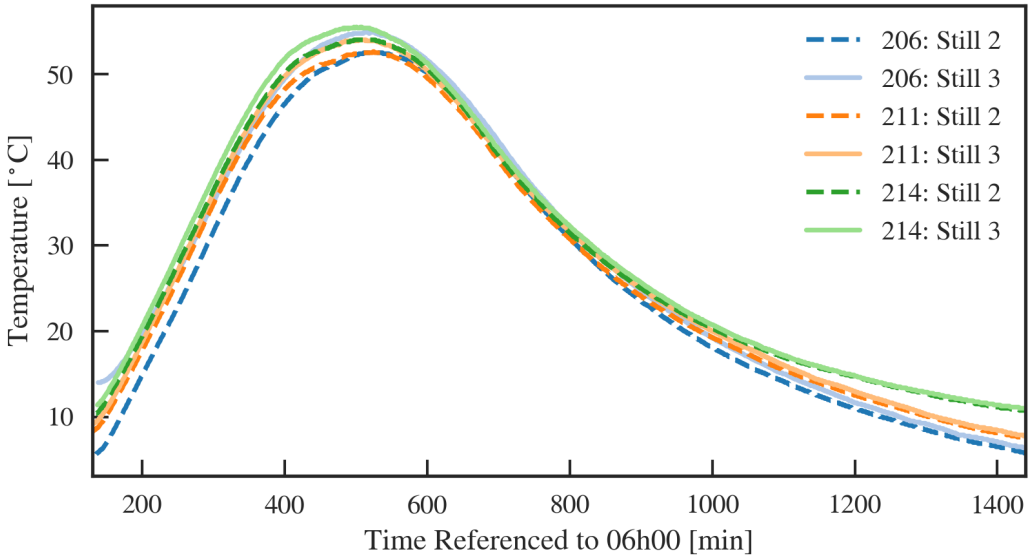

Figure 32: Water temperature for both Still 2 and Still 3 for a random selection of days during the baseline experiments.

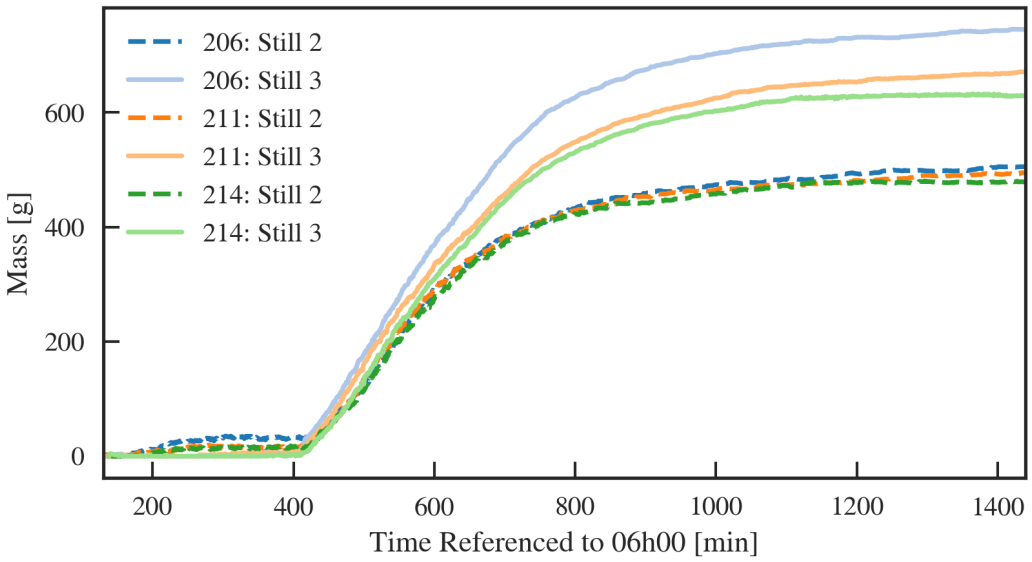

Figure 33: Mass of condensate versus time for both Still 2 and Still 3 for a random selection of days during the baseline experiments.

4.5 Reducing Energy Losses

From the energy balance analysis the relative magnitudes of the different loss terms can be seen. While some energy must be lost from the cover plate in order to allow for condensation to occur it is possible to try and reduce the conductive losses from the still

body. The following sections discuss the results from the experiments where the aim was to reduce the energy losses from the stills.

4.5.1 Insulation

Figure 34 shows the final mass of condensate produced in each still for each of the experiments described in Section 3.2.2, the experiment numbers in Figure 34 refer to those in Table 3. The final masses were corrected using the amount of solar irradiation received on a given day, as described in Section 3.3.2, to make the comparison easier.

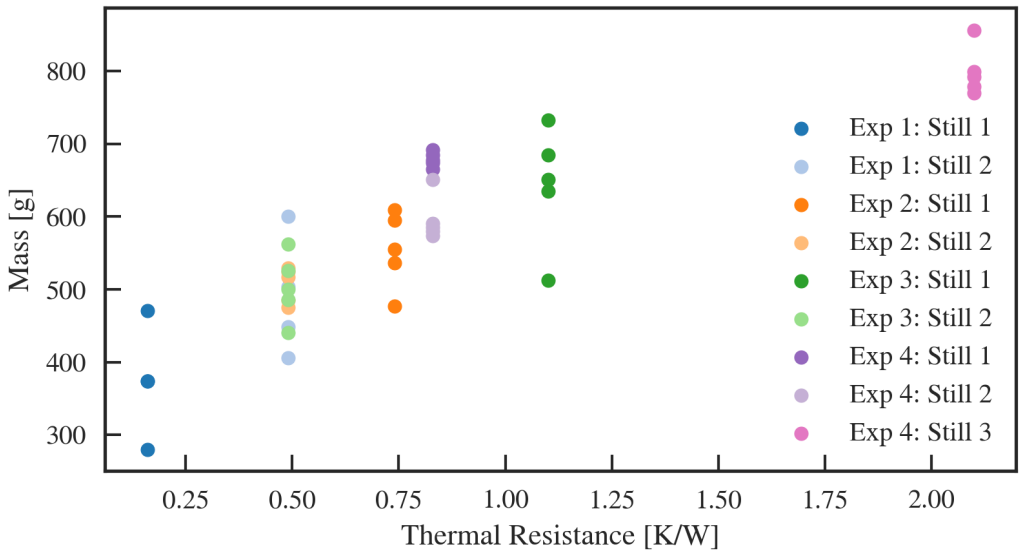

Figure 34: Mass of condensate plotted against the thermal resistance calculated for a unit area of the still, the masses have been corrected for the amount of incident irradiation received on a given day.

It is clear from Figure 34 that the higher thermal resistance results in a larger yield of condensate. However, diminishing returns are expected; at some point the effect which increasing the thickness of insulation has on the performance of the still is not large enough to compensate for the additional cost. This is perhaps better seen in Figure 35. In Figure 35 the change in thermal resistance for a given experiment is plotted on the x-axis and the resulting improvement in yield on the y-axis (Refer to Table 3 for the different experiment descriptions).

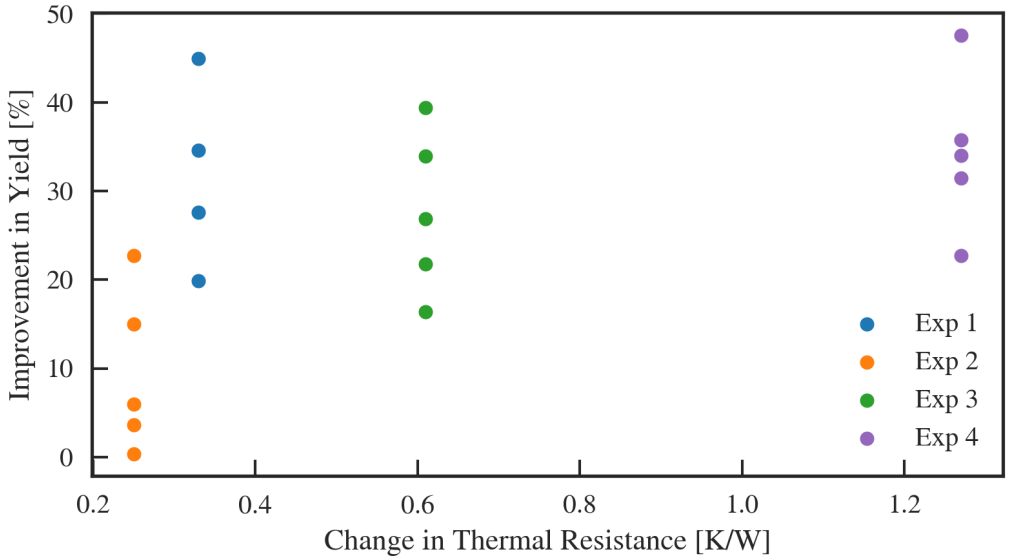

Figure 35: Percentage increase in yield for each day plotted against the corresponding change in thermal resistance between the different stills for each experiment set.

Experiment one, three, and four had vastly different changes in thermal resistance associated with each, but the improvement in yield shown in Figure 35 is comparable for all three of the experiments. Looking at Figure 34, as the thermal resistance changed from $0.16\,\mathrm{K}\cdot\mathrm{W}^{-1}$ to $1.1\,\mathrm{K}\cdot\mathrm{W}^{-1}$ the amount of condensate produced increased from around 0.4 kg to 0.65 kg. This is a large improvement in productivity for a sizeable increase in thermal resistance. However, increasing the thermal resistance from $1.1\,\mathrm{K}\cdot\mathrm{W}^{-1}$ to $2.1\,\mathrm{K}\cdot\mathrm{W}^{-1}$ only caused the yield to increase from 0.65 kg to 0.8 kg, the increase in yield is smaller for a larger increase in thermal resistance.

Figure 36 shows the condensate collection over time for a random day representing each thermal resistance. It can be seen that both the final mass of condensate and the rate of condensation increase as the thermal resistance is increased. This is expected, increasing the amount of insulation improves the energy retention capability of the system which should allow for accelerated evaporation and subsequently condensation. To comment on the energy retention the maximum water temperatures experienced by each still are seen in Figure 37.

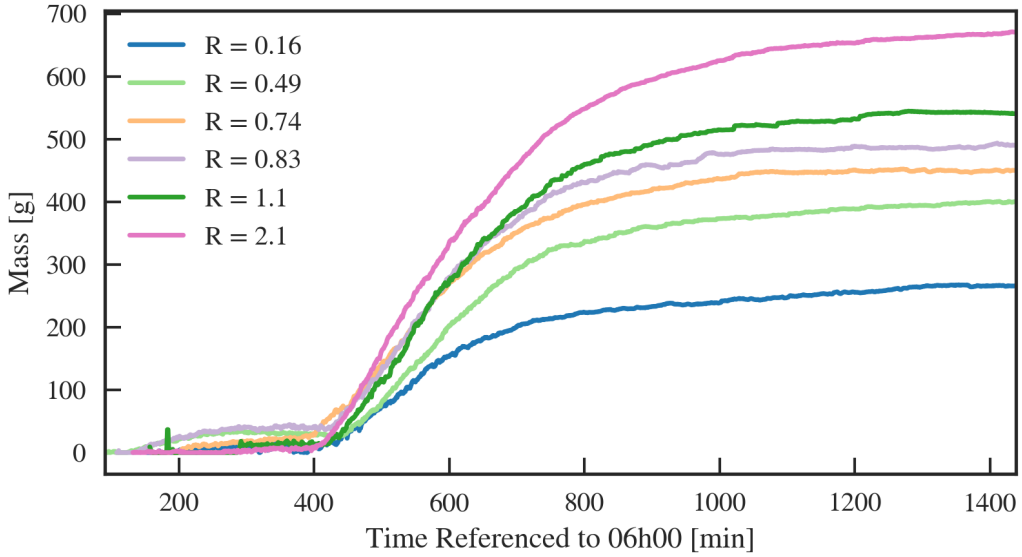

Figure 36: Mass of condensate for stills with specific thermal resistances, calculated for a unit area of the still, selected from various days over the course of the experiments.

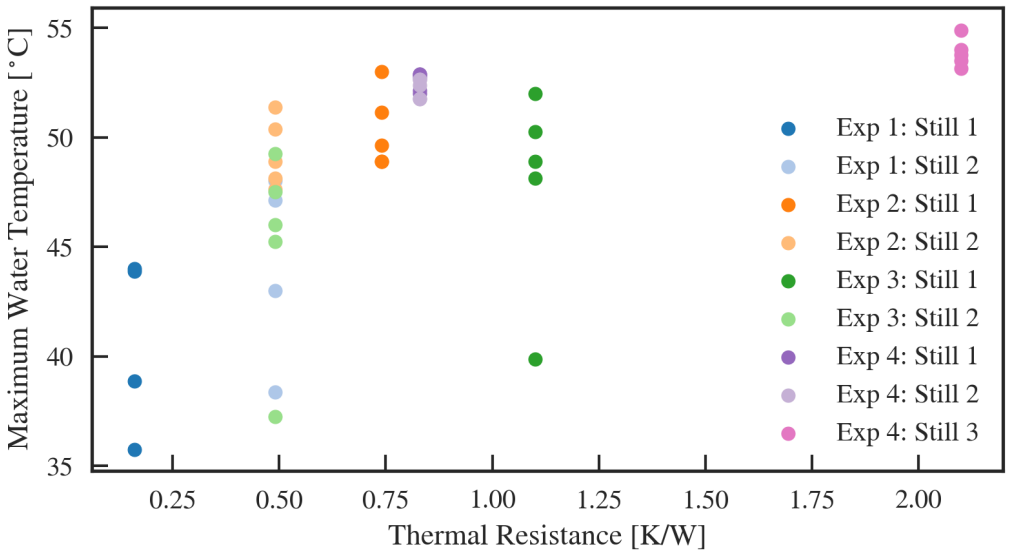

Figure 37: Maximum water temperature plotted against the thermal resistance calculated for a unit area of the still.

To some extent the maximum water temperature is seen to increase with an increasing thermal resistance, these temperatures could not be corrected in a similar fashion to the yield data to account for varying intensities of solar irradiation so it should be taken into consideration that the effect of the thermal resistance was not isolated in Figure 37. The outliers in experiments two and three are from days that experienced unusually low amounts of solar irradiation, up to 30 % less than the other days, due to cloud cover.

Despite the maximum water temperatures being low on those two days the difference between Still 1 and 2 is still observed.

4.5.2 Internal Reflectors

Aluminium was added to the back of the still in order to redirect energy from the back wall into the water and reduce conductive losses, Figure 38 shows how the back wall temperature was changed.

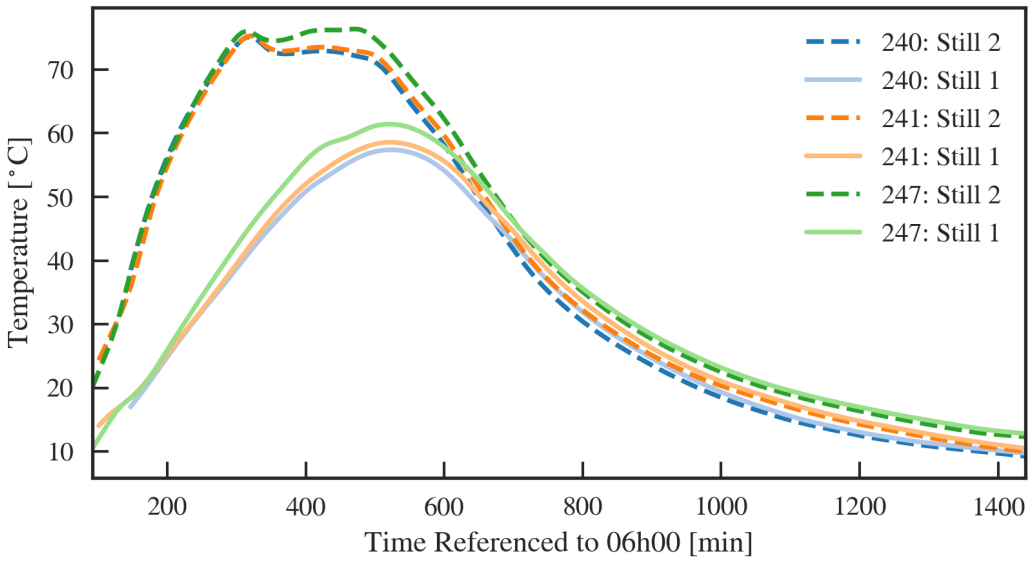

Figure 38: Temperature of the back wall of the still for days where aluminium was added to the back of Still 1, Still 2 was the reference still.

The temperature of the back wall was decreased by more than 10 °C when compared to the reference still, Still 2. Visual inspection of the stills during operation showed that condensate formation on the covers differed between Still 1 and Still 2. Still 1, having the aluminium panel, had condensate forming over the entire cover plate from early on while Still 2 took longer for condensate to form on the portion of cover nearest to the back wall. This can be seen in figures A.5 and A.6 in Appendix A. The energy balance for a selection of days where aluminium was added to the back of Still 1 can be seen in Figure 39.

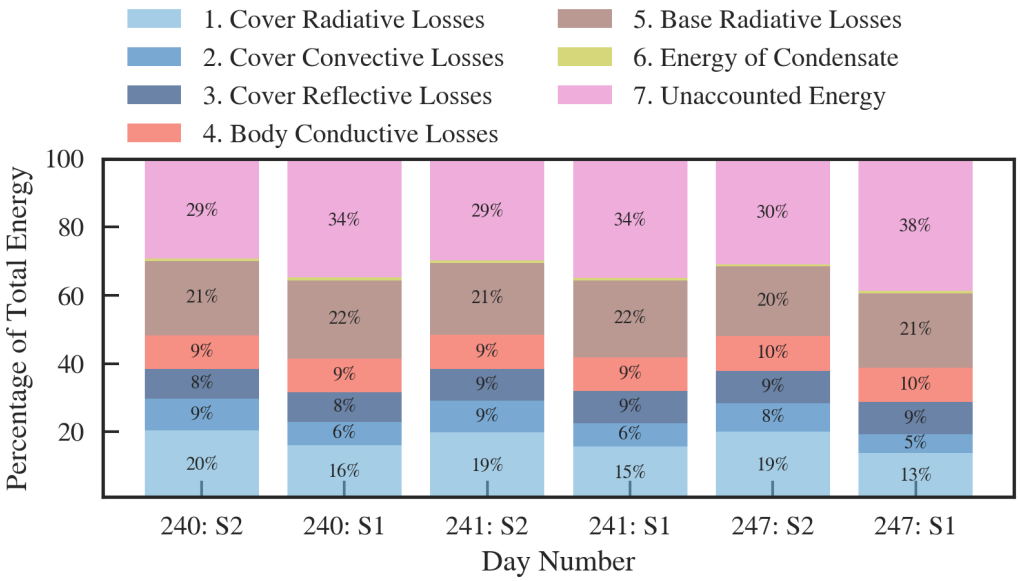

Figure 39: The energy balance for days where aluminium was added to the back of Still 1, Still 2 was the reference still.

The results from the energy balance do not differ greatly from the baseline tests shown previously in Figure 28 except for the significantly larger percentage of unaccounted energy in both of the stills. The cover losses are greater in Still 2 than in Still 1, and Still 1 has a higher amount of unaccounted energy. The unaccounted energy is probably due to reflection within the still. Previously, any light that was reflected from the surface of the water would likely meet one of the dark walls of the still. Given that the largest wall was now a reflective surface it is possible that this reflected light was reflected once more, up and out of the still.

Additionally, the reflective backplate would no longer absorb as much of the radiation emitted from the base as it previously would. Given that the radiation originates at the base of the still it is likely that much of it would be reflected up and out of the cover.

Looking at the effect which the addition of the aluminium had on the water temperature, in Figure 40. Considering that the approximate heat capacity of plywood is $1210\,\mathrm{J}\cdot\mathrm{kg}^{-1}\cdot\mathrm{K}^{-1}$ whereas the heat capacity of water is $4186\,\mathrm{J}\cdot\mathrm{kg}^{-1}\cdot\mathrm{K}^{-1}$ the large decrease in wood temperature (around 10 °C) for a relatively small increase in water temperature, 3 °C on average, is not unexpected. The lower water temperature in Still 1 in the evening can be explained by the absence of a significant amount of energy which would otherwise have been stored in the wood and released to the air in the still during the night.

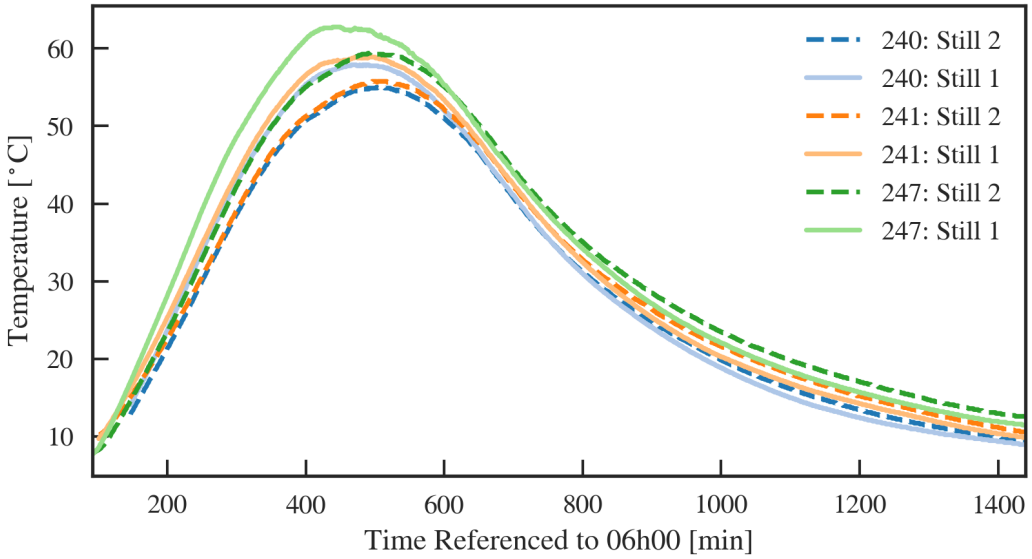

Figure 40: Temperature of the water for days where aluminium was added to the back of Still 1, Still 2 was the reference still.

Table 7 summarises the yields of the two stills as well as the change in performance due to the addition of the aluminium. The column containing the corrected increase in yield is calculated taking into account the inherent difference in performance determined during the baseline tests previously discussed in Section 4.4.

Table 7: Water Produced in Experiments with Back Reflectors.

Day Number	Still 2 Yield	Still 1 Yield	Increase in Yield	Corrected Yield Increase
240	0.606 kg	0.798 kg	31 %	12 %
241	0.624 kg	0.793 kg	27 %	8 %
247	0.589 kg	0.646 kg	9 %	−6 %

On days 240 and 241 the addition of aluminium proved beneficial to the performance of the still, but on day 247, after the aluminium had been in the still for several days, the performance of the still was hindered by the presence of the aluminium. This reflects the results observed in the energy balance analysis in Figure 39, and the efficiencies shown in Table 8. On day 247 from the energy balance in Still 1 it can be seen that there was an unusually large amount of unaccounted energy and reduced cover losses. Recall that a portion of the cover losses are necessary for condensation to occur, if the cover losses become too small condensation is less likely to occur. As the aluminium reflected the majority of incident radiation while the wood absorbed the energy, the aluminium was

typically at a significantly lower temperature than the wood when there was no incident irradiation. If the temperature of the aluminium was similar to that of the cover, where condensation was meant to occur, it is likely that condensation would have occurred on the aluminium and resulted in a decrease in yield due to that condensate being lost.

Oxidation of the aluminium over time increased the surface area by roughening it and adding nucleation sites for condensation. The presence of nucleation sites while being at a lower temperature promoted condensation; this condensate formation on the aluminium was observed during operation of the still. Additionally, as mentioned previously, the reflective surface may have reflected a portion of the energy out of the still instead of directing all the energy to the water resulting in a higher unaccounted energy than usual.

Table 8: Efficiencies for Experiments with Back Reflectors.

Day Number	Still 1 Efficiency	Still 2 Efficiency
240	12.7 %	9.8 %
241	11.9 %	9.5 %
247	9.8 %	9.0 %

When aluminium panels were added to the sides of Still 1 in addition to the panel on the back, the still performed significantly worse than when there was only aluminium on the back. Figure 41 shows the energy balance for these experiments. The energy balance in Still 1 looks much the same as it did on day 247 in Figure 39, large amounts of unaccounted energy and unusually low cover losses.

The yield result for these experiments are shown in Table 9, the progressive deterioration in the performance of Still 1 can be seen clearly in the decrease in improvement when referenced to Still 2 as well as the rapid decrease in efficiency of Still 1 in Table 10.

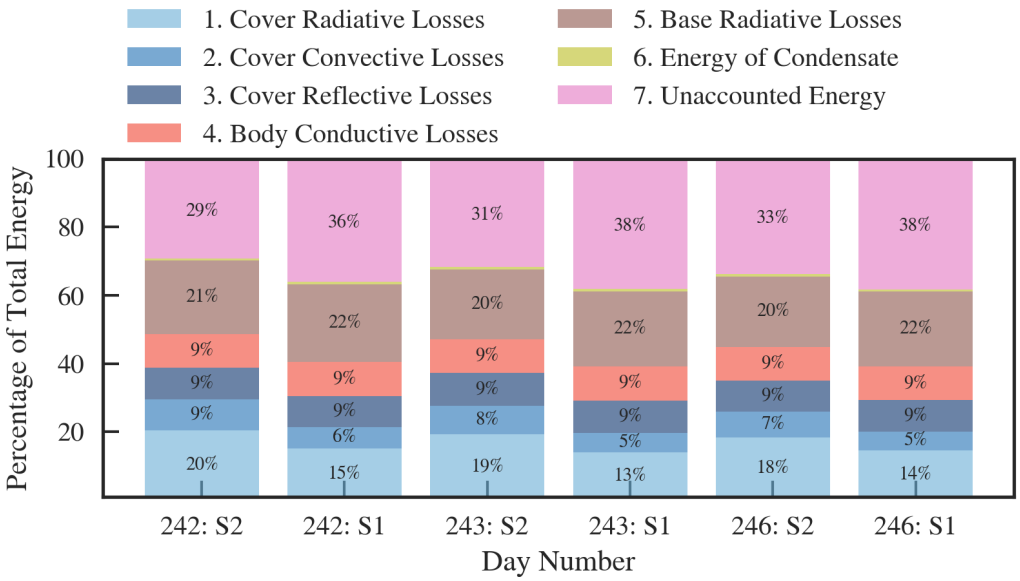

Figure 41: The energy balance for days where aluminium was added to the back and sides of Still 1, Still 2 was the reference still.

Table 9: Water Produced in Experiments with Back and Side Reflectors.

Day Number	Still 2 Yield	Still 1 Yield	Yield Increase	Corrected Yield Increase
242	0.644 kg	0.743 kg	15 %	−1 %
243	0.579 kg	0.622 kg	7 %	−8 %
246	0.588 kg	0.582 kg	−1 %	−15 %
248	0.506 kg	0.487 kg	−3 %	−17 %
249	0.497 kg	0.465 kg	−6 %	−20 %

Table 10: Efficiencies for Experiments with Back and Side Reflectors.

Day Number	Still 1 Efficiency	Still 2 Efficiency
242	11.2 %	9.8 %
243	9.7 %	9.1 %
246	8.6 %	8.8 %
248	8.2 %	8.6 %
249	7.9 %	8.4 %

Figure 42 shows the condensate collected over time for the two stills, for a selection of days where the side and back aluminium panels were in Still 1. The condensate collection

begins earlier and appears to occur at a higher rate in Still 1 over the course of the day, but the rate decreases rapidly as the experiment progresses. Table 11 shows the amount of water produced in each still during the day and night respectively.

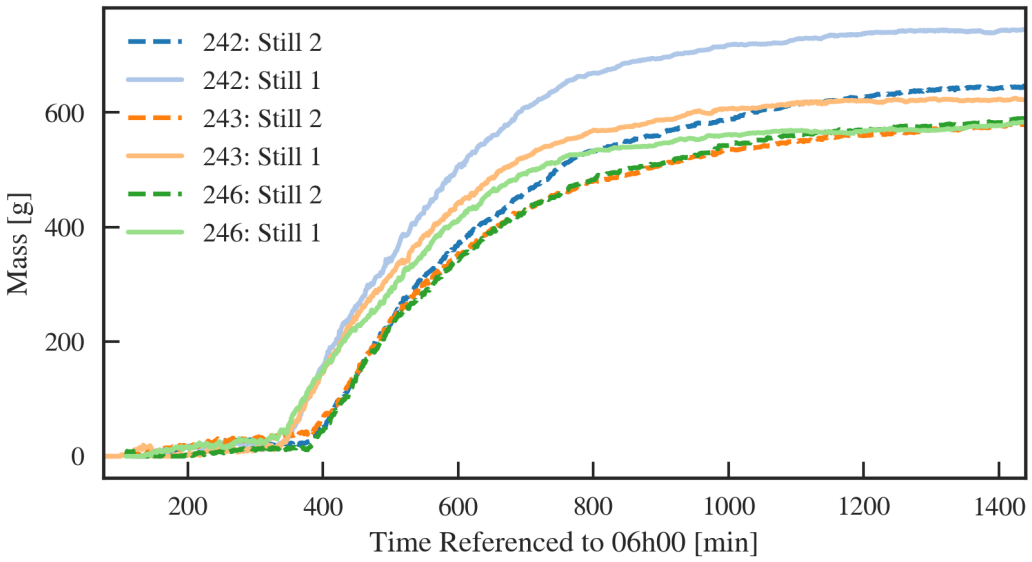

Figure 42: Mass of condensate produced on days where aluminium was added to the back, and sides, of Still 1, Still 2 was the reference still.

Table 11: Day-time and Night-time yield comparison.

Day Number	Still 2 Day Yield	Still 1 Day Yield	Still 2 Night Yield	Still 1 Night Yield
242	0.476 kg	0.623 kg	0.168 kg	0.121 kg
243	0.443 kg	0.536 kg	0.134 kg	0.085 kg
246	0.443 kg	0.503 kg	0.145 kg	0.079 kg
248	0.389 kg	0.427 kg	0.116 kg	0.060 kg
249	0.380 kg	0.425 kg	0.116 kg	0.039 kg

From this data it can be seen that Still 1, with the aluminium panels, consistently produces more water than Still 2 during daylight hours while Still 2 produces more water over night. There are two possible explanations for this behaviour. The sides of the still do not reach temperatures as high as the back wall due to the sides being in shadow for more of the day, due to the lower heat capacity of aluminium when compared to the wood it is likely that overnight the temperature of the aluminium is low enough that condensation occurs preferentially on the aluminium side panels instead of on the cover, explaining the decrease in night-time yield seen in Still 1. Additionally, as the wood

temperature has been lowered by approximately 10 °C on all sides by the addition of the aluminium there is less energy stored in the system to be released back into the water overnight to aid evaporation.

While literature suggests that the addition of internal reflectors is good for the performance of the still the results do not reflect this. The increased driving force for evaporation was seen, and is shown in Figure 43, but due to the absence of sufficient area for condensation to occur the net effect was negative. The reflector surface should preferably be resistant to corrosion and oxidation in order to eliminate the formation of nucleation sites and discourage condensate formation on the reflector surfaces. The conductivity and angle of the reflector is also likely to affect the performance and should be investigated further.

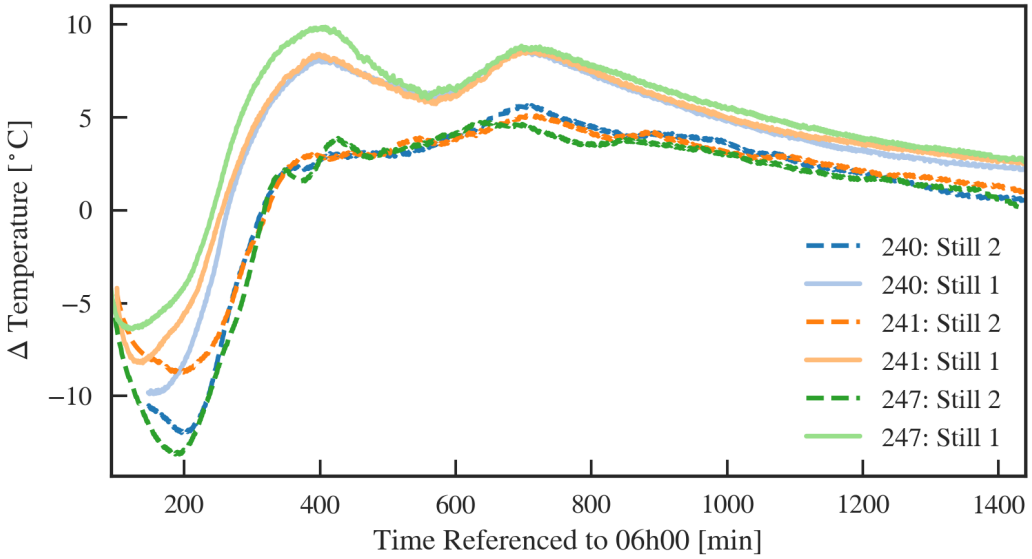

Figure 43: Difference between water temperature and cover temperature for days where aluminium was added to the back of Still 1, Still 2 was the reference still.

4.6 Increasing Evaporation Rate

4.6.1 PVC Tarpaulin

In the first set of tests with the PVC tarpaulin added to Still 1 a definite improvement in performance was seen when compared to the reference still, Still 2. After running the experiment with the carbon black nanofluid the PVC was tested again and an additional improvement immediately seen. Consider the yields given in Table 12. Days 261 through to 264 were the initial tests with PVC, the percentage improvement was 38 % on average

with small variance. From day 274 onwards, the percentage improvement in yield in Still 1 when compared to Still 2 was 98 % on average. This was excluding the outliers on days 285 and 296, these days experienced slightly lower amounts of incident irradiation as well as rain. Rain, in particular, makes results difficult to compare.

Table 12: Water Produced in Experiments with PVC.

Day Number	Still 2 Yield	Still 1 Yield	Yield Increase	Corrected Yield Increase
261	0.549 kg	0.895 kg	63 %	39 %
262	0.497 kg	0.821 kg	65 %	41 %
263	0.413 kg	0.647 kg	56 %	34 %
264	0.223 kg	0.362 kg	62 %	38 %
274	0.462 kg	1.07 kg	132 %	98 %
275	0.469 kg	1.13 kg	140 %	106 %
285	0.320 kg	0.91 kg	184 %	143 %
292	0.425 kg	1.06 kg	150 %	113 %
295	0.457 kg	0.977 kg	113 %	82 %
296	0.372 kg	0.773 kg	107 %	77 %
297	0.486 kg	1.08 kg	122 %	90 %
298	0.452 kg	1.05 kg	133 %	98 %
299	0.461 kg	1.09 kg	137 %	102 %

In Figure 44 the energy balance analysis for a day before the change in improvement, and two days after the change, is shown. The first thing to note is the increased base radiative losses from Still 1 due to increased absorbance of irradiation and subsequently higher base temperatures. The reduced cover losses in Still 1 are also noteworthy; if the absorbance of the base of the still has been increased the reflection would be decreased and likely result in a lower cover temperature causing the reduced losses. The reason for the change in the percentage of unaccounted energy between the initial experiments and later experiments seen in both stills is unclear. A small increase in the energy of the condensate leaving the system can be seen in the energy balance for Still 1 indicating substantially more water is being produced in this still.

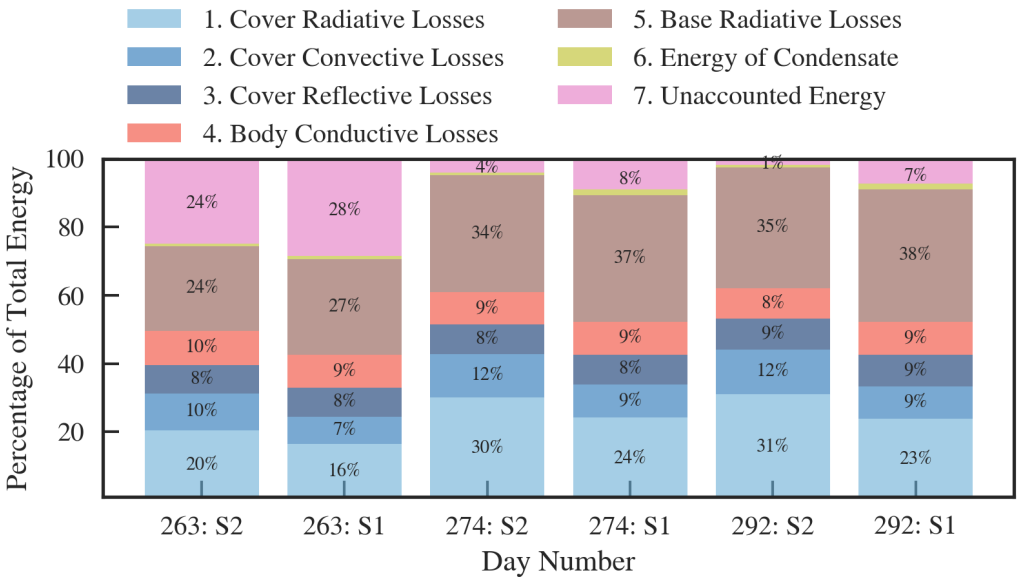

Figure 44: The energy balance analysis for a selection of days where PVC was added to Still 1, Still 2 was the reference still.

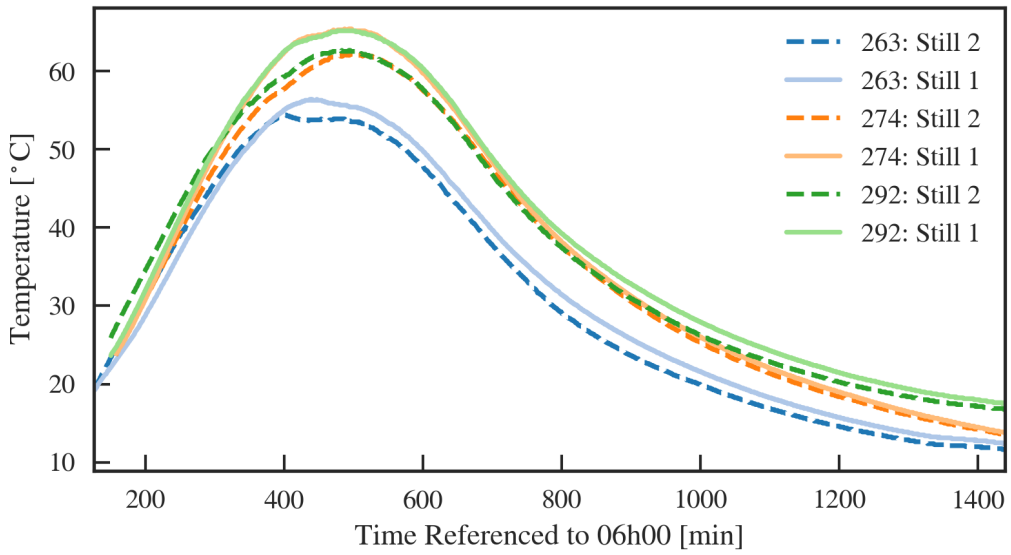

Figure 45: Water temperatures for a selection of days where PVC was added to Still 1, Still 2 was the reference still.

Figure 45 shows the higher water temperatures seen by Still 1. In the first four days of the PVC experiments the water temperature was on average 2 °C hotter in Still 1 than in Still 2, increasing to between a 3 °C and 4 °C difference in the later experiments. This suggests that the absorbance of the PVC was modified between the sets of experiments. This is not impossible as something present in the nanofluid, such as the surfactant, may have modified the surface. An alternative is that traces of nanoparticles may have remained

on the surfaces despite the extensive cleaning of the still. The surface was not tested for modification at this point in time as removing the PVC to sample would result in the Still being un-usable, the stills are being used for additional tests and cannot currently be disassembled.

The cover temperatures for the two stills can be seen in Figure 46. The temperature in Still 1 is significantly lower, confirming the reason for the reduced cover losses seen in Figure 44. The cover losses were reduced but condensation rate increased, as seen in Figure 47. Recall in Section 4.2 it was shown that cover losses are necessary for condensation to occur; the decrease in cover losses and increase in condensation observed in the PVC experiments indicates that an optimum should exist between cover losses and driving force for condensation.

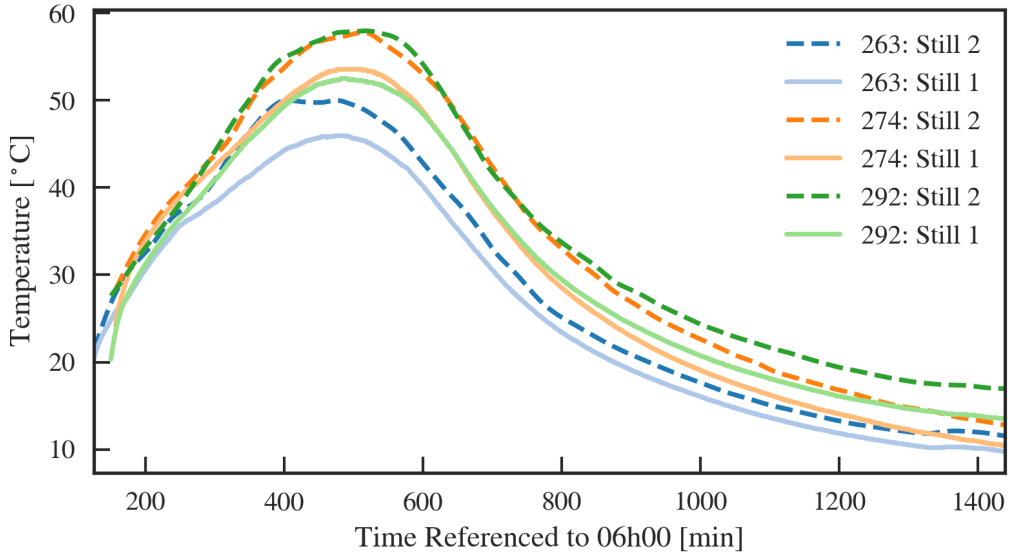

Figure 46: Cover temperatures for a selection of days where PVC was added to Still 1, Still 2 was the reference still.

In Figure 47 the increased rate of condensation in Still 1 is seen. The difference between day 263 and the other two days is immediately visible in the decreased yield and the reduced rate of condensation. The onset time for condensate collection is also between 10 and 20 minutes earlier in Still 1 than in Still 2.

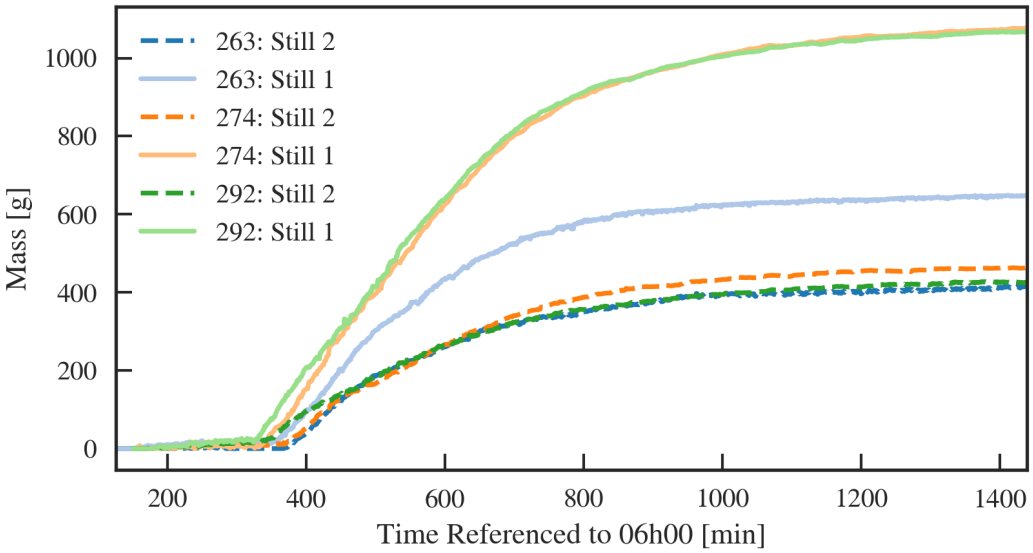

Figure 47: Mass of condensate for a selection of days where PVC was added to Still 1, Still 2 was the reference still.

Looking at Table 13, the efficiency of Still 1 is more than double that of Still 2 in the later experiments. The PVC is definitely a better absorber surface than the Durapond sealant.

Table 13: Efficiencies for Experiments with PVC.

Day Number	Still 1 Efficiency	Still 2 Efficiency
261	21.1 %	12.9 %
262	19.5 %	11.8 %
263	16.6 %	10.5 %
264	14.9 %	9.2 %
274	23.1 %	10.0 %
275	24.1 %	10.0 %
285	21.7 %	7.5 %
292	23.6 %	9.2 %
295	20.9 %	9.7 %
296	20.0 %	9.6 %
297	23.5 %	10.6 %
298	23.3 %	10.0 %
299	26.2 %	11.0 %

4.6.2 Carbon Black Nanofluid

The addition of the carbon black nanofluid to Still 1 was intended to increase the absorbance as described in Section 2.3.11. The energy balance for these experiments is shown in Figure 48.

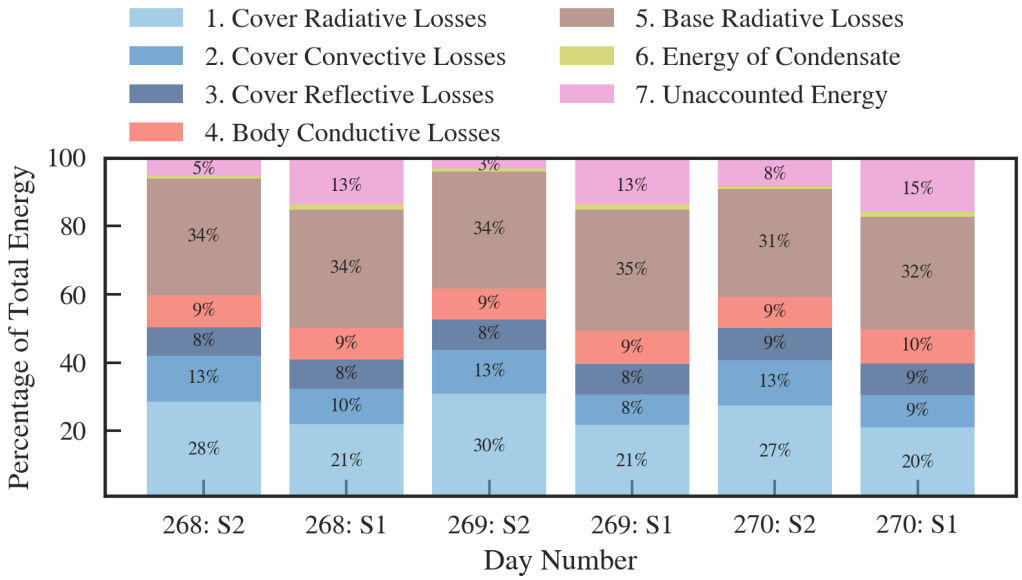

Figure 48: The energy balance analysis for the experiments where a carbon black nanofluid was added to Still 1, Still 2 was the reference still.

The energy of condensate is larger in Still 1 than in Still 2, indicating an improvement in performance of the still. The cover losses are lower in Still 1 than in Still 2, as with the PVC. Literature states (Section 2.3.11) that a problem with the use of nanofluids is that the cover heats up significantly in the presence of the nanofluid so it is unexpected for the cover losses to be so much lower. Reduced cover losses could be caused by the nanofluid modifying the surface tension of the water in a way that reduces the amount of evaporation for a given increase in water temperature. Figure 49 shows the cover temperatures for the experiments in question.

While the difference in maximum cover temperatures between the two stills remains between 2 °C and 4 °C, the cover temperature in Still 1 was significantly cooler than in Still 2 in the later part of the day, from around 17h00 onwards. This is likely the reason for the reduced cover losses. The lower cover temperature over night could be due to an increased heat capacity of the fluid caused by the addition of the carbon black particles, if the fluid retains more heat there is less energy being released back to the cover.

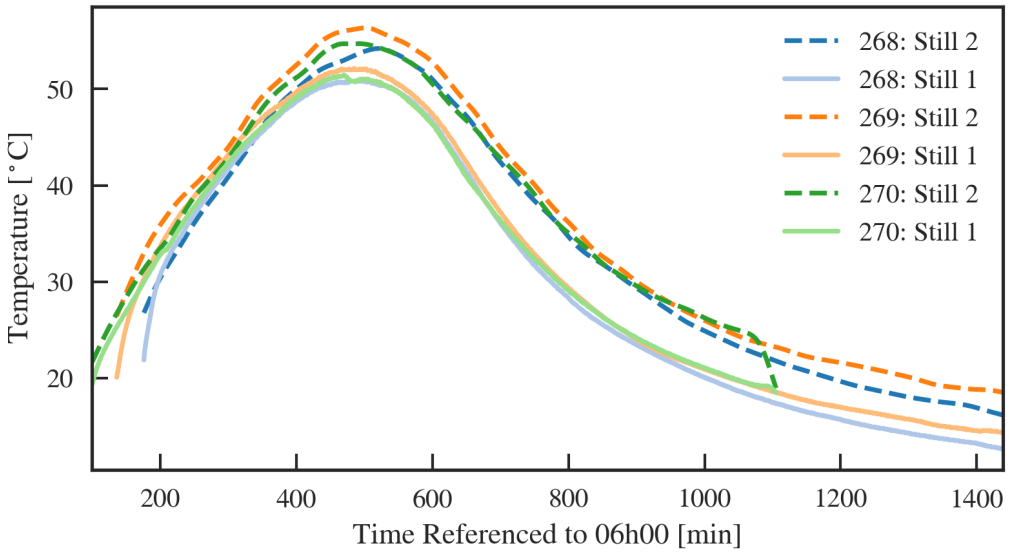

Figure 49: Cover temperatures for both stills for the experiments where a carbon black nanofluid was added to Still 1, Still 2 was the reference still.

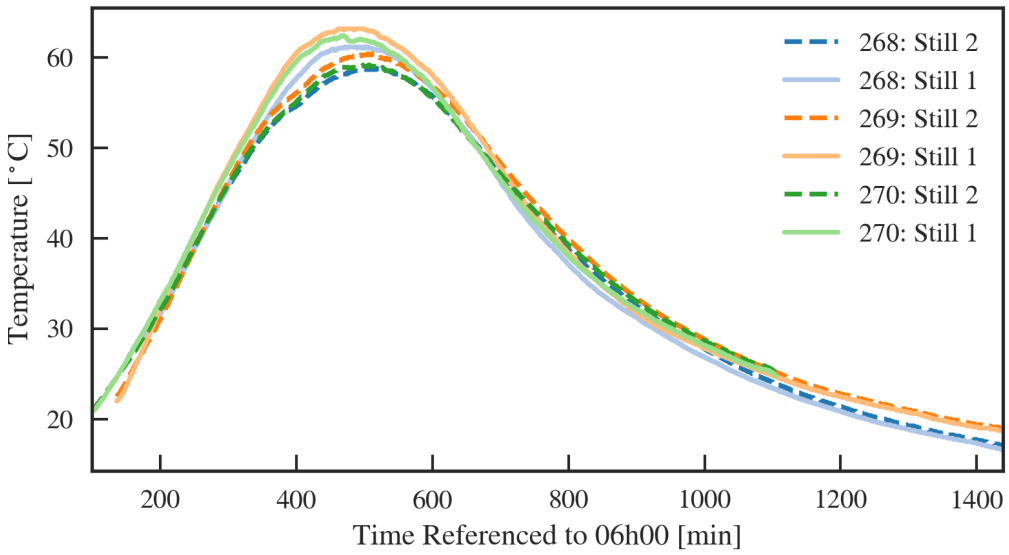

Figure 50: Water temperatures for both stills for the experiments where a carbon black nanofluid was added to Still 1, Still 2 was the reference still.

Figure 50, showing the water temperatures, does not support the suggestion of heat retention in the water as the water temperature drops to roughly the same temperature in both stills. An alternative explanation is the nanoparticles causing a diffused emittance of light reducing the amount directly incident on the cover. Figure 50 shows that Still 1 experienced maximum water temperatures roughly 3 °C higher than Still 2 and that those maximums were reached between 30 and 40 minutes earlier than in Still 2. This

suggests that the nanofluid did improve the absorbance of solar irradiation. The earlier maximums in water temperature suggest that an earlier onset of condensation would be observed in Still 1. This can be seen in Figure 51 and the values of the onset time for condensate collection are given in Table 14.

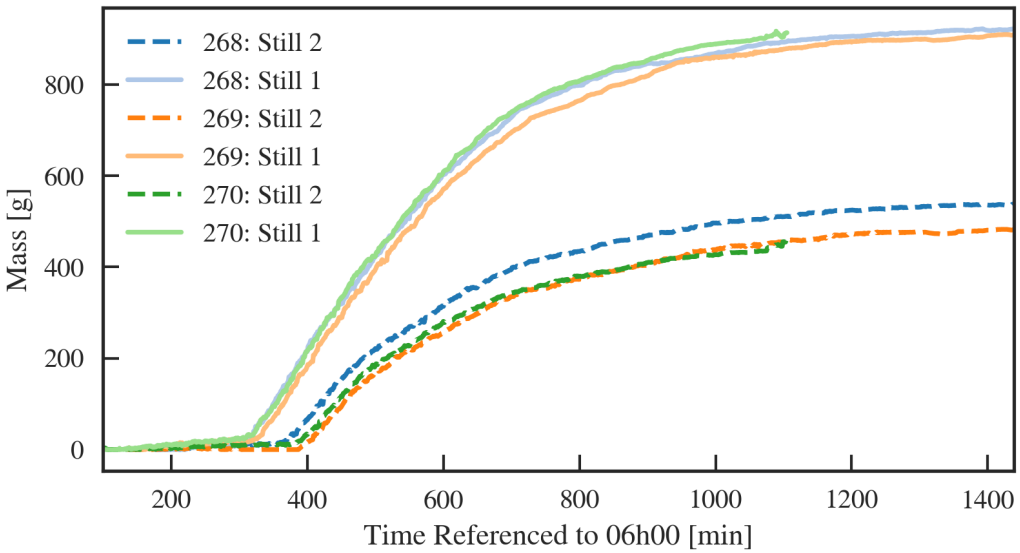

Figure 51: Mass of condensate produced in both stills for the experiments where a carbon black nanofluid was added to Still 1, Still 2 was the reference still.

Table 14: Onset Time comparison for experiments with carbon black nanofluid.

Day Number	Still 1	Still 2
268	11h10	12h10
269	11h30	12h30
270	11h20	12h30

From Figure 51 it appears that the rate of condensation is higher in Still 1 than in Still 2. The calculated condensation rate and modelled evaporation rate, obtained as described in Section 3.3.3 are plotted for each of the stills in Figure 52. It is immediately evident that the rate of evaporation and condensation were higher in Still 1 than in Still 2.

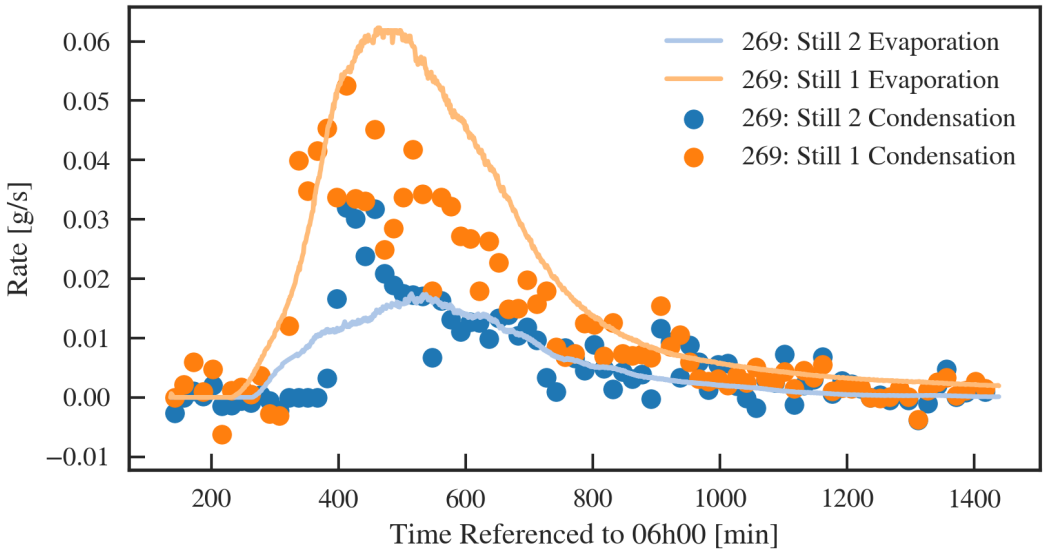

Figure 52: Calculated condensation rate and modelled evaporation rate in both stills for the experiments where a carbon black nanofluid was added to Still 1, Still 2 was the reference still.

Table 15 shows the final yields and the improvement in yield in Still 1 when compared to Still 2. The results show a progressive improvement in yield. Looking at the mass of condensate in Figure 51 it appears that the yield in Still 2 on day 269 was larger than usual and the increase in yield calculated for that day may be lower than expected due to this.

Table 15: Water produced by each still in experiments using the carbon black nanofluid, and the increase in yield.

Day Number	Still 2 Yield	Still 1 Yield	Yield Increase	Corrected Yield Increase
268	0.536 kg	0.920 kg	71 %	46 %
269	0.481 kg	0.908 kg	88 %	61 %
270	0.450 kg	0.909 kg	101 %	72 %

Considering the efficiencies in Table 16 it can be seen that the efficiency of Still 1 increased over the course of the experiments. This improvement in performance over time is unexpected as the nanofluid was observed to degrade rapidly over the three day period. The particles began settling out of solution from the first day. A control sample of the nanofluid was kept at a constant temperature in the laboratory to compare the behaviour; the lab sample remained stable. When discussing the stability of a nanofluid,

agglomeration is one of the main factors to consider. When the particles begin forming agglomerates the surfactant is no longer managing to maintain an even suspension of particles in the nanofluid. Figure 53 shows the particle size distribution within the nanofluid at the start and at the end of the experiments.

Table 16: Efficiencies for experiments with carbon black nanofluid.

Day Number	Still 1 Efficiency	Still 2 Efficiency
268	21.2 %	12.3 %
269	21.5 %	11.3 %
270	22.1 %	11.2 %

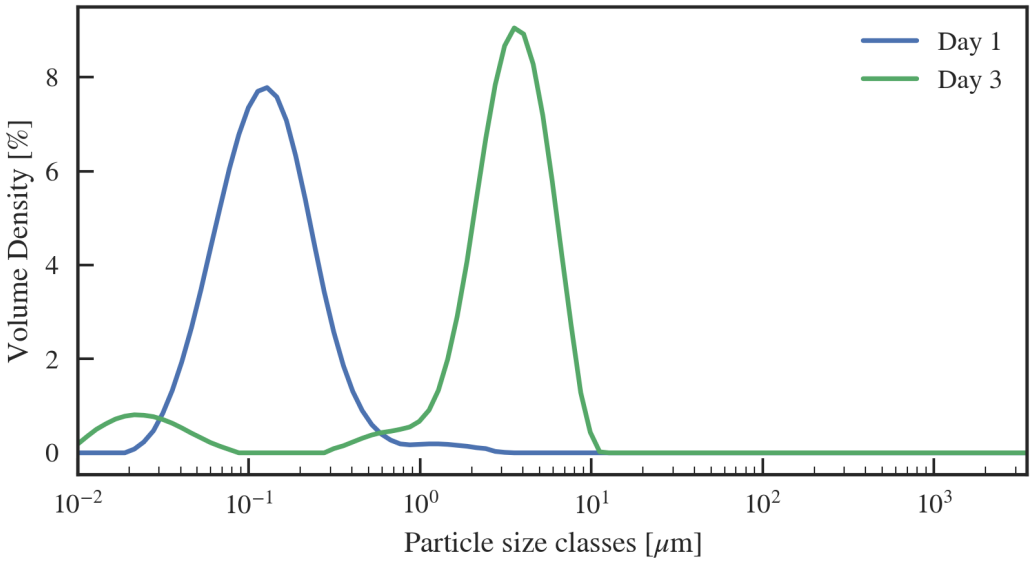

Figure 53: Particle size analysis results for the carbon nanofluid, before addition to the solar stills and after three days of operation.

The nanofluid, post synthesis, had an average particle size of 0.132 µm diameter, following exposure to sunlight and multiple heating-cooling cycles in the operation of the solar still, the average particle size increased to a diameter of 3.44 µm. This shows severe agglomerate formation within the nanofluid, indicative of a deterioration in stability, and can explain the settling observed in the system.

A sample of the nanofluid was taken each day and analysed in the UV-VIS spectrophotometer and the results shown in Figure 54. The results were compared to the control sample from the laboratory. It can be seen that the absorbance of the fluid decreased drastically as the particles settled out over the three days. However, the increase in efficiency

indicates that the nanofluid is as effective when the particles are simply agglomerated on the base of the still forming a highly absorptive layer.

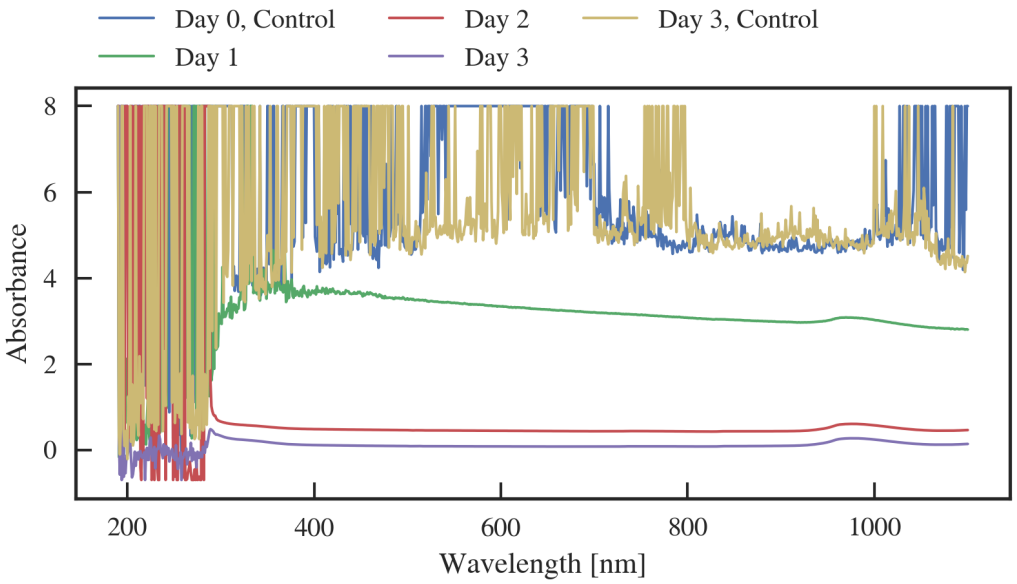

Figure 54: UV-VIS analysis results for the carbon nanofluid, day 0 refers to before the fluid was added to the still, days 1, 2, and 3, are after each of the days that the fluid was in the still.

The reason for the erratic nature of the absorbance spectrum of the control experiments was the high concentration of particles, some of which scattered the light or completely stopped light from passing through the cell.

4.6.3 Charcoal

Activated carbon is known for its large surface area, when used in the solar still this area is used to absorb incident irradiation. The additional area for absorbance of solar irradiation should increase the rate at which the energy is absorbed. In Figure 55 the energy balance for a selection of days is shown.

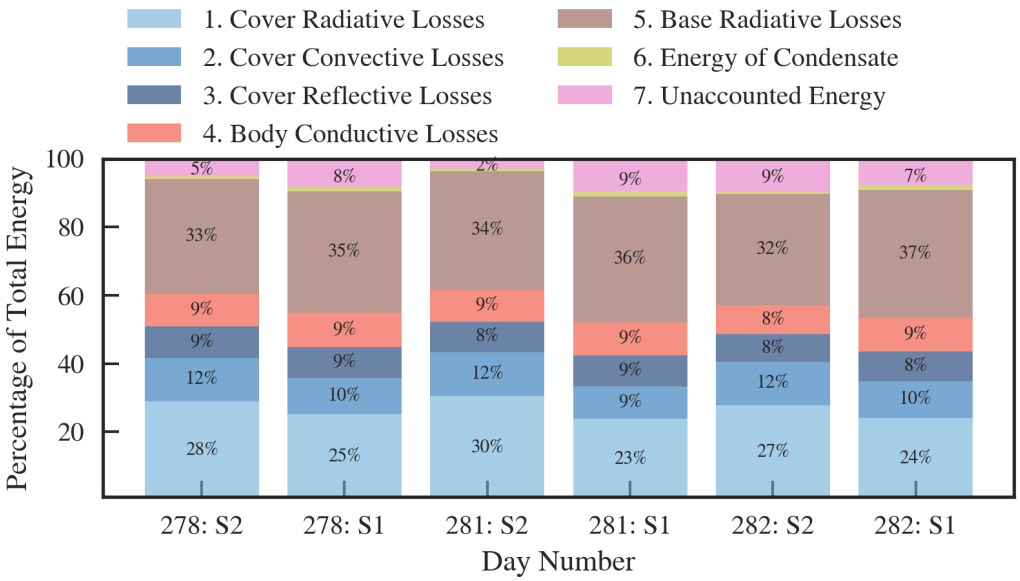

Figure 55: Energy balance analysis for a selection of days where activated charcoal was added to Still 1, Still 2 was the reference still.

The base radiative losses in Still 1 are likely underestimated as the charcoal will be at a slightly higher, but unknown, temperature. The effect of the charcoal on the absorbance is seen in the increase in radiative losses indicating higher internal temperatures, as well as the increased energy of condensate. The reduced cover losses can be explained by reduced reflection and back radiation from the base of the still leaving via the cover; the irregular shape of the charcoal results in much of the irradiation being reabsorbed by the charcoal as it is reflected and radiated at erratic angles.

To better comment on the cover losses, Figure 56 shows the cover temperatures in the two stills. The difference in maximum cover temperatures is between 3 °C and 5 °C which is larger than before, but the cover does not remain as cool overnight so the overall effect on the losses is not as prominent as when the carbon black nanofluid was added to the still.

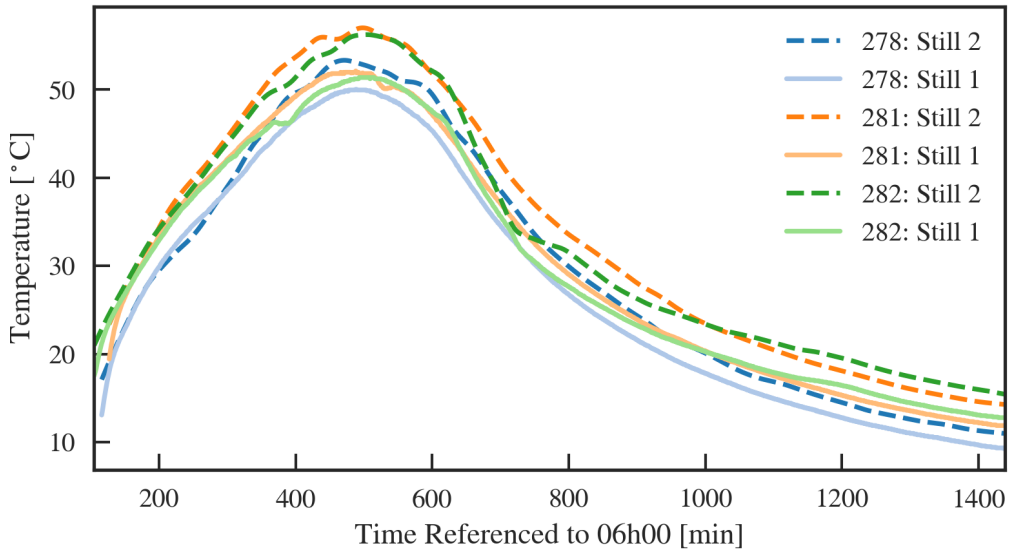

Figure 56: Cover temperatures for a selection of days where activated charcoal was added to Still 1, Still 2 was the reference still.

The water temperatures are seen in Figure 57, with Still 1 reaching temperatures around 2 °C higher than Still 2. The rate of increase of water temperature was not seen to vary significantly between the stills.

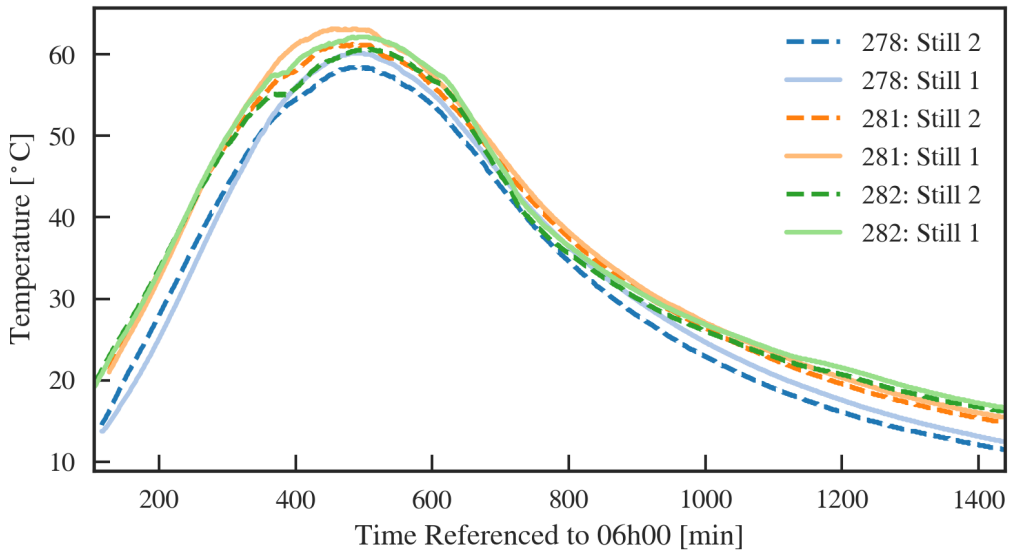

Figure 57: Water temperatures for a selection of days where activated charcoal was added to Still 1, Still 2 was the reference still.

Figure 58 shows that the relative humidity in Still 1 is lower than in Still 2. This would suggest evaporation as a limiting factor in the performance of the still. However, the

mass of condensate produced in Still 1 was significantly more than in Still 2, this is seen in Figure 59. The data thus suggests that the small temperature differences in Still 1 had a huge effect on the condensation ability.

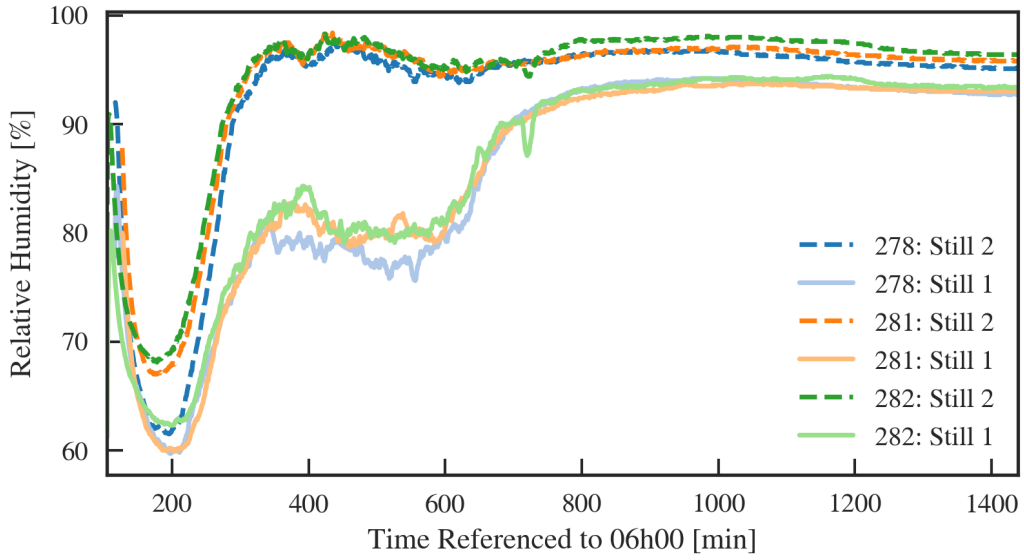

Figure 58: Relative humidity for a selection of days where activated charcoal was added to Still 1, Still 2 was the reference still.

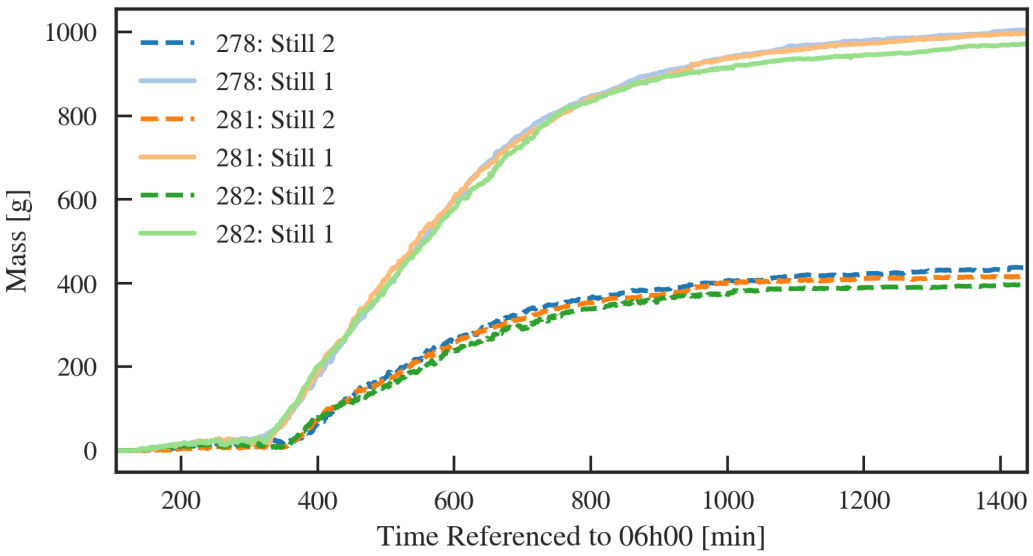

Figure 59: Mass of condensate produced for a selection of days where activated charcoal was added to Still 1, Still 2 was the reference still.

Table 17 shows the yields of the two stills and Table 18 the efficiencies. The addition of charcoal to Still 1 resulted in efficiencies more than double that in Still 2 making it a promising addition.

Table 17: Water produced by each still in experiments using the activated charcoal, and the increase in yield.

Day Number	Still 2 Yield	Still 1 Yield	Yield Increase	Corrected Yield Increase
276	0.204 kg	0.473 kg	130 %	98 %
277	0.295 kg	0.640 kg	116 %	85 %
278	0.437 kg	1.005 kg	129 %	96 %
281	0.416 kg	0.996 kg	139 %	104 %
282	0.396 kg	0.971 kg	144 %	109 %

Table 18: Efficiencies for experiments with charcoal.

Day Number	Still 1 Efficiency	Still 2 Efficiency
276	19.8 %	8.2 %
277	18.6 %	8.5 %
278	21.6 %	9.4 %
281	21.9 %	9.1 %
282	21.8 %	8.2 %

4.6.4 Carbon Felt

When the carbon felt was added to the still it floated just beneath the surface of the water and the entirety of the carbon felt was wetted by a thin layer of water.

Figure 60 shows the energy balance analysis for a selection of days during the experiments. As with the previous sets of experiments the cover losses were lower in comparison to Still 2, the energy of condensate was higher, and the unaccounted energy was also higher. The larger unaccounted energy in Still 1 is likely due to the radiative base losses being underestimated; the surface radiating towards the cover is the top of the felt. The temperature of the top of the felt is unknown as the water film was too thin for it to be measured accurately, the radiative losses were calculated using the base temperature which would have been lower than the top surface of the felt.

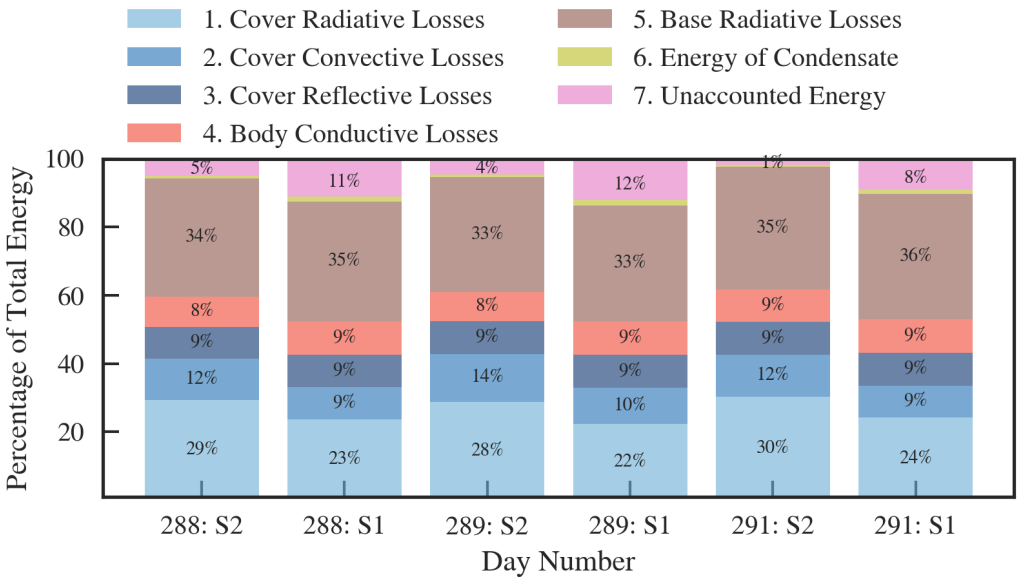

Figure 60: Energy balance analysis for a selection of days where carbon felt was added to Still 1, Still 2 was the reference still.

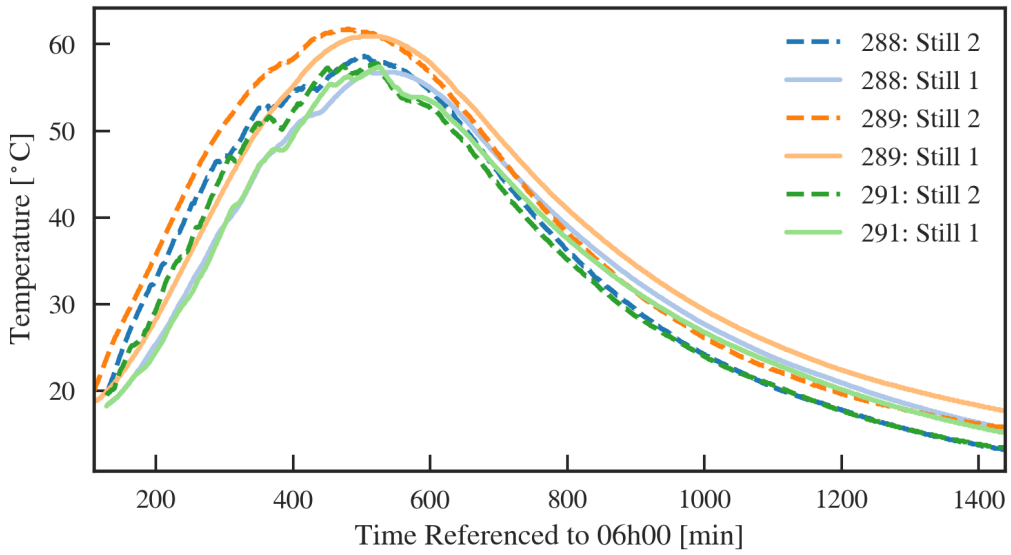

Figure 61: Temperature of the water for days where carbon felt was added to Still 1, Still 2 was the reference still.

In Figure 61 it can be seen that the bulk water temperature was lower for the first half of the day in Still 1, the still with the carbon felt, this is due to the solar irradiation being absorbed by the carbon felt near the surface of the water and heating up the thin film of water above the felt quicker, and to higher temperatures, than the bulk. The higher water temperatures in Still 1 overnight can be explained by the carbon felt retaining more energy in the water due to the additional thermal mass. This lower bulk temperature during

the portion of the day where most evaporation and condensation occurs is beneficial; the water heats up from the surface reaching higher temperatures due to the small volume of water directly exposed to irradiation, unfortunately, as mentioned previously, due to the thinness of the film an accurate measurement of the temperature of the film could not be obtained. This surface heating effect allows for significantly higher evaporation rates, and subsequently condensation rates, as can be seen in Figure 62.

The onset time for condensate collection is consistently 30 to 50 minutes earlier in Still 1 than in Still 2, and the rate of condensation in Still 1 is significantly higher, and remains so for a longer period of time likely due to the higher water temperatures overnight.

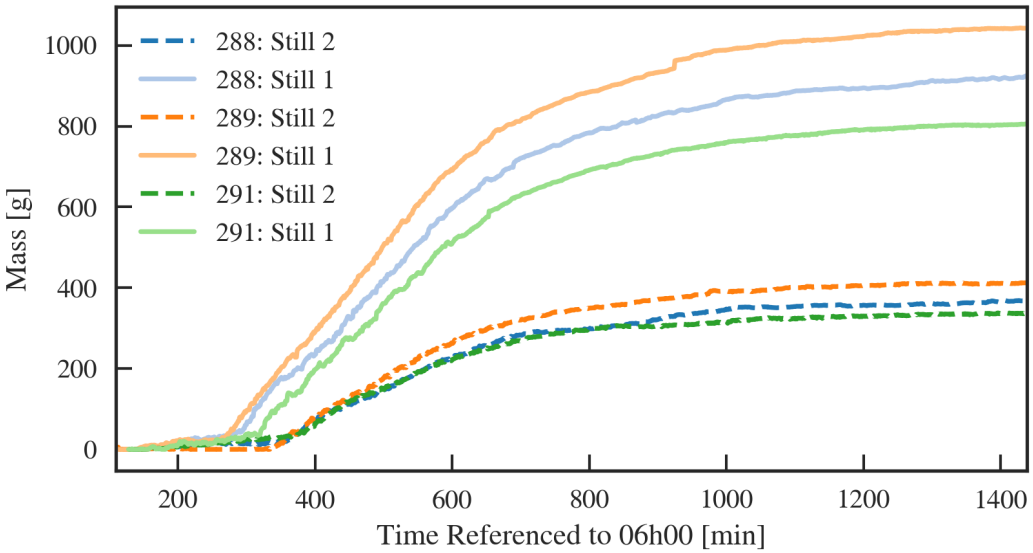

Figure 62: Load cell curves for a selection of days where carbon felt was added to Still 1, Still 2 was the reference still.

Looking at the relative humidities within the stills in Figure 63, Still 2 very quickly reached a relative humidity of 100 % indicating saturation of the air within the still. Still 1, however, remained at a comparably low relative humidity for the entire portion of the day where most of the condensation occurs. This indicates that the condensation in Still 1 was significantly better than in Still 2, if evaporation was responsible for the low relative humidity the amount of condensate produced would not be higher in Still 1 than in Still 2. This is a very similar result to those observed with the addition of charcoal.

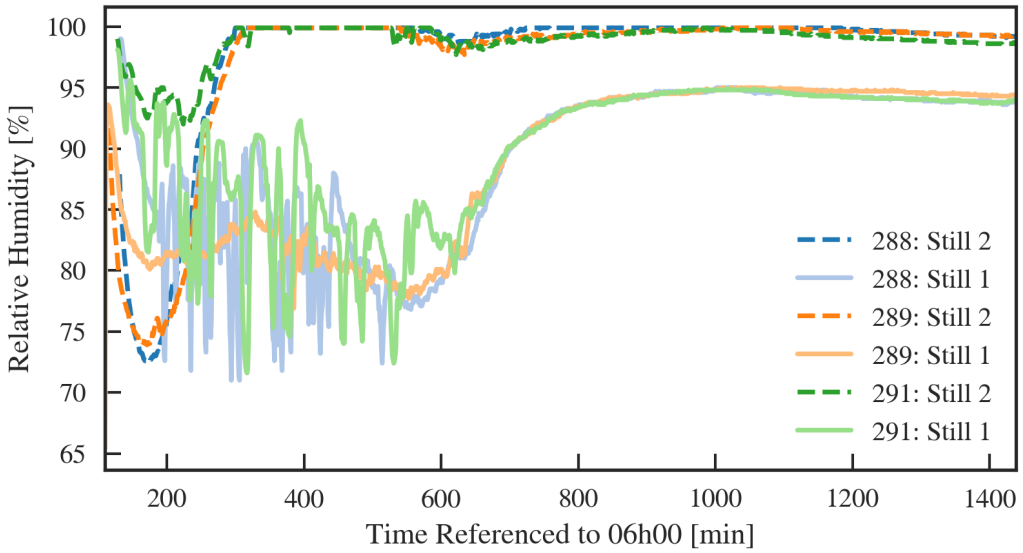

Figure 63: Relative humidities for a selection of days where carbon felt was added to Still 1, Still 2 was the reference still.

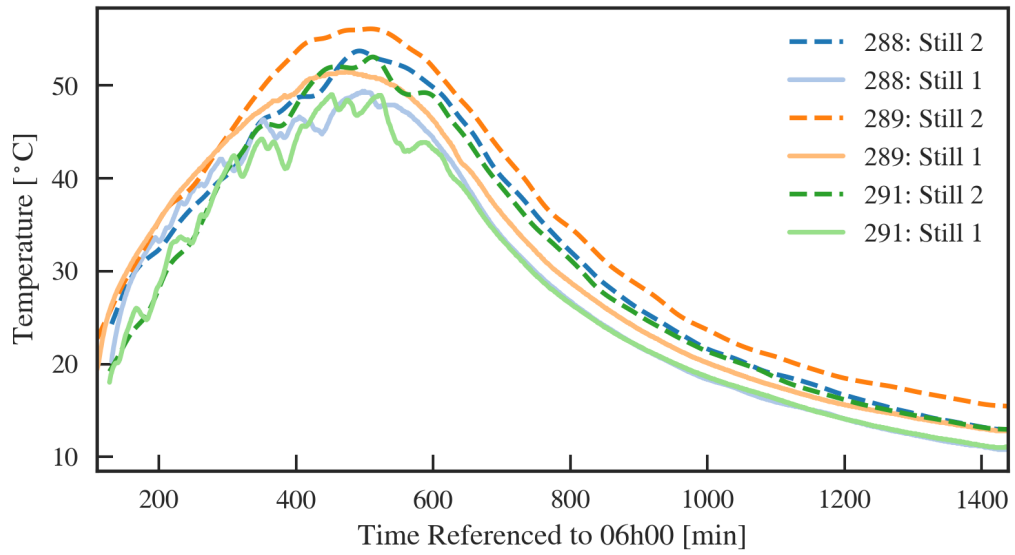

Figure 64: Cover temperatures for a selection of days where carbon felt was added to Still 1, Still 2 was the reference still.

This difference in condensation rate is unexpected as the modifications were focussed on increasing the evaporation rate. The cover temperatures in Figure 64 suggest that the increased condensation rate was due to the lower cover temperature in Still 1; a higher driving force for condensation to occur exists when the temperature of the condensation surface is lower. The air temperatures in the stills show that Still 1 had a higher air temperature, indicating an improved rate of evaporation in Still 1 compared to Still 2.

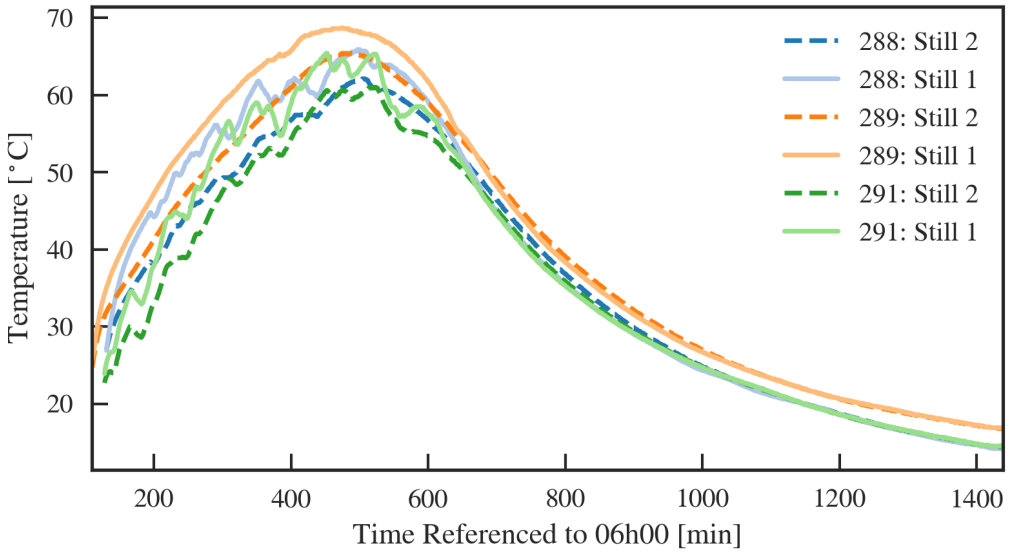

Figure 65: Air temperatures inside the stills for a selection of days where carbon felt was added to Still 1, Still 2 was the reference still.

The lower cover temperature in Still 1 can be explained by the difference in absorber surface between the stills. The absorber surface in Still 1 is the carbon felt while the absorber surface in Still 2 is the Durapond coated base of the still. The carbon felt absorbs significantly more of the incident irradiation and reflects less of the energy, the surface is matt in comparison the the Durapond. Reducing the reflection from the absorber can result in a decrease in cover temperature. Another contributing factor is the texture of the absorber surface. Still 2 has a relatively smooth absorber surface, this means that the reflection of incident irradiation, and radiation from the absorber are all directed to the walls and cover of the still. In Still 1, the rough fibrous nature of the carbon felt causes a large portion of the reflected irradiation and energy radiated back from the absorber to be reabsorbed by the carbon felt instead of the cover.

Table 19 shows the yields in each of the two stills as well as the increase in yield due to the addition of the carbon felt.

Table 19: Water produced by each still in experiments using the carbon felt, and the increase in yield.

Day Number	Still 2 Yield	Still 1 Yield	Yield Increase	Corrected Yield Increase
288	0.368 kg	0.921 kg	150 %	114 %
289	0.411 kg	1.042 kg	153 %	116 %
290	0.354 kg	0.844 kg	138 %	104 %
291	0.336 kg	0.808 kg	139 %	105 %

It is clear that the presence of the carbon felt greatly improved the performance of the still, while it was intended to increase the evaporation rate the apparent increase in condensation rate was of equal benefit. Attempts should be made to obtain the temperature of the water film to better comment on the increase in evaporation rate in isolation. The efficiencies observed in Table 20 are comparable and, possibly slightly higher on average, to those in the charcoal experiments.

Table 20: Efficiencies for experiments with carbon felt.

Day Number	Still 1 Efficiency	Still 2 Efficiency
288	21.8 %	8.6 %
289	22.2 %	8.7 %
290	21.1 %	8.6 %
291	20.4 %	8.4 %

4.7 Increasing Condensation Rate

While most of the experiments were focussed on reducing the energy losses from the still and increasing the evaporation rate some tests were done on increasing the rate of condensation or simply trying to gain a better understanding of the process of condensation within the system.

4.7.1 Grooved Cover

As described in Section 3.2.4 grooves were added to a portion of the cover plate of Still 3. These grooves increased the internal area of the cover plate by 4 %. An additional

effect of the addition of grooves to the cover is the increased scattering of light when it enters the still, possibly resulting in the water heating up more uniformly, and also more reflection back into the still of light reflected from the inside of the cover. The geometry is modified such that the light is more likely to remain in the still.

The effects of this are seen in Figure 66 where the maximum water temperatures in Still 3 are as much as 4 °C higher than in Still 2.

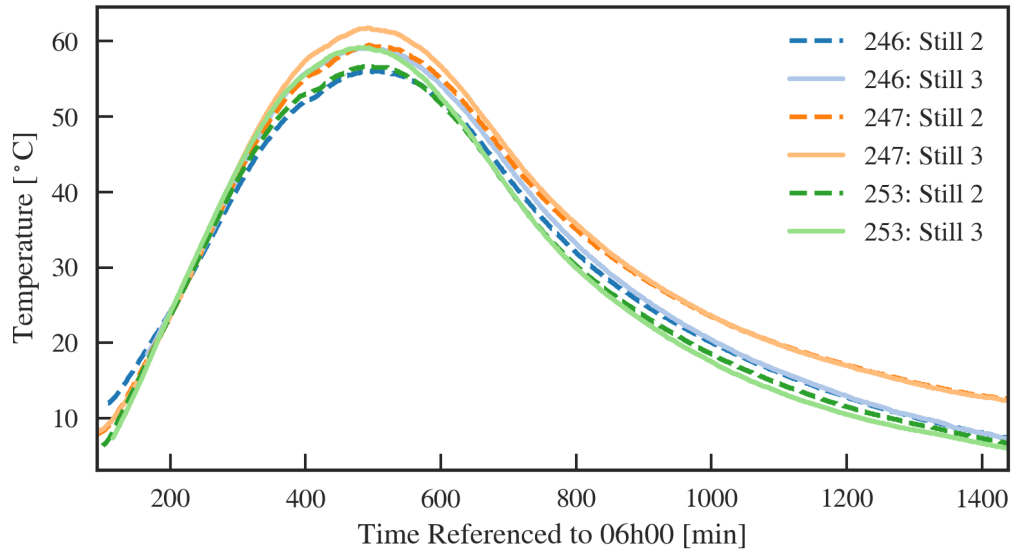

Figure 66: Water temperatures inside the stills for a selection of days where the grooved cover was on Still 3, Still 2 was the reference still.

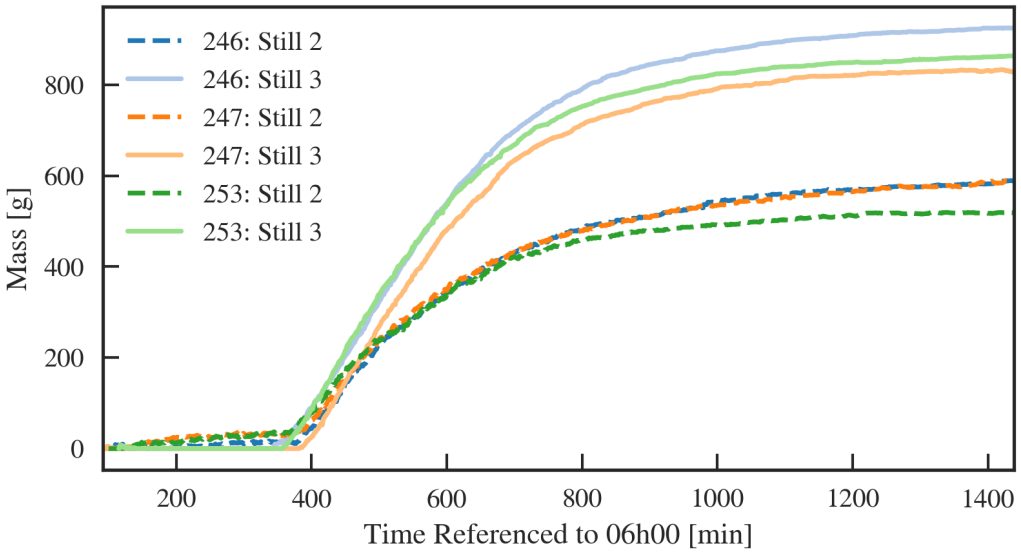

Figure 67: Mass of water produced for a selection of days where the grooved cover was on Still 3, Still 2 was the reference still.

Figure 67 shows the mass of condensate produced in the two stills. While the onset time for condensate collection remains roughly constant at around 12h30, the rate of water production is higher in Still 3 than in Still 2, as it was in the baseline tests in Section 4.4. The summary of the yields in Table 21 indicates an improvement in performance when compared to the baseline experiments.

Table 21: Water produced by each still in experiments with a grooved cover, and the increase in yield.

Day Number	Still 2 Yield	Still 3 Yield	Yield Increase	Corrected Yield Increase
246	0.588 kg	0.924 kg	57 %	20 %
247	0.589 kg	0.830 kg	41 %	7 %
248	0.506 kg	0.708 kg	40 %	7 %
249	0.497 kg	0.676 kg	36 %	4 %
250	0.049 kg	0.103 kg	106 %	60 %
253	0.518 kg	0.863 kg	66 %	27 %
254	0.540 kg	0.842 kg	56 %	19 %
255	0.559 kg	0.881 kg	57 %	20 %

Taking day 250 as an outlier, the improvement in yield varies from 4 % to 27 %. Day 250 was a day with particularly low solar irradiation, only 31 % of the normal irradiation intensity on a sunny day. On these days with low irradiation the still's behaviour was observed to be relatively erratic; insufficient data is currently available at these low irradiation intensities to correctly comment on the reasons for the performance of the stills on these days. The reason for the poor performance of Still 3 on days 247, 248, and 249 is not clear from the available data; water temperatures and cover temperatures were comparable to the other days, no obvious differences were observed.

One additional thing worth noting, drops that form in the grooves have a chance of being larger than drops that form on the flat surface and also have a higher chance of making it to the bottom of the cover without dropping back into the still. This is due to the larger contact area which a drop will have with the PMMA cover when in the groove. Due to PMMA being slightly hydrophilic the adhesion is significantly larger when the contact area is increased. Given the observation made in Section 4.1 regarding drops falling back into the still this is likely a contributing factor to the improvement offered by the grooves.

4.7.2 Heat Sink

Figure 68 shows the condensate collection in Still 2 and 3 for days where the heat sink was added to a portion of the cover on Still 3. While this looks remarkably similar to the previous set of results it can be seen that the onset of condensate collection was earlier in Still 3 than in Still 2, with the difference being 30 minutes on average. This is explained best by Figure 69. It was observed in Still 3 that the drops on the cover plate grew quickest in the area under the heat sink and began to move down the cover much earlier than other droplets.

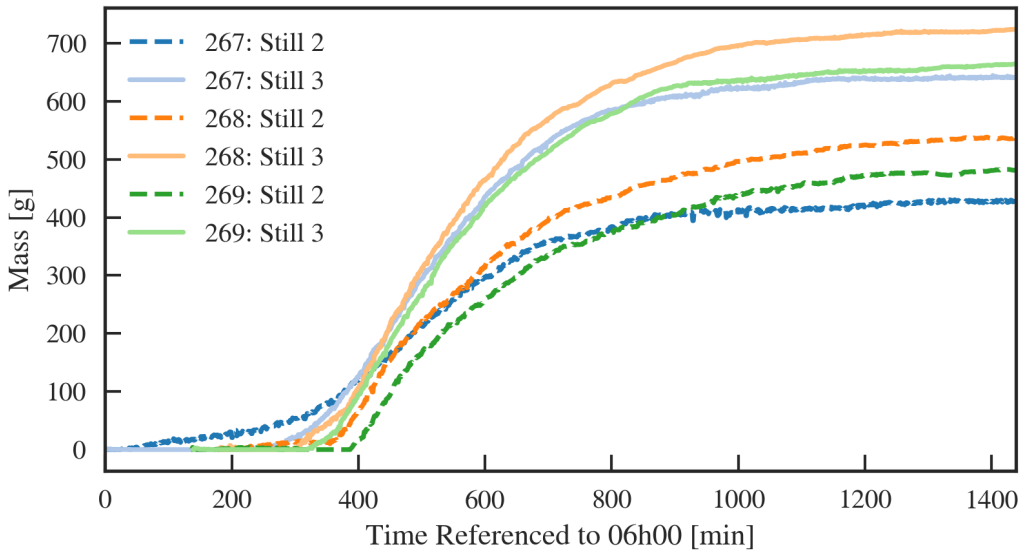

Figure 68: Mass of water produced for a selection of days where the heat sink was on Still 3, Still 2 was the reference still.

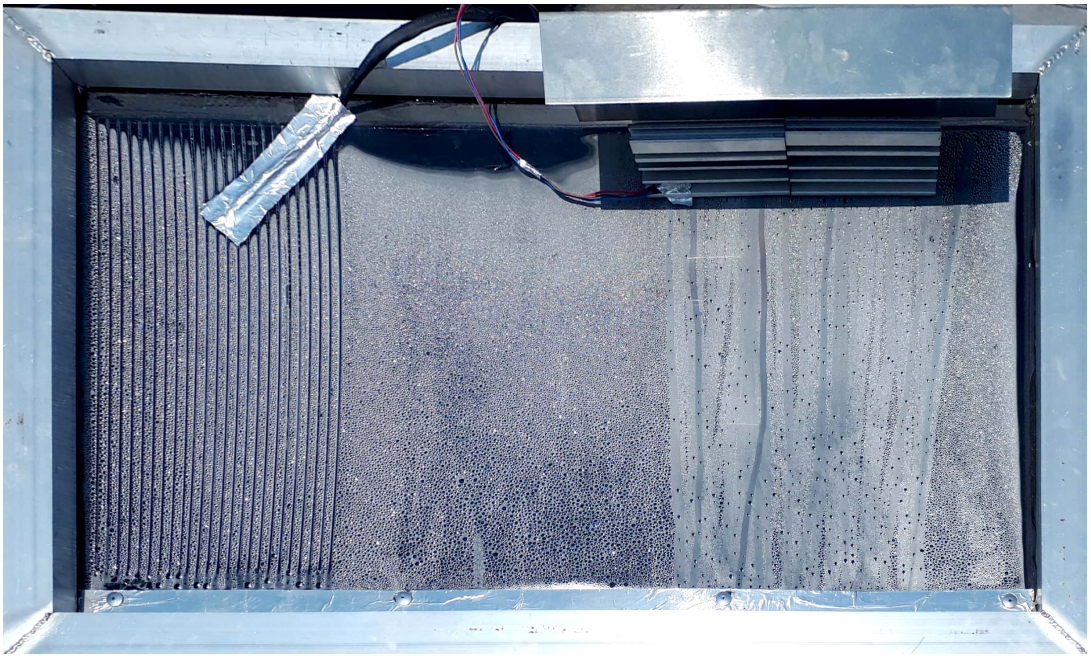

Figure 69: A top down view of the cover of Still 3, with the heat sink and grooves, showing the preferential movement of droplets in the area under the heat sink.

This preferential drop formation in the area under the heat sink is due to the additional energy which the heat sink is able to dissipate from the cover. This suggests that if more energy is allowed to leave the cover plate accelerated drop formation can be achieved and the performance of the still potentially improved.

Table 22 shows the final yields in each of the two stills as well as the increase in performance between Still 2 and 3. It should be recalled that Still 3 experienced a leak at some point during the experiment (See Section 4.1) resulting in the insulation material becoming wet with water from inside the still. This could explain the erratic behaviour observed in the results from Still 3.

Table 22: Water produced by each still in experiments with the added heat sink, and the increase in yield.

Day Number	Still 2 Yield	Still 3 Yield	Yield Increase	Corrected Yield Increase
261	0.549 kg	0.742 kg	35 %	3 %
262	0.497 kg	0.636 kg	28 %	−2 %
263	0.413 kg	0.544 kg	31 %	0.5 %
264	0.223 kg	0.347 kg	55 %	18 %
267	0.427 kg	0.641 kg	50 %	14 %
268	0.536 kg	0.723 kg	35 %	3 %
269	0.481 kg	0.663 kg	37 %	5 %
276	0.204 kg	0.364 kg	77 %	36 %
278	0.437 kg	0.781 kg	78 %	36 %

4.7.3 Tapping on Cover

As described in Section 3.2.4, to check if drop movement was hindering the rate at which condensation occurred the cover was tapped on at regular intervals to force drop movement down the cover. It was observed that the vibrations resulted in a large portion of water falling back into the still instead of running down the cover, but despite this the following was seen.

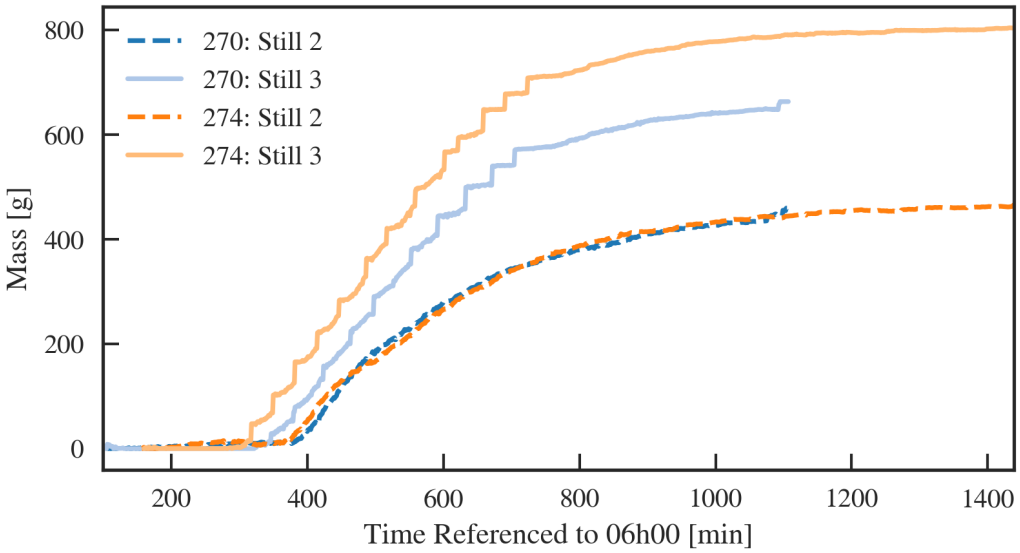

Figure 70: Mass of water produced for two of the days where the cover of Still 3 was tapped, Still 2 was the reference still.

In Figure 70 spikes in the rate of condensation can be seen in the form of steps in the condensate mass curve. These represent the points at which the cover was tapped and all the drops that had accumulated on the cover were collected. The condensate began forming immediately after the cover was cleared of drops, and no dips in the humidity of Still 3 can be seen in Figure 71 indicating that the rate of evaporation was more than sufficient to keep up with the increased rate of condensation.

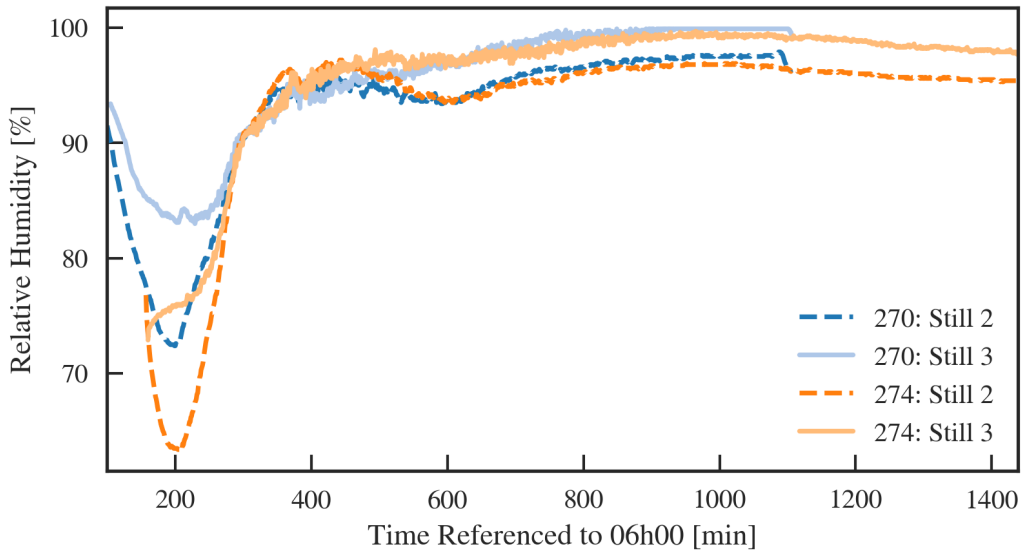

Figure 71: Relative humidity for two of the days where the cover of Still 3 was tapped, Still 2 was the reference still.

Table 23 shows the final masses and improvement in yield between the two stills. It should be noted that the yield improvement data for day 270 is not comparable to the other days as the system experienced a power failure and stopped logging before the end of the experiment.

Table 23: Water produced by each still in experiments where the cover of Still 3 was tapped, and the increase in yield.

Day Number	Still 2 Yield	Still 3 Yield	Yield Increase	Corrected Yield Increase
270	0.450 kg	0.658 kg	46 %	11 %
274	0.462 kg	0.803 kg	73 %	32 %
275	0.469 kg	0.821 kg	75 %	33 %

It appears that should accelerated droplet movement be achieved more water can be produced due to the area being available for condensation to occur on. Drop-wise con-

densation is the preferred mode of condensation and is achieved when the cover has minimal stationary drops already on the cover.

4.7.4 External Tubes

The addition of the external tubes produced no noteworthy results. They did not modify the temperatures in the still or greatly improve the yield. On average only between 0.01 kg and 0.02 kg of water were collected in the tubes. This shows that the natural convection in the still was insufficient to allow for the movement of wet air into the cooler tubes where condensation could occur. If circulation was forced it is likely that the tubes would have a larger effect. Another possibility would be to increase the diameter of the tubes, at the cost of additional losses, to allow for easy, unrestricted, movement of air. It should be noted that the scope of this investigation excluded forced circulation of air within the still.

4.8 Revised Design

As discussed in Section 3, Still 4 was built at the end of the project making use of knowledge gained during the project. In Figure 72 the energy balance analysis is shown. The conductive losses in Still 4 are roughly a third of those in Still 2, Still 4 also has higher radiative losses due to higher temperatures inside the still. The cover losses of the two stills are relatively similar with neither being consistently higher or lower than the other. Still 4 also has a higher energy of condensate indicating better performance.

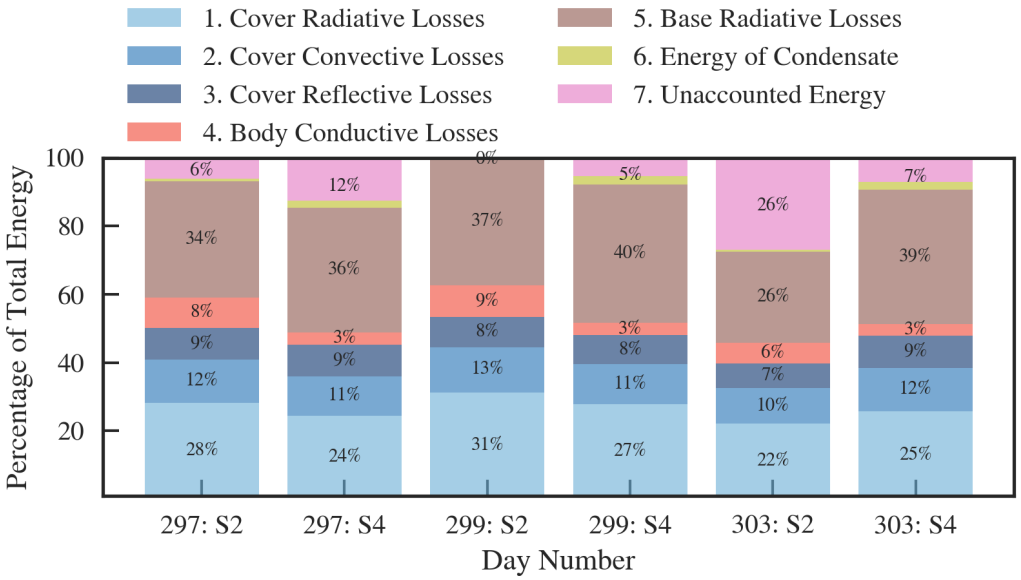

Figure 72: Energy balance analysis for a selection of days comparing Still 2 and Still 4.

Figure 73 shows the water temperatures, Still 4 experiences significantly higher water temperatures due to the absence of the plywood which absorbs large amounts of energy. The maximum temperature of water in Still 4 is on average 11 °C higher than in Still 2. It also reaches this maximum temperature earlier, approximately 45 minutes earlier, which results in an earlier onset in condensate collection as can be seen in Figure 74. The lower water temperatures in Still 4 overnight are partially due to the absence of the plywood which, in Still 2, releases the energy it stored during the day causing the water to cool down more slowly.

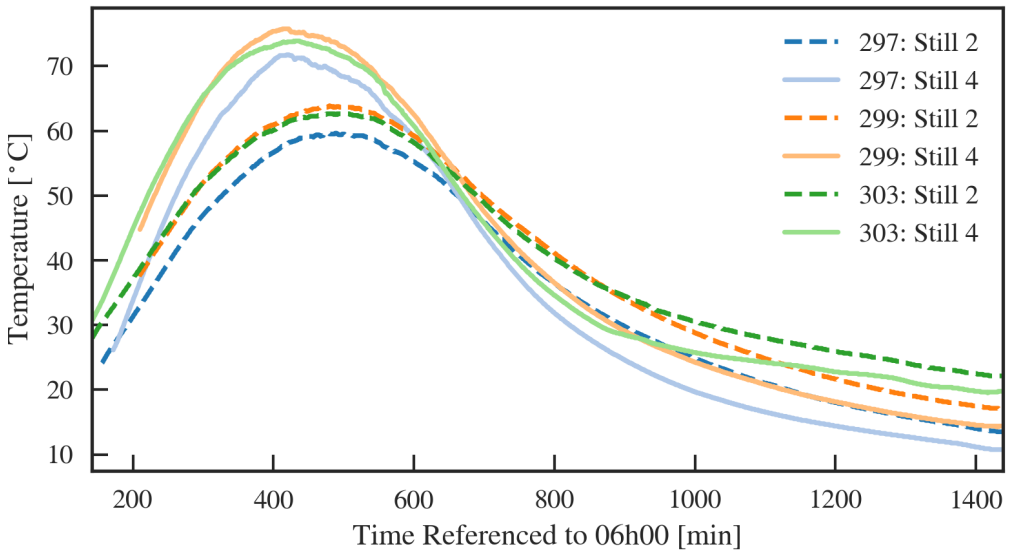

Figure 73: Water temperatures for a selection of days comparing Still 2 and Still 4.

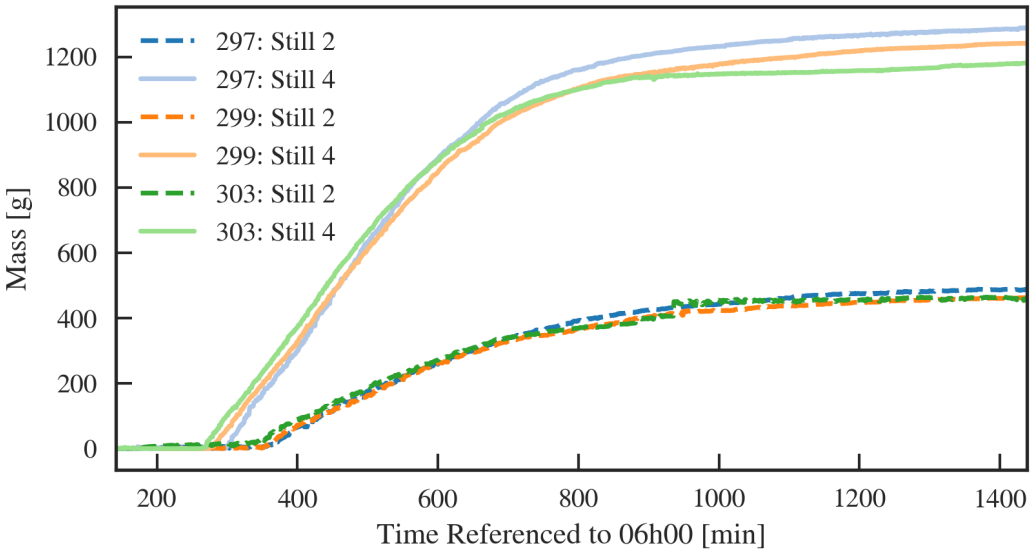

Figure 74: Mass of condensate produced for a selection of days comparing Still 2 and Still 4.

In Figure 74 the high rate of condensation in Still 4 when compared to Still 2 can be seen. This high rate of condensation is a contributing factor to the lower overnight water temperatures observed in Still 4. The onset of condensate collection is also on average 30 minutes earlier in Still 4. Table 24 shows the yields, improvement in yields, and efficiencies of the two stills. Excluding the outliers on days 305 and 306 which can be attributed to rain, Still 4 is significantly better than Still 2 and operates with the highest efficiency of any of the modifications made throughout the project.

Table 24: Efficiencies and Water Produced in Still 2 and Still 4 During Comparison Experiments.

Day Number	Still 2 Yield	Still 4 Yield	Increase in Yield	Still 2 Efficiency	Still 4 Efficiency
297	0.486 kg	1.29 kg	164 %	10.6 %	27.1 %
298	0.452 kg	1.25 kg	176 %	10.0 %	27.2 %
299	0.461 kg	1.24 kg	169 %	11.0 %	28.4 %
302	0.410 kg	1.20 kg	193 %	9.3 %	26.4 %
303	0.455 kg	1.18 kg	158 %	7.6 %	26.2 %
304	0.256 kg	0.726 kg	183 %	7.7 %	24.6 %
305	0.066 kg	0.232 kg	250 %	4.9 %	16.5 %
306	0.314 kg	1.05 kg	232 %	7.5 %	24.6 %

5 Conclusions and Recommendations

Four simple basin solar stills were built and analysed. The stills operated completely off grid and were easy to maintain. While the capital investment of the stills was small enough to obtain the cost target, the yields of the stills were not high enough. The energy balance analysis could be used to identify points of improvement in the system. Areas where improvements could be made include the radiative losses from the base, the conductive losses from the body of the still, and the cover losses.

The yield of the still was observed to have a strong linear relation to the amount of incident irradiation received by the still and a weak linear relation to the ambient temperature with the yield improving as the ambient temperature increases. Looking at the loss terms it was considered likely that the improvement in performance was due to a decrease in losses when ambient temperatures were higher. However, the efficiency was not strongly dependent on the temperature or the incident irradiation.

The effect of insulation was found to be significant as the yield was higher in stills with higher thermal resistance. However there were diminishing returns on investment observed as the thermal resistance increased past $0.74\,\mathrm{K}\cdot\mathrm{W}^{-1}$. Increasing the thermal resistance by $0.25\,\mathrm{K}\cdot\mathrm{W}^{-1}$, $0.33\,\mathrm{K}\cdot\mathrm{W}^{-1}$, and $0.58\,\mathrm{K}\cdot\mathrm{W}^{-1}$ resulted in increases in yield of 9 %, 30 %, and 27 % on average.

Adding aluminium as an internal reflector significantly decreased the temperatures of the sides of the still but had numerous negative effects. These were increasing the amount of radiation which was reflected out of the still as well as providing an alternative surface for condensation to occur on. The net effect of the addition of aluminium was negative despite the reduction in side temperatures of 10 °C and increase in water temperature of 3 °C which was achieved. The performance worsened over time as oxidation caused an increase in nucleation sites on the aluminium. Should reflectors not susceptible to oxidation be used, and angled better, the performance may be improved, however it is clear that many factors are involved in the addition of internal reflectors.

Based on the experiments which focused on increasing the evaporation rate the following observation was made: increasing the absorbance of solar irradiation can increase the yield not only due to the higher water temperature but due to the reduced reflection of radiation from the base which results in lower cover temperatures. The addition of PVC resulted in an increase in yield of 98 % on average when compared to the reference still and had efficiencies in the range of 20 % to 26 %. This indicated that a significantly larger portion of the cover losses were usefully utilised.

The carbon black nanofluid degraded with the heating cooling cycles but the efficiency of the still remained roughly constant at 21 % despite the settling of particles. This suggests that a layer of highly absorbent material at the base of the still would be as, if not more, effective than the nanofluid given the cost and complications involved in the synthesis of the nanofluid. The increase in performance when compared to the reference still varied between 46 % and 72 %. The main advantage of the nanofluid was the significantly cooler cover temperatures experienced in the latter half of the day.

The addition of activated charcoal had similar results as the cover temperature was decreased, water temperature was increased, and yield improved by 98 % compared to the reference still. The efficiencies observed in the still with charcoal were on average 20 %, slightly less efficient than with the nanofluid despite the larger improvement in yield. Adding carbon felt to the still caused the bulk water temperatures to be lower due to heating a thin film of water on the surface of the felt at a higher rate. The cover temperatures were lower and the yield was improved by up to 110 % with efficiencies of 21 %.

The addition of grooves to the cover did improve the performance slightly. It is unclear if this was due to the increased area, larger drops which formed in the grooves, or increased scattering of light inside the still and allowing less radiation to leave the still. The addition of the heat sink had no obvious effect on the yield of the still but did cause drops to form more quickly in the area underneath the heat sink which resulted in earlier drop movement in this area. The erratic behaviour of these two tests could be due to the leak which occurred in Still 3. Manual tapping on the cover improved the yield significantly, suggesting that should the area be cleared of droplets more quickly the performance of the still could be improved. The addition of external condensation area had no conclusive results at this stage.

The revised design of the basin still, using information gained during the project, performed significantly better than the reference still. The water was up to 11 °C hotter in Still 4 and heated up at a significantly higher rate. The improvement in yield was roughly 180 % when compared to the reference still and the efficiency was on average 26 %, the highest efficiency achieved yet.

It is recommended that future stills be built of materials with low heat capacity in order to increase the rate at which the water heats up. The stills should also make use of an absorber material with a low reflectivity as well as high absorbance in order to reduce the cover temperature.

The use of a textured, or grooved, cover should be further investigated as the shape and orientation of the grooves may be able to significantly reduce the amount of condensate

that drips back into the still. It would be beneficial to future analysis if a method could be found to determine the amount of condensate that is lost in this manner.

Further experiments should be performed regarding the addition of external condenser area, possibly implementing forced convection, to determine if this is a viable addition to a basin solar still.

References

Abdallah, S, Badran, O and Abu-Khader, MM (Jan. 25, 2008) "Performance evaluation of a modified design of a single slope solar still" *Desalination*, *219*, (1): 222–230 ISSN: 0011-9164.

Abdel-Rehim, ZS and Lasheen, A (Oct. 1, 2005) "Improving the performance of solar desalination systems" *Renewable Energy*, *30*, (13): 1955–1971 ISSN: 0960-1481.

Abu-Hijleh, BAK and Rababa'h, HM (June 2003) "Experimental study of a solar still with sponge cubes in basin" *Energy Conversion and Management*, *44*, (9): 1411–1418 ISSN: 0196-8904.

Akash, BA, Mohsen, MS, Osta, O and Elayan, Y (May 1, 1998) "Experimental evaluation of a single-basin solar still using different absorbing materials" *Renewable Energy*, 6th Arab International Solar Energy Conference: Bringing Solar Energy into the Daylight *14*, (1–4): 307–310 ISSN: 0960-1481.

Ayoub, J and Alward, R (Oct. 1, 1996) "Water requirements and remote arid areas: the need for small-scale desalination" *Desalination*, *107*, (2): 131–147 ISSN: 0011-9164.

Badran, OO and Al-Tahaineh, HA (Nov. 1, 2005) "The effect of coupling a flat-plate collector on the solar still productivity" *Desalination*, *183*, (1): 137–142 ISSN: 0011-9164.

Bester, JJG (2017) "Carbon black nanofluid synthesis for use in concentrated solar power applications" Dissertation, University of Pretoria.

Bhardwaj, R, ten Kortenaar, MV and Mudde, RF (Oct. 1, 2013) "Influence of condensation surface on solar distillation" *Desalination*, *326*, 37–45 ISSN: 0011-9164.

Bhardwaj, R, ten Kortenaar, MV and Mudde, RF (Sept. 15, 2015) "Maximized production of water by increasing area of condensation surface for solar distillation" *Applied Energy*, *154*, 480–490 ISSN: 0306-2619.

Bouchekima, B (Oct. 10, 2003) "A small solar desalination plant for the production of drinking water in remote arid areas of southern Algeria" *Desalination*, *159*, (2): 197–204 ISSN: 0011-9164.

Çengel, YA and Ghajar, AJ (2015) *Heat and Mass Transfer: Fundamentals & applications*, 5th McGraw-Hill, New York.

Chandrashekara, M and Yadav, A (Jan. 2017) "Water desalination system using solar heat: A review" *Renewable and Sustainable Energy Reviews*, *67*, 1308–1330 ISSN: 1364-0321.

Class O Armaflex® (2013) ND/1208/2K/002 Armacell.

Corrigan, T (2009) "Socio-economic Problems Facing Africa: Insights from six APRM Country Review Reports" *South African Institute of International Affairs*,

Coulson, JM, Richardson, JF, Backhurst, JR and Harker, JH (1999) *Coulson and Richardson's Chemical Engineering Volume 1: Fluid Flow, Heat Transfer and Mass Transfer*, Sixth Edition Butterworth Heinemann, Oxford.

Data Sheet: Waterproofing, Durapond (Aug. 2014) Duram Smart Paint.

Delyannis, EE (Dec. 1, 1987) "Status of solar assisted desalination: A review" *Desalination*, Proceedings of the THIRD WORLD CONGRESS ON DESALINATION AND WATER REUSE *67*, (Supplement C): 3–19 ISSN: 0011-9164.

Deshmukh, HS and Thombre, SB (May 15, 2017) "Solar distillation with single basin solar still using sensible heat storage materials" *Desalination*, *410*, (Supplement C): 91–98 ISSN: 0011-9164.

Dimri, V, Sarkar, B, Singh, U and Tiwari, GN (July 30, 2008) "Effect of condensing cover material on yield of an active solar still: an experimental validation" *Desalination*, *227*, (1): 178–189 ISSN: 0011-9164.

DS18B20 - Programmable Resolution 1-Wire Digital Thermometer (2018) 19-7487 Rev. 5 Maxim Integrated.

Dunkle, RV (1961) "Solar water distillation : the roof type still and a multiple effect diffusion still" in: *Proceedings of International Heat Transfer Conference* (Boulder, Colorado) vol. Part V University of Colorado: pp. 895–902.

Eilers, PHC (July 2003) "A Perfect Smoother" *Analytical Chemistry*, *75*, (14): 3631–3636 ISSN: 0003-2700.

Elango, C, Gunasekaran, N and Sampathkumar, K (July 2015) "Thermal models of solar still—A comprehensive review" *Renewable and Sustainable Energy Reviews*, *47*, 856–911 ISSN: 1364-0321.

Elango, T, Kannan, A and Murugavel, KK (Mar. 16, 2015) "Performance study on single basin single slope solar still with different water nanofluids" *Desalination*, *360*, 45–51 ISSN: 0011-9164.

Eldalil, KMS (Feb. 1, 2010) "Improving the performance of solar still using vibratory harmonic effect" *Desalination*, *251*, (1): 3–11 ISSN: 0011-9164.

Eltawil, MA and Zhengming, Z (Dec. 15, 2009) "Wind turbine-inclined still collector integration with solar still for brackish water desalination" *Desalination*, *249*, (2): 490–497 ISSN: 0011-9164.

Estahbanati, MRK, Ahsan, A, Feilizadeh, M, Jafarpur, K, Ashrafmansouri, S and Feilizadeh, M (Mar. 1, 2016) "Theoretical and experimental investigation on internal reflectors in a single-slope solar still" *Applied Energy*, *165*, (Supplement C): 537–547 ISSN: 0306-2619.

Feilizadeh, M, Estahbanati, MRK, Ahsan, A, Jafarpur, K and Mersaghian, A (Aug. 15, 2016) "Effects of water and basin depths in single basin solar stills: An experimental and theoretical study" *Energy Conversion and Management*, *122*, (Supplement C): 174–181 ISSN: 0196-8904.

Feilizadeh, M, Soltanieh, M, Estahbanati, MRK, Jafarpur, K and Ashrafmansouri, S (Dec. 15, 2017) "Optimization of geometrical dimensions of single-slope basin-type solar stills" *Desalination*, *424*, (Supplement C): 159–168 ISSN: 0011-9164.

Fourier, J (1822) *Theorie analytique de la chaleur*, Firmin Didot, pere et fils.

Gupta, B, Shankar, P, Sharma, R and Baredar, P (Jan. 1, 2016) "Performance Enhancement Using Nano Particles in Modified Passive Solar Still" *Procedia Technology*, 1st Global Colloquium on Recent Advancements and Effectual Researches in Engineering, Science and Technology - RAEREST 2016 on April 22nd & 23rd April 2016 *25*, 1209–1216 ISSN: 2212-0173.

He, T and Yan, L (Nov. 30, 2009) "Application of alternative energy integration technology in seawater desalination" *Desalination*, *249*, (1): 104–108 ISSN: 0011-9164.

Hedden, S and Cilliers, J (Sept. 2014) "Parched prospects - the emerging water crisis in South Africa" *Institute for Security Studies*, ISSN: 1026-0404.

Al-Hussaini, H and Smith, IK (Nov. 1, 1995) "Enhancing of solar still productivity using vacuum technology" *Energy Conversion and Management*, *36*, (11): 1047–1051 ISSN: 0196-8904.

Ibrahim, AGM and Elshamarka, SE (Aug. 1, 2015) "Performance study of a modified basin type solar still" *Solar Energy*, *118*, 397–409 ISSN: 0038-092X.

IsoBoard (2018) *Properties: ISOBOARD – EXTRUDED POLYSTYRENE (XPS)* URL: `https://isoboard.com/insulation/properties/` (visited on 05/15/2018).

Jamil, B and Akhtar, N (July 15, 2017) "Effect of specific height on the performance of a single slope solar still: An experimental study" *Desalination*, *414*, (Supplement C): 73–88 ISSN: 0011-9164.

Joseph, J, Saravanan, R and Renganarayanan, S (Mar. 1, 2005) "Studies on a single-stage solar desalination system for domestic applications" *Desalination*, *173*, (1): 77–82 ISSN: 0011-9164.

Kabeel, AE, Omara, ZM and Essa, FA (Feb. 1, 2014a) "Enhancement of modified solar still integrated with external condenser using nanofluids: An experimental approach" *Energy Conversion and Management*, *78*, 493–498 ISSN: 0196-8904.

Kabeel, AE, Omara, ZM and Essa, FA (Oct. 1, 2014b) "Improving the performance of solar still by using nanofluids and providing vacuum" *Energy Conversion and Management*, *86*, 268–274 ISSN: 0196-8904.

Kabeel, AE, Omara, ZM and Essa, FA (June 2017) "Numerical investigation of modified solar still using nanofluids and external condenser" *Journal of the Taiwan Institute of Chemical Engineers*, *75*, 77–86 ISSN: 1876-1070.

Kalogirou, SA (Jan. 1, 2005) "Seawater desalination using renewable energy sources" *Progress in Energy and Combustion Science*, *31*, (3): 242–281 ISSN: 0360-1285.

Kalogirou, SA (2014) *Solar Energy Engineering: Processes and Systems*, Second Edition Academic Press, Boston.

Karagiannis, IC and Soldatos, PG (Mar. 1, 2008) "Water desalination cost literature: review and assessment" *Desalination*, European Desalination Society and Center for Research and Technology Hellas (CERTH), Sani Resort 22–25 April 2007, Halkidiki, Greece *223*, (1): 448–456 ISSN: 0011-9164.

Khalifa, AJN and Hamood, AM (Sept. 1, 2009a) "Effect of insulation thickness on the productivity of basin type solar stills: An experimental verification under local climate" *Energy Conversion and Management*, *50*, (9): 2457–2461 ISSN: 0196-8904.

Khalifa, AJN and Hamood, AM (Aug. 1, 2009b) "On the verification of the effect of water depth on the performance of basin type solar stills" *Solar Energy*, *83*, (8): 1312–1321 ISSN: 0038-092X.

Khalifa, AJN and Hamood, AM (Nov. 30, 2009c) "Performance correlations for basin type solar stills" *Desalination*, *249*, (1): 24–28 ISSN: 0011-9164.

Al-Kharabsheh, S and Goswami, DY (Aug. 1, 2003) "Analysis of an innovative water desalination system using low-grade solar heat" *Desalination*, *156*, (1): 323–332 ISSN: 0011-9164.

Kumar, RA, Esakkimuthu, G and Murugavel, KK (Dec. 1, 2016) "Performance enhancement of a single basin single slope solar still using agitation effect and external condenser" *Desalination*, *399*, 198–202 ISSN: 0011-9164.

Lal, RK, Mishra, S, Dwivedi, JP and Dwivedi, H (Jan. 2017) "A Comprehensive Study of the Different Parameters of Solar Still" *Materials Today: Proceedings*, 5th International Conference of Materials Processing and Characterization (ICMPC 2016) *4*, (2, Part A): 3572–3580 ISSN: 2214-7853.

Lemmon, EW, McLinden, MO and Friend, DG (2018) "Thermophysical Properties of Fluid Systems", in: *NIST Chemistry WebBook, NIST Standard Reference Database Number 69*, Linstrom, PJ and Mallard, WG (Eds.), National Institute of Standards and Technology, Gaithersburg MD (visited on 09/20/2018).

Li, C, Goswami, Y and Stefanakos, E (Mar. 2013) "Solar assisted sea water desalination: A review" *Renewable and Sustainable Energy Reviews*, *19*, 136–163 ISSN: 1364-0321.

Madani, AA and Zaki, GM (Jan. 1, 1995) "Yield of solar stills with porous basins" *Applied Energy*, Fifth Arab International Solar Energy Conference *52*, (2): 273–281 ISSN: 0306-2619.

Mahian, O, Kianifar, A, Kalogirou, SA, Pop, I and Wongwises, S (Feb. 1, 2013) "A review of the applications of nanofluids in solar energy" *International Journal of Heat and Mass Transfer*, *57*, (2): 582–594 ISSN: 0017-9310.

Malik, MAS, Tiwari, GN, Kumar, A and Sodha, MS (1982) *Solar Distillation*, First Edition Pergamon Press, Oxford, UK.

Matrawy, KK, Alosaimy, AS and Mahrous, AF (Nov. 15, 2015) "Modeling and experimental study of a corrugated wick type solar still: Comparative study with a simple basin type" *Energy Conversion and Management*, *105*, (Supplement C): 1261–1268 ISSN: 0196-8904.

Monowe, P, Masale, M, Nijegorodov, N and Vasilenko, V (Oct. 3, 2011) "A portable single-basin solar still with an external reflecting booster and an outside condenser" *Desalination*, *280*, (1–3): 332–338 ISSN: 0011-9164.

Murugavel, KK, Chockalingam, KKSK and Srithar, K (Mar. 1, 2008) "Progresses in improving the effectiveness of the single basin passive solar still" *Desalination*, *220*, (1): 677–686 ISSN: 0011-9164.

Nafey, AS, Abdelkader, M, Abdelmotalip, A and Mabrouk, AA (Nov. 1, 2000) "Parameters affecting solar still productivity" *Energy Conversion and Management*, *41*, (16): 1797–1809 ISSN: 0196-8904.

Omara, ZM, Abdullah, AS, Kabeel, AE and Essa, FA (Oct. 1, 2017) "The cooling techniques of the solar stills' glass covers - A review" *Renewable and Sustainable Energy Reviews*, *78*, 176–193 ISSN: 1364-0321.

Omara, ZM, Kabeel, AE and Abdullah, AS (Feb. 1, 2017) "A review of solar still performance with reflectors" *Renewable and Sustainable Energy Reviews*, *68*, (Part 1): 638–649 ISSN: 1364-0321.

Omara, ZM, Kabeel, AE and Essa, FA (Oct. 1, 2015) "Effect of using nanofluids and providing vacuum on the yield of corrugated wick solar still" *Energy Conversion and Management*, *103*, 965–972 ISSN: 0196-8904.

Owner's Manual, Pyranometer, Models SP-212 and SP-215 (2018) Apogee Instruments, Inc.

Phadatare, MK and Verma, SK (Nov. 5, 2007) "Influence of water depth on internal heat and mass transfer in a plastic solar still" *Desalination*, *217*, (1–3): 267–275 ISSN: 0011-9164.

Pugsley, A, Zacharopoulos, A, Mondol, JD and Smyth, M (Apr. 1, 2016) "Global applicability of solar desalination" *Renewable Energy*, *88*, (Supplement C): 200–219 ISSN: 0960-1481.

Rabhi, K, Nciri, R, Nasri, F, Ali, C and Bacha, HB (Aug. 15, 2017) "Experimental performance analysis of a modified single-basin single-slope solar still with pin fins absorber and condenser" *Desalination*, *416*, 86–93 ISSN: 0011-9164.

Rajaseenivasan, T, Prakash, R, Vijayakumar, K and Srithar, K (Aug. 1, 2017) "Mathematical and experimental investigation on the influence of basin height variation and stirring of water by solar PV panels in solar still" *Desalination*, *415*, (Supplement C): 67–75 ISSN: 0011-9164.

El-Sebaii, AA, Aboul-Enein, S, Ramadan, MRI and El-Bialy, E (Jan. 1, 2000) "Year-round performance of a modified single-basin solar still with mica plate as a suspended absorber" *Energy*, *25*, (1): 35–49 ISSN: 0360-5442.

Shanmugan, S, Rajamohan, P and Mutharasu, D (Sept. 30, 2008) "Performance study on an acrylic mirror boosted solar distillation unit utilizing seawater" *Desalination*, *230*, (1): 281–287 ISSN: 0011-9164.

Sharon, H and Reddy, KS (Jan. 1, 2015) "A review of solar energy driven desalination technologies" *Renewable and Sustainable Energy Reviews*, *41*, (Supplement C): 1080–1118 ISSN: 1364-0321.

Sharshir, SW, Peng, G, Wu, L, Yang, N, Essa, FA, Elsheikh, AH, Mohamed, SIT and Kabeel, AE (Feb. 25, 2017) "Enhancing the solar still performance using nanofluids and glass cover cooling: Experimental study" *Applied Thermal Engineering*, *113*, 684–693 ISSN: 1359-4311.

Sharshir, SW, Yang, N, Peng, G and Kabeel, AE (May 5, 2016) "Factors affecting solar stills productivity and improvement techniques: A detailed review" *Applied Thermal Engineering*, *100*, 267–284 ISSN: 1359-4311.

Singh, HN and Tiwari, GN (Aug. 15, 2004) "Monthly performance of passive and active solar stills for different Indian climatic conditions" *Desalination*, *168*, (Supplement C): 145–150 ISSN: 0011-9164.

Smith, JM, Van Ness, HC and Abbott, MM (2005) *Introduction to Chemical Engineering Thermodynamics*, 7th McGraw-Hill, New York.

Song, J, Li, T, Wright-Contreras, L and Law, AW (July 4, 2017) "A review of the current status of small-scale seawater reverse osmosis desalination" *Water International*, *42*, (5): 618–631 ISSN: 0250-8060.

Srivastava, PK and Agrawal, SK (Feb. 15, 2013) "Experimental and theoretical analysis of single sloped basin type solar still consisting of multiple low thermal inertia floating porous absorbers" *Desalination*, *311*, (Supplement C): 198–205 ISSN: 0011-9164.

El-Swify, ME and Metias, MZ (Aug. 1, 2002) "Performance of double exposure solar still" *Renewable Energy*, *26*, (4): 531–547 ISSN: 0960-1481.

Szulmayer, W (Mar. 1, 1973) "Solar stills with low thermal inertia" *Solar Energy*, *14*, (4): 415–421 ISSN: 0038-092X.

Taghvaei, H, Taghvaei, H, Jafarpur, K, Estahbanati, MRK, Feilizadeh, M, Feilizadeh, M and Ardekani, AS (Aug. 15, 2014) "A thorough investigation of the effects of water depth on the performance of active solar stills" *Desalination*, *347*, (Supplement C): 77–85 ISSN: 0011-9164.

Tanaka, H (June 1, 2009a) "Effect of inclination of external reflector of basin type still in summer" *Desalination*, *242*, (1): 205–214 ISSN: 0011-9164.

Tanaka, H (Nov. 30, 2009b) "Experimental study of a basin type solar still with internal and external reflectors in winter" *Desalination*, *249*, (1): 130–134 ISSN: 0011-9164.

Temperature and Humidity Module - AM2302 Product Manual (2018) Aosong Electronics.

Tiwari, AK and Tiwari, GN (Aug. 5, 2006) "Effect of water depths on heat and mass transfer in a passive solar still: in summer climatic condition" *Desalination*, *195*, (1): 78–94 ISSN: 0011-9164.

Tiwari, GN, Thomas, JM and Khan, E (July 1, 1994) "Optimisation of glass cover inclination for maximum yield in a solar still" *Heat Recovery Systems and CHP*, *14*, (4): 447–455 ISSN: 0890-4332.

Tiwari, GN, Tiwari, A and Shyam (2016) *Handbook of Solar Energy: Theory, Analysis and Applications*, Springer.

Velmurugan, V, Gopalakrishnan, M, Raghu, R and Srithar, K (Oct. 1, 2008) "Single basin solar still with fin for enhancing productivity" *Energy Conversion and Management*, *49*, (10): 2602–2608 ISSN: 0196-8904.

Wypych, G (2016) *Handbook of Polymers*, 2nd Edition ChemTec Publishing, Toronto, Canada.

Yadav, S and Sudhakar, K (July 1, 2015) "Different domestic designs of solar stills: A review" *Renewable and Sustainable Energy Reviews*, *47*, 718–731 ISSN: 1364-0321.

A Additional Figures and Images

Figure A.1: A photograph from the front of two of the basin stills during operation, clearly showing the stills mounted on their frames.

Figure A.2: A photograph of two of the basin stills during operation; the pyranometer is visible on the foremost still.

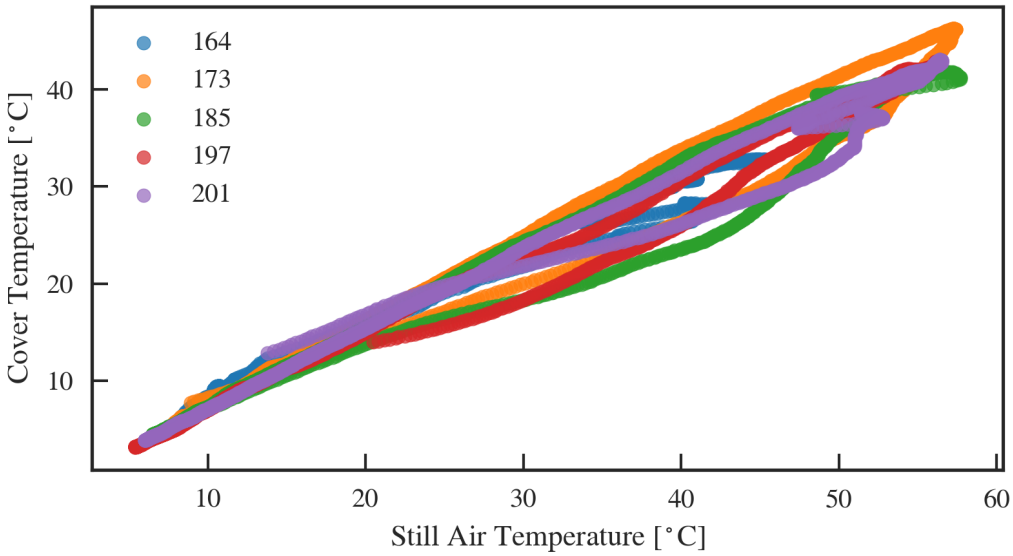

Figure A.3: The linear relationship between the inside cover temperature and the air temperature within the still for a selection of days, the equation $T_{cover} = 0.75T_{air} + 0.2$ was found to accurately represent this relationship.

Figure A.4: The inside surface of the still after a couple months of operation, showing the deterioration of the Durapond sealant.

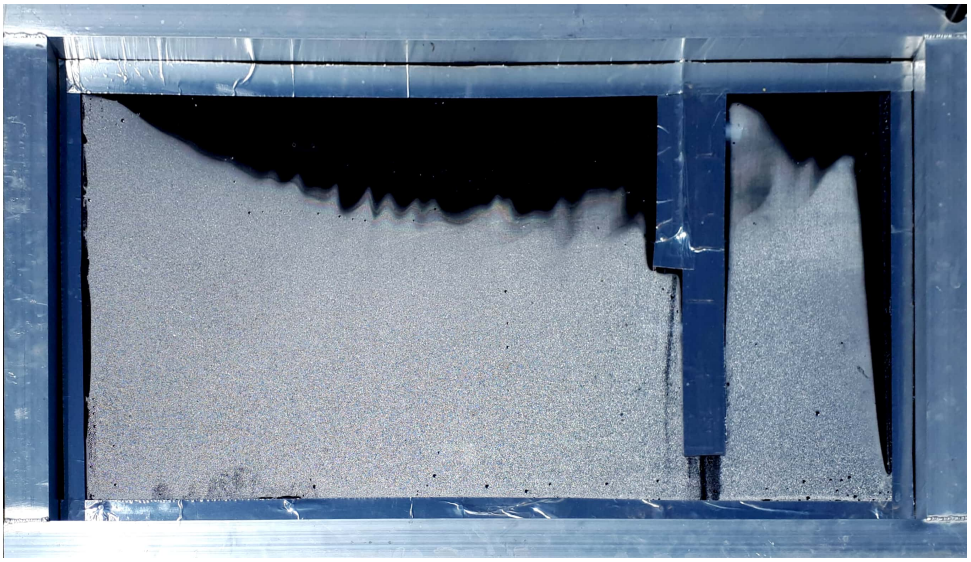

Figure A.5: A top down view of the cover plate of Still 2 on day 240, photo taken at 10h20.

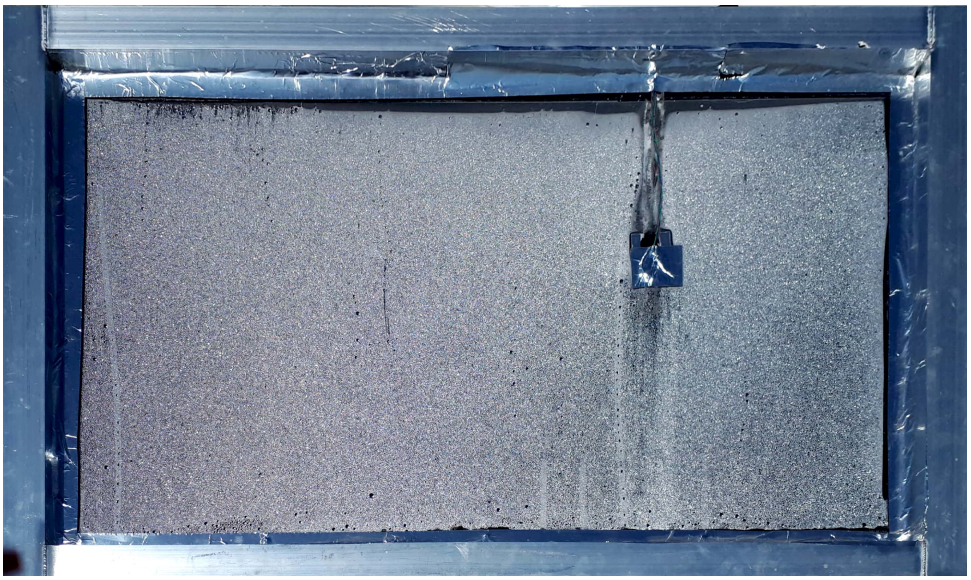

Figure A.6: A top down view of the cover plate of Still 1 on day 240, where aluminium had been added to the back wall of the still, photo taken at 10h21.